

Vegetation ecology of forest-savanna ecotones in the Comoé National Park (Ivory Coast):
Border and ecotone detection, core-area analysis, and ecotone dynamics

Dissertation

zur

Erlangung des akademischen Grades

Doctor rerum naturalium (Dr. rer. nat.)

der Mathematischen-Naturwissenschaftlichen Fakultät

der Universität Rostock

Institut für Biowissenschaften (IfBI)

Abteilung Allgemeine und Spezielle Botanik

vorgelegt von

Klaus Josef Hennenberg, geb. am 18.12.1970 in Münster (Westf.)

aus Rostock

Rostock, 17.12.2004

Gutachter:

Prof. Dr. Stefan Porembski

Prof. Dr. Wilhelm Barthlott

Prof. Dr. Florian Jeltsch

Tag der Verteidigung: 23.05.2005

Contents

Contents	3
List of Figures	5
List of Tables	7
List of Abbreviations	8
Summary	10
Zusammenfassung	12
1 Introduction.....	14
1.1 Transect analysis.....	17
1.1.1 Transect analysis of univariate data.....	17
1.1.2 Transect analysis of multivariate data	18
1.2 Biomass and surface fires along forest-savanna ecotones	18
1.3 Microclimate along forest-savanna ecotones.....	19
1.4 Vegetation composition along forest-savanna ecotones.....	20
1.5 Core-area analysis.....	21
1.6 Dynamics of forest-savanna ecotones	22
2 Material and Methods	24
2.1 Study area	24
2.1.1 Climate.....	25
2.1.2 Geology and soils	26
2.1.3 Vegetation.....	27
2.1.4 Characteristics of <i>Anogeissus leiocarpus</i>	29
2.2 Sampling design.....	29
2.3 Sampling of vegetation	31
2.3.1 Vegetation structure and composition	31
2.3.2 Sampling of tree and shrub individuals	32
2.3.3 Density measurement of tree and shrub individuals.....	33
2.3.4 Sampling of surface biomass	33
2.4 Sampling of abiotic parameters	33
2.4.1 Microclimatic parameters	33
2.4.2 Fire occurrence, shading, and soil depth	34

2.5	Border-and-ecotone-detection analysis (BEDA) for univariate transect data	35
2.6	Statistical analysis.....	37
2.6.1	General transect description	37
2.6.2	Surface biomass and surface-fire probability	37
2.6.3	Microclimate.....	38
2.6.4	Vegetation composition	38
2.6.5	Core-area analysis.....	39
2.6.6	Size-class distribution of tree species	40
3	Results.....	42
3.1	General transect description	42
3.2	Surface biomass and surface-fire probability	45
3.3	Seasonal variability in microclimatic borders and ecotones.....	50
3.4	Border and ecotone detection by means of vegetation composition	56
3.5	Core-area analysis.....	59
3.6	Size-class distribution of tree species with a focus on <i>Anogeissus leiocarpus</i>	62
4	Discussion.....	69
4.1	Border and ecotone detection	69
4.1.1	Border-and-ecotone detection analysis (BEDA) for univariate transect data...69	
4.1.2	SMWDA and MWRA for multivariate transect data	70
4.2	Relation of surface biomass and surface fire	71
4.3	Seasonal variability in microclimatic borders and ecotones.....	74
4.4	Border and ecotone detection by means of vegetation composition	76
4.5	Core-area analysis.....	77
4.6	Dynamics of forest-savanna ecotones and the role of <i>Anogeissus leiocarpus</i>	80
5	Conclusions.....	84
	References.....	87
	Acknowledgements.....	102
	Appendix.....	104

List of Figures

Fig. 1.1. The hierarchical continuum model combined with the climax pattern hypothesis expressed as species response curves along a single environmental gradient.....	20
Fig. 2.1. Map of the study area in the southwestern part of the Comoé National Park, Ivory Coast, West Africa.	25
Fig. 2.2. Mean monthly and mean annual rainfall for three climate stations in northeastern Ivory Coast and for the climate station at the research camp of the University of Würzburg in the southwestern part of the CNP.....	26
Fig. 2.3. Idealized model of the vegetation distribution along a topographical gradient of a pediplain.....	28
Fig. 2.4. Distribution of dominant vegetation types in the northern and southern part of the CNP.....	29
Fig. 2.5. Sampling designs along forest-savanna transects being adapted to the study parameters.....	31
Fig. 2.6. Scheme of the border-and-ecotone detection analysis (BEDA).....	35
Fig. 2.7. Demonstration of the method to value the width of an ecotone at a significant border detected by the split-moving-window dissimilarity analysis (SMWDA) using moving-window regression analysis (MWRA).....	39
Fig. 3.1. Values of three structural parameters and soil depth along eight studied transects ...	43
Fig. 3.2. Sample scores of the first and second DCA axes for the cover of all species along the intensely studied transect.....	44
Fig. 3.3. Box-plot of dry mass of grasses, herbs, and litter for biomass plots in the savanna, forest belt, and closed forest.....	45
Fig. 3.4. Non-linear regression of grass volume and mass of dry grasses.....	46
Fig. 3.5. Distribution of dry mass of grass and burned area along eight forest-savanna transects.....	46
Fig. 3.6. Dry mass of grasses versus total vegetation cover above 1 m and soil depth along eight forest-savanna transects.....	47
Fig. 3.7. Graphic comparison of the non-linear mixed effects model and the fixed model for the parameter dry mass of grasses along eight forest-savanna transects.....	49
Fig. 3.8. Ignition probability in dependence on dry mass of grasses.....	50
Fig. 3.9. 3D-presentation of two five-day courses of vapor pressure deficit (VPD) measured during the dry and rainy season along the intensely studied transect.....	51
Fig. 3.10. Courses of three microclimatic parameters at the reference site in the open savanna in the CNP during the study period from 02/08/2002 to 08/30/2002.....	52
Fig. 3.11. Five-day mean of diurnal amplitude of vapor pressure deficit (VPD _{ampl.}) measured along the intensely studied transect from 08/30/2002 to 09/04/2002.....	52
Fig. 3.12. Borders and ecotones detected by BEDA for three standardized microclimatic parameters for five measuring periods.....	54

Fig. 3.13. Five-day mean of diurnal amplitude of vapor pressure deficit ($VPD_{\text{ampl.}}$) and the standardized values ($\text{stdVPD}_{\text{ampl.}}$) for five measurement periods.....	55
Fig. 3.14. Pooled average Z scores computed by SMWDA and slopes calculated by MWRA for the intensely studied transect for vegetation composition	57
Fig. 3.15. Sum of relative core area (rCA) for 31 studied semi-deciduous forest islands and number of forest islands containing a specific rCA in dependence on DEI.	59
Fig. 3.16. Map of the studied forest islands in the southwestern part of the CNP and the remaining core area (CA) assuming a DEI of 55 m.....	60
Fig. 3.17. Relative core area (rCA) assuming a DEI of 55 m versus total area (TA) of semi-deciduous forest islands	61
Fig. 3.18. Size of forest islands required to guarantee that a forest island contains a relative core area (rCA) of 50% in dependence on DEI	61
Fig. 3.19. Diameter-classes distribution of <i>Anogeissus leiocarpus</i> and of all trees (including <i>A. leiocarpus</i>) along eight forest-savanna transects and in a human-influenced monodominant <i>Anogeissus</i> stand.....	62
Fig. 3.20. Map of clumped occurrence of the different diameter classes of <i>Anogeissus leiocarpus</i> in a human-influenced monodominant <i>Anogeissus</i> stand.....	63
Fig. 3.21. Sample scores of the first and second PCA axes for (a) the abundance of four diameter classes of <i>Anogeissus leiocarpus</i> and (b) for structural vegetation data from the transect segments of eight forest-savanna transects and the <i>Anogeissus</i> stand.....	65
Fig. 4.1. Maximum height of a grass tuft of <i>Hyparrhenia</i> sp. versus annual rainfall from 1993 to 2001	74
Fig. 4.2. Occurrence probability of <i>Antiaris africana</i> and <i>Majidea fosteri</i> in dependence on the area of forest islands	78
Fig. 5.1. Modeling approach for the planned forest boundary model	85
Fig. A. 1. Graphic comparison of the non-linear mixed effects model and the fixed model for the structural parameter cover of grasses and grass litter	105
Fig. A. 2. Graphic comparison of the non-linear mixed effects model and the fixed model for the structural parameter cover above 1 m	106
Fig. A. 3. Graphic comparison of the non-linear mixed effects model and the fixed model for the structural parameter cover of woody climbers.....	107

List of Tables

Table 3.1. Results of BEDA for three structural parameters assuming no random effect between transects (fixed model)	43
Table 3.2. Results of BEDA for dry mass of grasses for eight forest-savanna transect	48
Table 3.3. Results of random effects of linear mixed effects models with a cubic term computed as approximations of sigmoidal non-linear models for three microclimatic parameters ($\text{stdT}_{\text{mean}}$, $\text{stdH}_{5\text{-quantil}}$, and $\text{stdVPD}_{\text{ampl.}}$)	54
Table 3.4. Width of the forest belt visible in the field and DEI detected for tree species larger than 20 cm dbh along eight forest-savanna transects	58
Table 3.5. Mean abundance of four diameter classes of 10 dominant tree species in transect segments with high abundance of <i>Anogeissus leiocarpus</i>	65
Table 3.6. Regression analysis of diameter class DC1 of 10 dominant tree species and three environmental parameters	67
Table. A. 1. Summary of detected DEI regarding different parameters studied along forest-savanna transects in the CNP	108
Appendix A. Estimation of total area (<i>TA</i>) in dependence on an aspired relative core area ..	104

List of Abbreviations

a, c	Asymptotes of the sigmoidal non-linear regression model, each reflecting the conditions of a parameter in one of two adjacent habitats
ANOVA	Analysis of variance
AS	monodominant <i>Anogeissus leiocarpus</i> stand (= <i>Anogeissus</i> stand)
B	Inflection point of the sigmoidal non-linear regression model, reflecting the location of the border between two habitats
B-Eco	Belt-ecotone segment
BIOTA	Biodiversity Monitoring Transect Analysis in Africa
b	x -coordinate of B
CA	Core area of forest islands
d	Slope of the sigmoidal non-linear regression model
dbh	diameter at breast height
DC1-DC5	Diameter classes (DC1: 0-1 cm dbh, DC2: 1-6 cm dbh, DC3: 6-30 cm dbh, DC4: > 30 cm dbh, DC5: dead trees > 30 cm dbh)
DCA	Detrended corespondance analysis
DEI	Depth-of-edge influence
$E1, E2$	Locations of the limits of an ecotone that is associated to a border, B
$e1, e2$	x -coordinates of $E1$ and $E2$
F-Eco	Forest-ecotone segment
For	Closed-forest segment
glm	R-function for generalized linear models
$H_{5\%}$ -quantil	Five-day mean of diurnal 5%-quantil of relative air humidity
IST	Intensely studied transect (T4)
lme	R-function for linear mixed effects models

loess	R-function for non-parametric smoothing models
MP1-MP5	Measurement period of 40 days each from 02/08 to 08/30/2002
MWRA	Moving-window regression analysis
nlme	R-function for non-linear mixed effects models
nls	R-function for non-linear regression models
PCA	Principal component analysis
<i>rCA</i>	Relative core area of forest islands
r_s	Spearman's rank correlation coefficient
<i>SD</i>	Standard deviation unit
SMWDA	Split-moving-window dissimilarity analysis
T1-T8	Numeration of the studied transects
<i>TA</i>	Total area of forest islands
T_{mean}	Five-day mean of diurnal mean air temperature
Sav	savanna segment
S-Eco	savanna-ecotone segment
stdH _{5%-quantil}	Five-day mean of standardized diurnal 5%-quantil of relative air humidity
stdT _{mean}	Five-day mean of standardized diurnal mean air temperature
stdVPD _{ampl.}	Five-day mean of standardized diurnal amplitude of vapor pressure deficit
VPD _{ampl.}	Five-day mean of diurnal amplitude of vapor pressure deficit

Summary

Loss of biodiversity is mainly caused by changes in climate and land use. The latter is currently taking place most strongly in the tropics, especially due to continuous deforestation which often creates a fragmented landscape. Forest-edge effects – measured as depth-of-edge influence (DEI) – can profoundly reduce the area of ecological forest interior (core area). The size of forest-core areas is a central issue in the protection of forest-interior species at the landscape scale, and the dynamics of ecotones between forests and adjacent habitats are important for the understanding of forest succession or regression. Especially in the tropics, these aspects have not been well studied.

The study sites of the present thesis were located in the southwestern part of the Comoé National Park (CNP) in northeastern Ivory Coast (northern Guinea zone, West Africa). Inside the protected area of the CNP, a mosaic of forest islands, savannas, and gallery forests can be found that is representative for large areas of the northern Guinea and the southern Sudanian zone in West Africa. Within the CNP, important human impacts are uncontrolled annual burning of the savanna and poaching. Outside of the CNP, strong deforestation occurred during the last decades. The aim of the present thesis was to analyze the forest-savanna ecotone of semi-deciduous forest islands with regard to DEI, forest-core area and forest succession in order to understand basic processes significant for nature protection and forest management.

In the CNP, seven large islands of a dry variant of semi-deciduous forest (*Celtis* spp. and *Triplochiton scleroxylon* type) with a size of 21 to 146 ha were selected. At eight locations randomly chosen, transects with a length of 300 to 350 m were installed perpendicularly to the forest-savanna ecotone. In addition, a single stand dominated by the pioneer tree species *Anogeissus leiocarpus* (Combretaceae) was included into the study. This species was also dominant in the forest belts of the studied transects.

Four topics were addressed in the present thesis. The first topic deals with filling a methodological gap in statistic analyses of transect data along ecotones. With regard to univariate transect data, a new border-and-ecotone detection analysis (BEDA) was developed and confidence intervals were derived for the characteristic parameters that describe border and ecotone properties. For the analysis of multivariate data, two existing methods, the ‘split-moving-window dissimilarity analysis’ and the ‘moving-window regression analysis’, were combined for determining significant borders and width of the associated ecotones. Both approaches proved to be objective and reliable methods for transect analysis.

In the context of the second topic, the methods outlined in the first topic were successfully applied to data on vegetation composition, structural vegetation parameters, surface biomass, occurrence of surface fires, microclimate, and soil depth recorded along the forest-savanna transects. The smallest DEI of 0 m occurred for fire occurrence, whereas the largest DEI of 148 m was detected for grass biomass. However, most DEI values were found between 20 and 60 m and were, thus, comparable to published values for tropical and temperate forests. But the DEI of different parameters were only rarely related with each other, even though the parameters themselves were correlated with each other. For example, the covers of grasses and vegetation layers above 1 m were negatively correlated, but DEI values were 11.4 ± 9.8 m and 32.0 ± 15.5 m, respectively. Hence, for the application in the core-area analysis, no generalized DEI can be given, but each parameter of interest must be investigated separately.

The third topic deals with the calculation of core areas of forest islands in the CNP by applying a GIS-based non-additive core-area model. For a given DEI of 55 m (e.g. species composition of trees > 20 cm dbh), only 9 of 31 forest islands contained a relative core area ($rCA = \text{core area} / \text{total area}$) larger than 50%. An rCA of 50% can be expected for forest islands with a size of 36.6 ha. For a DEI of 120 m (e.g. cover of woody climbers), only one forest island contained an rCA larger than 50%, and to allow for an rCA of 50% forest islands must be larger than 250 ha. Since areas protected from deforestation are rare in the northern Guinea and southern Sudanian zone, the results of the core-area analysis are of high importance for the development of forest protection plans in these regions.

The fourth topic addresses successional processes at the forest-savanna ecotone. The analysis of the distribution of tree-size classes along the studied transects revealed sequential series of both tree species and tree-size classes of individual species. At the forest border, *Anogeissus leiocarpus* was the most abundant tree. Juveniles (< 1 cm dbh) reached highest density values (mean of 502 individuals/ha) at savanna sites at the outer periphery of the forests. Forest tree species regenerated well at forest sites, but also in the shade of *A. leiocarpus*. It is concluded that the studied forest islands advance against savanna by sequential succession. The potential of *A. leiocarpus* to act as an important pioneer in the succession from savanna to forest due to its effective regeneration at savanna sites and subsequent modification of site conditions, especially fire intensity by shading out savanna grasses, is discussed. With regard to the distribution pattern of tree-size classes and structural vegetation parameters, the monodominant *Anogeissus* stand was most similar to transect segments near the forest border and may be interpreted as a successional stage towards a semi-deciduous forest island.

The results presented in this study provide a profound understanding of processes at forest-savanna ecotones and deliver a sound data base for nature protection and forest management in the northern Guinea and southern Sudanian zone in West Africa. In addition, these data may serve as basis for both long-term studies and modeling of the dynamics of forest-savanna ecotones in the Comoé National Park.

Zusammenfassung

Verlust biologischer Vielfalt wird vor allem durch Klimawandel und Veränderungen der Landnutzung hervorgerufen. Letztere treten besonders stark in den Tropen auf, wo derzeit eine fortschreitende Entwaldung zu einer Fragmentierung der Landschaft führt. Waldrandeffekte, gemessen als *depth-of-edge influence* (DEI), verringern zusätzlich die ökologische Kernfläche des Waldes (*core area*). Zur Entwicklung von Schutzkonzepten für Waldarten ist die Größenbestimmung des *core area* von besonderer Bedeutung. Zudem spielt die Dynamik von Waldrändern eine wichtige Rolle in der Waldsukzession und -regression. Besonders in den Tropen sind diese Aspekte noch unzureichend verstanden.

Die Untersuchungen der vorliegenden Arbeit fanden im südwestlichen Teil des Comoé-Nationalparks (CNP) in der Guinea-Zone im Nordosten der Elfenbeinküste (Westafrika) statt. Der CNP setzt sich aus einem Mosaik aus Inselwäldern, unterschiedlichen Savannenformationen und Galeriewäldern zusammen, welches als repräsentativ für weite Bereiche der Nord-Guinea- und der Süd-Sudan-Zone in Westafrika gilt. Menschliche Einflüsse im CNP beschränken sich vornehmlich auf Savannenfeuer und Wilderei. Außerhalb des CNP wurde während der letzten Jahrzehnte eine starke Entwaldung festgestellt. Ziel dieser Arbeit war die Analyse des Wald-Savanne-Ökotonen an tropischen halb-immergrünen Waldinseln in Bezug auf DEI, *core area* und Waldsukzession, um zu einem besseren Systemverständnis insbesondere in Hinblick auf Waldnaturschutz und -management in der Region beizutragen.

Im CNP wurden sieben große Waldinseln (21 – 146 ha) ausgewählt, die einer trockenen Variante halb-immergrüner Tropenwälder angehören (*Celtis* spp.- und *Triplochiton scleroxylon*-Typ). An acht Zufallspunkten wurden senkrecht zum Waldrand Wald-Savanne-Transekte mit einer Länge von 300 – 350 m angelegt. Zusätzlich wurde ein monodominanter *Anogeissus leiocarpus*-Bestand (Combretaceae) bearbeitet. Diese Pionierbaumart dominierte ebenfalls in den Waldrandbereichen der untersuchten Transekte.

In der vorliegenden Arbeit wurden folgende Themenbereiche bearbeitet. Mit dem ersten Themenbereich sollte eine Lücke in der statistischen Analyse von Transektdaten entlang von Ökotonen geschlossen werden. Zur Analyse univariater Daten wurde eine *border-and-ecotone detection analysis* (BEDA) einschließlich der Herleitung von Konfidenzintervallen entwickelt. Zur Analyse multivariater Daten wurden die Methoden von *split-moving-window dissimilarity analysis* und *moving-window regression analysis* kombiniert, um signifikante Grenzen und Breiten zugehöriger Ökotone zu bestimmen. Beide Ansätze erwiesen sich als objektive und verlässliche Verfahren zur Transektanalyse.

Diese Methoden wurden im zweiten Themenbereich entlang der acht Wald-Savanne-Transekte für die Parameter Vegetationszusammensetzung, Vegetationsstruktur, bodennahe Biomasse, Auftreten von Bodenfeuer, Mikroklima und Bodentiefe angewandt. Der kleinste DEI von 0 m wurde für das Auftreten von Bodenfeuer festgestellt, der größte DEI von 148 m für Grassbiomasse. Die meisten im CNP gemessenen DEI-Werte lagen jedoch zwischen 20 und 60 m und sind damit vergleichbar mit Werten aus anderen Studien an tropischen und temperaten Wäldern. Allerdings konnten die DEI-Werte unterschiedlicher Parameter selten in einen Zusammenhang gebracht werden, selbst wenn Korrelationen zwischen den Parametern vorlagen. So unterschieden sich beispielsweise für die negativ korrelierten Deckungsgrade von Gräsern und Vegetationsschichten > 1 m die DEI-Werte mit $11,4 \pm 9,8$ m und $32,0 \pm 15,5$ m deutlich. Für die Anwendung in *core area* Analysen kann daher kein genereller DEI angegeben werden, weshalb ökologisch interessierende Parameter getrennt zu betrachten sind.

Der dritte Themenbereich behandelt die Berechnung des *core area* von Waldinseln im CNP mit einem GIS-basierten, nicht-additiven *core area*-Modell. Bei einem DEI von 55 m (z.B. Baumindividuen > 20 cm BHD) enthielten nur 9 von 31 Waldinseln einen relativen *core area*-Wert ($rCA = \text{core area} / \text{Gesamtfläche}$) von mindestens 50%. Ein *rCA* von 50% war für Waldinseln ab 36,6 ha zu erwarten. Für einen DEI von 120 m (z.B. Deckungsgrad von Lianen) enthielt nur eine Waldinsel einen *rCA* von mehr als 50%, und ein *rCA* von 50% war bei Waldinseln ab 250 ha zu erwarten. Da in der Nord-Guinea- und der Süd-Sudan-Zone geschützte Gebiete selten sind, stellen die Ergebnisse der *core area*-Analyse einen wichtigen Beitrag zur Entwicklung von Schutz- und Managementplänen für Wälder in dieser Region dar.

Der vierte Themenbereich befasst sich mit Sukzessionsprozessen im Wald-Savanne-Ökoton. Verteilungsmuster von Baumgrößenklassen entlang der Transekte ergaben, dass sowohl Baumarten als auch Größenklassen einzelner Arten in einer sequenziellen Abfolge auftraten. Am Waldrand dominierte *Anogeissus leiocarpus*. Höchste Jungpflanzendichten (< 1 cm BHD: Mittelwert von 502 Individuen/ha) traten in der Savanne am Waldrand auf. Waldbaumarten verjüngten sich gut im Waldinneren, aber auch am Waldrand im Unterwuchs von *A. leiocarpus*. Es wurde geschlossen, dass die Waldinseln durch sequenzielle Sukzession in die Savanne vordringen. *A. leiocarpus* scheint sich als Pionierart effektiv an Savannenstandorten etablieren zu können und anschließend die Standortbedingungen besonders durch die Verringerung der Feuerintensität durch das Ausschatten von Gräsern zu verändern. Der monodominante *Anogeissus*-Bestand ähnelte für Verteilungsmuster von *A. leiocarpus* und der Vegetationsstruktur am meisten den Transektsegmenten an der Wald-Savanne-Grenze und kann als Sukzessionsstadium zum halb-immergrünen Tropenwald interpretiert werden.

Diese Arbeit trägt wesentlich zu einem besseren Systemverständnis des Wald-Savanne-Ökotons in Hinblick auf Waldnaturschutz und -management in der Nord-Guinea- und der Süd-Sudan-Zone in Westafrika bei. Zudem können die Daten als Grundlage für Langzeitstudien und Modellierungen der Dynamik des Wald-Savanne-Ökotons im CNP dienen.

1 Introduction

Global change is one of the most important causes that influence the loss of biodiversity around the world (Walker *et al.* 1999, Wolters *et al.* 2000, WBGU 2000). Two central processes of global change are the change in land use and climate change. Regarding the latter point, Thomas *et al.* (2004) recently predicted on the basis of mid-range climate-warming scenarios for 2050 considering about 20% of the Earth's terrestrial surface. Accordingly, about 15–37% of the species in the considered regions may become extinct as a result of shifts in species distribution and abundance. The second important process of global change, the change in land use, is currently taking place all over the world, but most strongly in the tropics (Turner 1996, Gascon *et al.* 2000, Fahrig 2003).

Tropical regions are the biologically most diverse areas in the world (e.g. Myers *et al.* 2000, Brooks *et al.* 2001, Küper *et al. in press*). Especially deforestation of tropical forests led to an enormous loss of intact natural habitats during the last century (Laurance *et al.* 1998, Laurance *et al.* 2001, Achard *et al.* 2002, Fearnside & Laurance 2003, Curran *et al.* 2004). Deforestation often occurs in heterogeneous patches and creates a landscape with fragmented forests. The threat of forest interior species by habitat loss, however, is then strengthened by island ecological processes (MacArthur & Wilson 1967, Cantrell *et al.* 2001, Lomolino & Weiser 2001, Fahrig 2003) and by edge effects as a result of an ecological transition zone between the two neighboring habitats (Laurance & Yensen 1991, Saunders *et al.* 1991, Murcia 1995, Laurance *et al.* 2002). Values for the depth-of-edge influence indicated in the literature range from meters (e.g. 0-6.5 m for canopy density, Didham & Lawton 1999) to kilometers (e.g. edge related fires, Cochrane & Laurance 2002).

In insular landscapes (Drake *et al.* 2002) – either created by humans, e.g. forest fragmentation, or by natural processes, e.g. soil patterns – ecologists face a fundamental challenge in understanding the structure and function of ecotones between neighboring habitats (Pickett & Cadenasso 1995, Kent *et al.* 1997). In this context, structural and functional aspects of ecotones can be distinguished as following:

- Structural aspects along ecotones are quantified in the literature by a wide range of different ecological parameters, from abiotic parameters, e.g. soil moisture and microclimate (Kapos 1989), to biotic parameters, e.g. species composition (Harper & Macdonald 2001) and vegetation structure (Matlack 1993).
- Concerning the functional aspects, an analogy of transition zones between two habitats to membranes in organisms or physical systems can be drawn where a selective flow

of material and energy occurs (Wiens *et al.* 1985, Risser 1995). Typical examples in the literature are the movement of animals (e.g. Schultz & Crone 2001, Holmquist 1998) and microclimate (e.g. Malcolm 1998).

These two aspects, however, are often interwoven. E.g. along the transition zone between forest and pasture the air temperature near the ground is directly influenced by the shading of trees (structural). In addition, air convection induced by differences in air temperature between the two habitats can result in a flow of energy (functional). This flow can be slowed down by the density of the vegetation (structural) at the border between the forest and the pasture. Thus, the air temperature measured at a location along a forest-pasture transect will be the result of an interaction of structural and functional aspects that are hard to distinguish (see Saunders *et al.* 1998 and Didham & Lawton 1999 as examples).

In tropical West Africa, most areas are profoundly altered by human activity (White 1983). In the Guinea zone in Ivory Coast, e.g., over 80% of the dense humid forest cover was cleared between 1900 and 1990 (Fairhead & Leach 1998, see also Chatelain *et al.* 1996a, Chatelain *et al.* 1996b). In many regions of the northern Guinea and southern Sudanian zone a patchy mosaic of tropical forests and savannas can be found (White 1983, Neumann & Müller-Haude 1999). In these regions, savanna formations are often interpreted as depredated formations of formerly closed deciduous and semi-deciduous forests that represent the respective climax stages (see reviews in Hopkins 1992 and Neumann & Müller-Haude 1999). But there is evidence from palynological studies that in the northern Guinea and Sudanian zone a mosaic of forests and savannas may have naturally coexisted long before human impact became stronger (Salzmann 2000). The study area of the present thesis was located in the protected areas of the Comoé National Park (CNP) in northeastern Ivory Coast (northern Guinea zone) where an mosaic of gallery forests, forest islands and savannas can be found (FGU-Kronberg 1979, Poilecot *et al.* 1991, Porembski 1991, Hovestadt *et al.* 1999).

BIOTA framework

BIOTA AFRICA (Biodiversity Monitoring Transect Analysis in Africa) is a cooperative, interdisciplinary and integrative research project with contributions from and in Benin, Burkina Faso, Germany, Ivory Coast, Kenya, Namibia and South Africa. The program was initiated in 1999 and is funded by the German Federal Ministry of Education and Research (BMBF). The project understands its activities as a contribution to the International Diversitas program, to the goals of the relevant UN conventions (UN 1992 and UN 1994) and to the Johannesburg Plan of Action of the World Summit on Sustainable Development (WSSD <http://www.iucn.org/wssd/>). The project aims at a holistic scientific contribution towards sustainable use and conservation of the biodiversity of the African continent. Goals of the project include the assessment of biodiversity changes by long-term monitoring, and causal

analysis with a focus on effects on biodiversity by anthropogenic land use and by climate change (compare <http://www.biota-africa.de>).

BIOTA AFRICA consists of three general parts in southern, East and West Africa. BIOTA WEST AFRICA aims to assess dimensions, spatial and temporal patterns, and functional roles of biodiversity in some of the most important African ecosystems (BIOTA West Africa 2003). During the pilot phase of the project (2001 - 2004), one center of research activity was set on ecosystems with a low human impact to gain reference data for the comparison of these sites with areas under stronger human impact that will be studied during the main project phase.

Ecotone concept and terminology

A landscape can be interpreted as a matrix of environmental gradients. Ecological theory assumes that the response of plant species to such environmental gradients leads to the formation of plant communities (overview in Kent *et al.* 1997 and Crawley 1997). Thereby, environmental gradients for single parameters may occur irregularly (steeply and flatly) or gradually, and plant species may show a response to gradients from linear to non-linear (thresholds) (Fagan *et al.* 2003). Gradients in plant-species composition will occur all over a landscape, but gradients will be especially strong and directed in the transition zone between plant communities (compare Fortin *et al.* 2000). The *border* between two habitats can be defined as a spatial locality where the magnitude of change is greatest (Fagan *et al.* 2003). In regard to plant communities the transition zone being associated with a border is called *ecotone* (Clements 1905, Leopold 1933, Griggs 1938), but the term *ecotone* is also used to describe transitional areas between vegetation zones on a continental scale (Kent *et al.* 1997). Van der Maarel (1990) distinguished between narrow and wide transition zones, *ecotones* and *ecoclines*. *Ecotones* may usually occur in man-made landscapes, and *ecoclines* can frequently be found as natural transition zones between plant communities (van der Maarel 1990, Kent *et al.* 1997). Following Wiens *et al.* (1985), the term *boundary* addresses functional aspects and dynamic processes at the transition zone between two habitats, but the terms *boundary* and *ecotone* are frequently used synonymously in the literature. In the present thesis the term *ecotone* is used to describe the transition zone between forests and savannas for both vegetation data and environmental data. The width of an *ecotone* can be marked as the area where considered parameters differ from both habitats (non-ecotone zones). Here, the borders of the *ecotone* are termed *ecotone limits* and, for reasons of simplicity within statistic analysis, conditions in non-ecotone zones are assumed to be homogeneous (non-directed gradients). The zone of *edge effects* and *depth-of-edge influence* (DEI) towards one of the two habitats describes the distance from the border to the respective limit of the *ecotone*.

Topics of the present thesis

The present thesis comprises four topics. The first deals with the methodological lack of statistic analyses of transect data along ecotones for both single parameters (e.g. grass biomass) and multivariate data sets (e.g. vegetation composition). Therefore, a focus is set on the development of new sets of analyses for border and ecotone detection (see Chapter 2.5 and 2.6.4).

The second topic treats the detection of borders and ecotones along forest-savanna transects and the detection of the depth-of-edge influence (DEI) towards the forest interior. On this, the new sets of analyses are applied to structural vegetation parameters and soil depth (Chapter 3.1), surface biomass in connection with occurrence of surface fires (Chapter 3.2), microclimatic parameters (Chapter 3.3), and multivariate vegetation data (Chapter 3.4).

The third topic addresses the calculation of core areas of forest islands in the study area. For this purpose, the gained knowledge on DEI towards the interior of the studied forest islands (second topic) is related to remaining forest core areas (Chapter 3.5).

The fourth topic deals with successional processes at the forest-savanna ecotone. Therefore the distribution of tree-size classes along forest-savanna boundaries are analyzed with a focus on the pioneer tree species *Anogeissus leiocarpus* (Chapter 3.6).

The topics addressed above are introduced and treated separately in the following six subchapters (Chapter 1.1 – 1.6).

1.1 Transect analysis

1.1.1 Transect analysis of univariate data

During the last decades a large number of studies has been published concerning the detection of borders and associated ecotones along ecological gradients especially in fragmented landscapes (see overview in Murcia 1995, Baker & Dillon 2000, Laurance *et al.* 2002). Knowledge on the depth-of-edge influence (DEI) into the habitat of interest is necessary to calculate its core area (Laurance & Yensen 1991, Fernandez *et al.* 2002). The majority of boundary studies in the literature present univariate parameters such as microclimatic parameters (Kapos 1989, Didham & Lawton 1999), vegetation structure (Matlack 1993), species richness and abundance of single species (Demaynadier & Hunter 1998, Harper & Macdonald 2002), as well as sample scores of the first axis of a detrended correspondence analysis (DCA) computed from a multivariate species data set (Lloyd *et al.* 2000, Walker *et al.* 2003). Analyses that were applied to detect the DEI are various. In general, they can be divided into two groups. (i) The first group comprises techniques that use transect replicates as replicates in the analysis itself. Typical approaches are analysis of variance and generalized

linear modeling (Honnay *et al.* 2002), nested analysis of covariance (Rheault *et al.* 2003), and randomization procedure (Harper & Macdonald 2001). Measurements of DEI are given as a single value for all transects included in the analysis. (ii) The second group contains techniques that analyze each single transect on its own. This yields DEI values for each transect and the variability between transects can be calculated. Thus, in general, the second group of analyses reveals more information than the first one. Examples are non-linear regression analysis (Brand & George 2001, Saunders *et al.* 1999) and piecewise linear regression analysis (Matlack 1993, Newmark 2001, Toms & Lesperance 2003). Especially piecewise linear regression analysis is a powerful tool, but it requires a rather high number of sampling points in each regression section along transects (Toms & Lesperance 2003).

In Chapter 2.5, a border-and-ecotone-detection analysis (BEDA) based on non-linear regression analysis is presented. The location of the border between habitats, the two limits of the associated ecotone, and finally the DEI, are calculated from the coefficient estimates of the model. In addition, confidence intervals for all calculated parameters are derived.

1.1.2 Transect analysis of multivariate data

Several multivariate methods have been developed to detect borders along ecological gradients, e.g. split-moving-window dissimilarity analysis (SMWDA) (Ludwig & Cornelius 1987, Cornelius & Reynolds 1991), Womble-methods (Jacquez *et al.* 2000, Fagan *et al.* 2003), and wavelet methods (Csillag & Kabos 2002, Bradshaw & Spies 1992). Kent *et al.* (1997) state that the moving-window analysis may have the greatest potential in the analysis of floristic data across transitional areas. For SMWDA, Cornelius & Reynolds (1991) provided a test statistic to decide whether a detected border is significant or not. However, regarding the width of associated ecotones, no standard method is available for multivariate data. One reason for this might be that – as ecotones are continuous by nature – no strictly objective measurement of the DEI is possible, but the selection of a criterion to define the limits of an ecotone is a subjective decision (Chen *et al.* 1996). To characterize the width of ecotones, Walker *et al.* (2003) recently used moving-window regression analysis (MWRA) along a coastal vegetation gradient in New Zealand.

In order to develop a methodologically coherent set of analyses, SMWDA and MWRA were combined in Chapter 2.6.4 to detect the significance of borders in multivariate data along continuously sampled transects and to determine the width of the associated ecotones.

1.2 Biomass and surface fires along forest-savanna ecotones

Fire is an important factor for the existence of savannas in general (Huntley *et al.* 1982, Bourlière 1983, Goldammer 1990, Scholes & Archer 1997, van Langevelde *et al.* 2003), and

its paramount importance has to be stressed especially for the distinctive physiognomy of humid savannas in West Africa (Swaine *et al.* 1992, Hochberg *et al.* 1994, Couteron & Kokou 1997, Gignoux *et al.* 1997) where fire exclusion experiments have yielded closed forest stands within 30-60 yr (Ramsey & Rose Innes 1963, Swaine *et al.* 1992, Louppe *et al.* 1995). Thus, fire plays an important role for the co-occurrence of forests and savannas that can be found in many West African regions (White 1983, Salzmann 2000, Salzmann *et al.* 2002).

Surface-fire probability and surface-fire intensity in savannas are strongly related to the amount of grass biomass as fuel (Stocks *et al.* 1996, Stott 2000). In West Africa, distribution pattern of forests and savannas are often explained by topography and water supply (e.g. Menaut & César 1979, see Chapter 2.1.3). Drier conditions on hilltops lead to a lower grass productivity and a lower fire probability that favors tree establishment. Thus, forest patches more likely occur on hilltops than on intermittently wetter slopes with a stronger fire influence where savannas dominate. In depressions, grasslands can be found, whereas watercourses are fringed by gallery forests. In accordance with this general description, Augustine (2003) showed in a semi-arid savanna in central Kenya that biomass of the herb layer declined from lower to upper topographical positions.

In this context, the impact of fire on vegetation dynamics in the transition zone between tropical forests and savannas is of particular interest, because these dynamics may influence the proportions of forest and savanna (Hennenberg *et al. in press*, Chapter 4.6). E.g., along gallery forest-savanna boundaries in Belize and Venezuela, Kellman & Meave (1997), Biddulph & Kellman 1998, and Kellman *et al.* (1998) found that surface fires were mostly prevented from penetrating the gallery forest by changes in fuel characteristics at the forest boundary.

In Chapter 3.2 data on (i) surface biomass with a focus on grass biomass along transects from savanna to the interior of forest islands are presented. (ii) Grass biomass production is related to environmental parameters. (iii) The depth-of-edge influence (DEI) towards the forest is computed in regard to grass biomass, and these values are compared with fire occurrence. (iv) The amount of grass biomass that is necessary for ignition is assessed.

1.3 Microclimate along forest-savanna ecotones

Since the 1940s, the role of microclimatic conditions has often been stressed concerning the growth and establishment of plants along forest borders and, thus, as a determining factor for vegetation composition along such gradients (Oosting & Kramer 1946, Kapos 1989, Matlack 1994, Williams-Linera *et al.* 1998). A physiological response of plants along microclimatic gradients at forest boundaries was shown, e.g., for $\delta^{13}\text{C}$ uptake of an understory species (Kapos *et al.* 1993) and transpiration of tree individuals (Giambelluca *et al.* 2003).

For microclimatic data measured during short time periods, Chen *et al.* (1995), Saunders *et al.* (1999) and Newmark (2001) showed that microclimatic conditions along forest boundaries varied with time of the day, but the annual variation was rarely investigated (e.g. Young & Mitchell 1994). In addition, Murcia (1995) pointed out that many boundary studies failed to select appropriate transect replicates. This ongoing problem is especially true for microclimatic studies where a high measuring expenditure is required (e.g. Didham & Lawton 1999 [four times $n = 1$], Davies-Colley *et al.* 2000 [$n = 1$], Redding *et al.* 2003 [$n = 1$]).

In Chapter 3.3, microclimatic parameters are presented that were recorded along eight forest-savanna transects from the peak of the dry season until the peak of the rainy season in 2002. The main aim of this chapter is to detect the DEI towards the interior of the studied forest islands and its seasonal variations on the basis of microclimatic parameters.

1.4 Vegetation composition along forest-savanna ecotones

The occurrence of vegetation types along ecological gradients as a response of a multiple set of species to a multiple set of environmental parameters is well known (Whittaker 1967). Typical examples are gradients of altitude (Vazquez & Givnish 1998) and salinity (Adam 1990). To explain patterns of ecotone and non-ecotone zones regarding species composition, Kent *et al.* (1997) combined the single environmental gradient model of Whittaker (1953, ‘climax pattern hypothesis’) and the ‘hierarchical continuum model’ of Collins *et al.* (1993, see details in Fig. 1.1). The main idea of this concept is that single species show specific responses along environmental gradients in combination with their different abilities to build up abundant populations in a region.

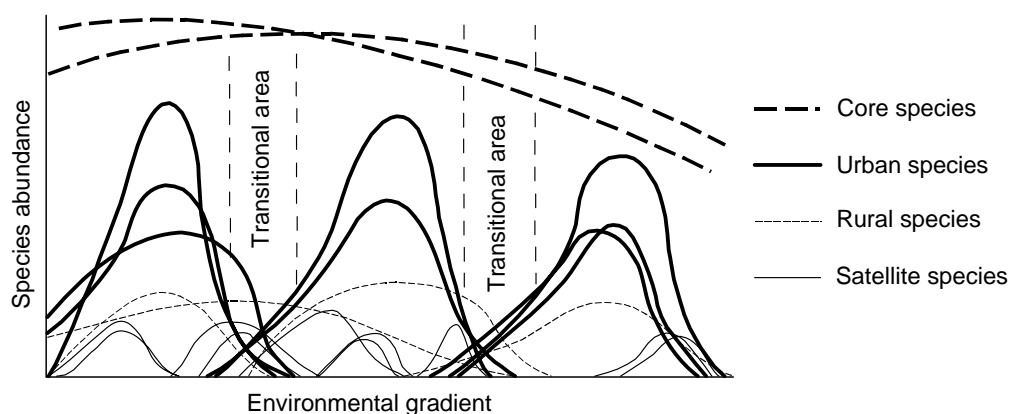


Fig. 1.1. The hierarchical continuum model (Collins *et al.* 1993) combined with the climax pattern hypothesis (Whittaker 1953) expressed as species response curves along a single environmental gradient (modified from Kent *et al.* 1997). Core species: species that are widely distributed across the region with high abundance; urban species: species with limited distribution but high abundance when they occur; rural species: species with widespread distribution but low abundance when they occur; satellite species: species with limited distribution in the region and low abundance.

For most vegetation parameters recorded in the field in respect to forest boundaries, a DEI has been estimated to be 60 m or less (reviews in Murcia 1995, Didham & Lawton 1999, Baker & Dillon 2000, and Laurance *et al.* 2002). Most of the studies were carried out at boundaries of temperate forests and mainly processed univariate data. Instead, ecotone studies that are based on multivariate plant-species data from tropical forests have not been conducted so far, though plant communities as a whole are well suited as they are an integral indicator for many ecological factors and processes that have been effective at a site, and changes in plant species composition along ecotones should reflect their gradients.

In Chapter 3.4, the combination of SMWDA and MWRA is applied to detect significant borders and associated ecotones along forest-savanna transects by means of vegetation composition. In addition, the DEI towards the forest interior is determined.

1.5 Core-area analysis

The size of forest-core areas is a central issue in the protection of forest-interior species at the landscape scale in both natural forest islands and anthropogenic forest fragments (Saunders *et al.* 1991, Drake *et al.* 2002, Fahrig 2003). Especially in the tropics the loss of forest-core area due to deforestation and increasing edge effects at the remaining forest fragments is one of the major causes of the general biodiversity decline (Laurance *et al.* 1998, Turner 1996).

From field data it became evident that the DEI can differ strongly between parameters (e.g. taxa, abiotic variables, ecological processes), forest types, forest-edge types, forest geometry, and the surrounding matrix (Murcia 1995 and Laurance *et al.* 2002). Respective knowledge on the DEI towards the forest interior can be used to approximate the forest-core area (Laurance & Yensen 1991, Chen *et al.* 1992, Fernandez *et al.* 2002), a parameter that is essential for forest management in insular landscapes (Gascon *et al.* 2000, Putz *et al.* 2001). Surprisingly, only two studies were found in the literature that did not use oversimplified core-area models (e.g. Laurance & Yensen 1991), but carried out a core-area analysis on forest fragments using GIS implements (Ranta *et al.* 1998, Russell & Jones 2001).

In the utilized regions south of the CNP on areas potentially covered by forest, Goetze *et al.* (*unpublished manuscript*) determined from remote-sensing data a deforestation rate averaging 40% that dominated over a reforestation rate of 14% during a 14-year time span (1988-2002). In contrast, de- and reforestation were almost absent from the studied area inside the CNP. This stresses the necessity of management of forests outside the CNP.

Referring to the DEI measured for various parameters (Chapter 3.1 – 3.4), the core area of forest islands of the studied forest type is computed for various DEI in Chapter 3.5. In addition, the minimal size of a forest island to contain a relative core area of at least 50% is determined.

1.6 Dynamics of forest-savanna ecotones

Throughout the Sudanian and Guinea region of West Africa, forest islands consisting of deciduous and evergreen tree species embedded in savannas are often interpreted as forest relicts of formerly continuous forests, and savannas as sites that are degraded by human activity (e.g. Aubréville 1949, Keay 1949, Chevalier 1951, Knapp 1973, Walter 1979, Anhof & Frankenberg 1991, Hopkins 1992, and Anhof 1994). This holistic ‘forest degradation hypothesis’ assumes the existence of a ‘climax stage’ as a final ecosystem of maximum stability in a succession process (Finegan 1984, McCook 1994). More recent interpretations of ecological systems reject the view of an inherent stability of ecosystems in favor of non-equilibrium and stochastic views (Gibson 1996, Perry 2002). Studies that emphasize sociological topics (Fairhead & Leach 1996) even claim humans as being responsible for the establishment of new forest islands for some areas in the Guinea region. For the Sudanian and northern Guinea zone in Nigeria, Keay (1959b) assumes that moist forest, savanna woodland, and transition woodland might have coexisted as a result of the interaction of climate and site conditions for a long time before human impact has become stronger. Palynological studies also support this view. In the Sudanian zone in northeastern Nigeria, for example, savanna vegetation and frequent fire occurred throughout the last 11.000 years. This leads to the conclusion that continuous dry or semi-deciduous forest has never completely displaced savanna vegetation (Salzmann 2000, Salzmann *et al.* 2002). Thus, the ecotone between forest and savanna can be interpreted to be a common natural element of the West African landscape. Assuming that forest and savanna co-occurrence has included dynamic processes and has taken place over long time periods, varying patterns of disappearance or shrinking and establishment or enlargement of forest islands in savanna by sequential succession (McCook 1994) would be expected to be a characteristic of this forest-savanna ecosystem. Such dynamics should particularly be observable in the forest-savanna ecotone (Gosz 1991).

For the northern Guinea and Sudanian zone, several authors documented a high abundance of *Anogeissus leiocarpus* (DC.) Guill. & Perr. (Combretaceae), a large deciduous tree, at forest borders (e.g. MacKay 1936, Letouzey 1969, Sobey 1978, Poilecot *et al.* 1991). Nansen *et al.* (2001) and Neumann & Müller-Haude (1999) point out that *A. leiocarpus* may play an important role in forest succession. In regard to successional processes, three questions are stressed in this thesis: (i) Do forest islands spread into savanna by sequential succession? (ii) Can monodominant *A. leiocarpus* stands be interpreted as a successional stage in the succession from savanna to forest? (iii) Which sites are favorable for the regeneration of *A. leiocarpus* compared to other dominant tree species?

To answer these questions, results obtained along forest-savanna transects and within one monodominant *A. leiocarpus* stand are presented in Chapter 3.6. Data refer to structural

vegetation parameters, distribution patterns of tree individuals with a focus on *A. leiocarpus*, regeneration of dominant tree species in the shade of *A. leiocarpus*, and regression analysis of offspring of dominant tree species and environmental parameters.

2 Material and Methods

2.1 Study area

The study was carried out in an area of 80 km² (8°47' - 8°41' N and 3°51' - 3°47' W) in the southwestern part of the Comoé National Park (CNP, Fig. 2.1). The study area is located in the plateau of the 'Massif de Pahradi' (Arnould 1961) and belongs to the water catchments of the Comoé river.

The CNP in northeastern Ivory Coast (Fig. 2.1) has an extension of 11,500 km² and is the largest national park in tropical West Africa. The section east of the Comoé river was protected as a game reserve since 1926 ('Refuge Nord de la Côte d'Ivoire') that was extended as the 'Réserve Totale de Faune de Bouna' in 1953. In 1968, the Comoé National Park was established including forest areas west of the Comoé river (Poilecot *et al.* 1991). The CNP was internationally approved in 1983 and declared as Biosphere Reserve und World Nature Heritage by the UNESCO.

Important human impacts in the CNP are nowadays uncontrolled annual burning of the savanna and poaching. Annual dry-season fires mainly occur in savannas and seldom enter dense forests. Most fires occur until the peak of the dry season in February (Lauginie 1995). A strong increase of poaching during the last 15 years has led to a dramatic decrease of wild animals, especially of large herbivores and top predators (Fischer & Linsenmair 2001). E.g., for the park area, populations of elephants and lions are almost extinct today. When the CNP was installed, all settlements were transferred to the outside of the protected area. As a result of the low value of soils in the CNP for cultivation and a high density of tsetse flies the population density of humans has already been relatively low before park installation (Lauginie 1995).

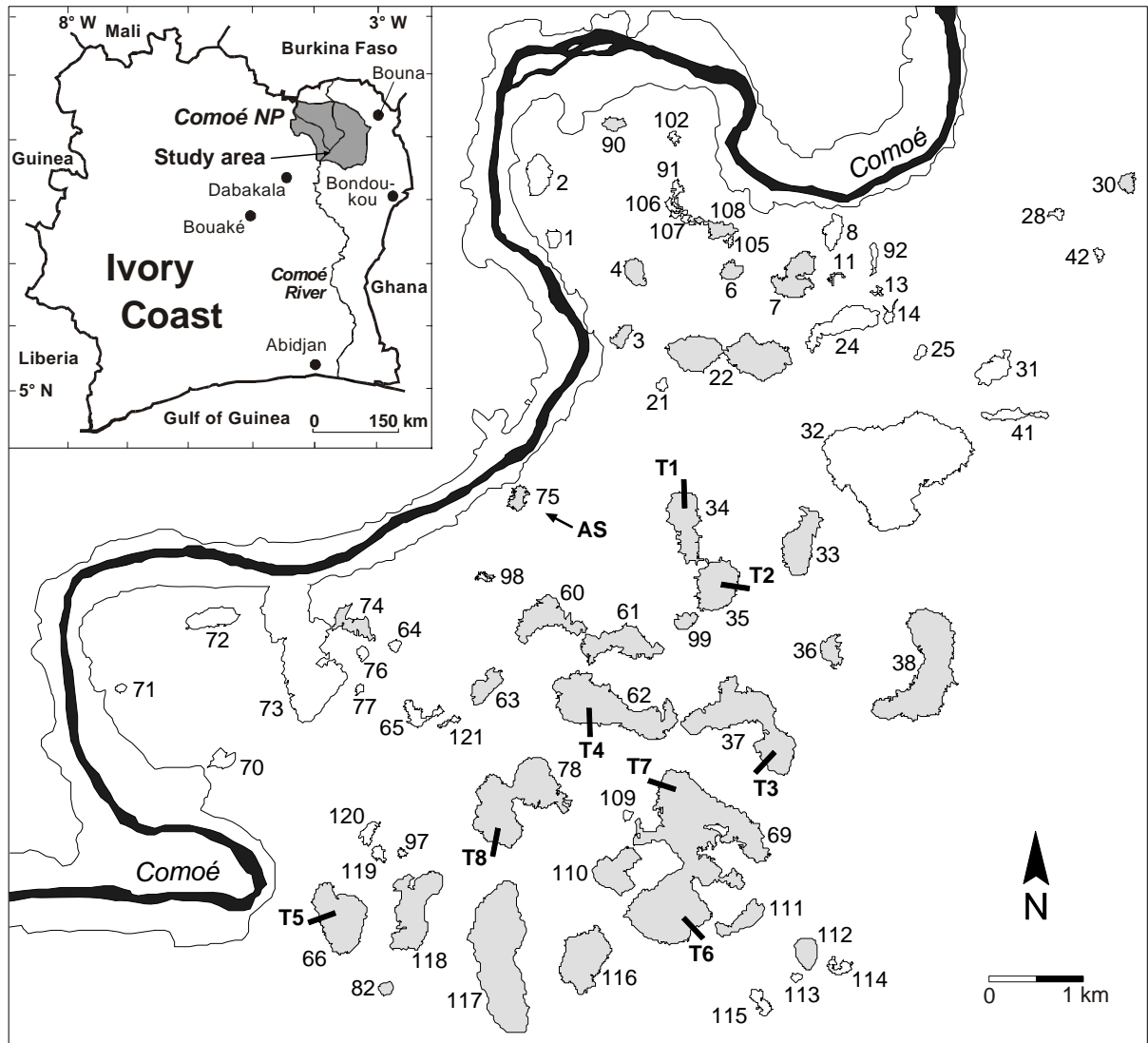


Fig. 2.1. Map of the study area in the southwestern part of the Comoé National Park (CNP), Ivory Coast, West Africa. Presented are forest islands larger than 0.5 ha that were mapped with a handheld GPS. The location of the Comoé river (black) and the borderline of the gallery forest were digitized from a satellite image (Landsat ETM+ image from December 2002). Gallery forest and forest islands that did not belong to the studied type of semi-deciduous forest are shown in white color. Studied forest islands were colored light-gray. Location of the eight studied forest-savanna transects (T1-T8) are marked with black bars. The numeration of forest islands is in accordance with Hovestadt *et al.* (1999). AS = monodominant *Anogeissus leiocarpus* stand (number 75).

2.1.1 Climate

The study area in the southern part of the CNP is located in the humid warm tropics (Lauer & Rafiqpoor 2002). Total annual rainfall measured at the climate station of the research camp of the University of Würzburg in the southern part of the CNP ranged from 856 to 1,248 mm (study period: 1993 – 2000, Fischer *et al.* 2002, see Fig. 2.2) and the annual mean temperature is about 26.5 to 27 °C (Ojo 1977). In connection with the south-north motion of the sun during the first half of each year the inter-tropical convergence zone (ITCZ) moves from its position near the equator north-ward to higher latitudes causing the onset of the rainy season (Ojo 1977). In consequence, the rainy season is influenced by the south-west monsoon, a

humid air stream blowing from the Gulf of Guinea (McGregor & Nieuwolt 1998). At the climate station in the CNP, about 90% of the annual rainfall occurred during the rainy season from March to October in most years (Fischer *et al.* 2002). This is in accordance with the rainfall distribution at the climate stations near the CNP in Bondoukou, Bouna, and Dabakala (Fig. 2.2). Fluctuations in daily temperature and humidity are low during the rainy season. At the beginning of the dry season, the south motion of the ITCZ leads to dry winds ('Harmattan') blowing from northeast (central Sahara). The dry season is characterized by high daytime temperatures (33 to >40 °C), rather cool nights (10 to 15 °C), and occasionally very low relative humidity (<10%).

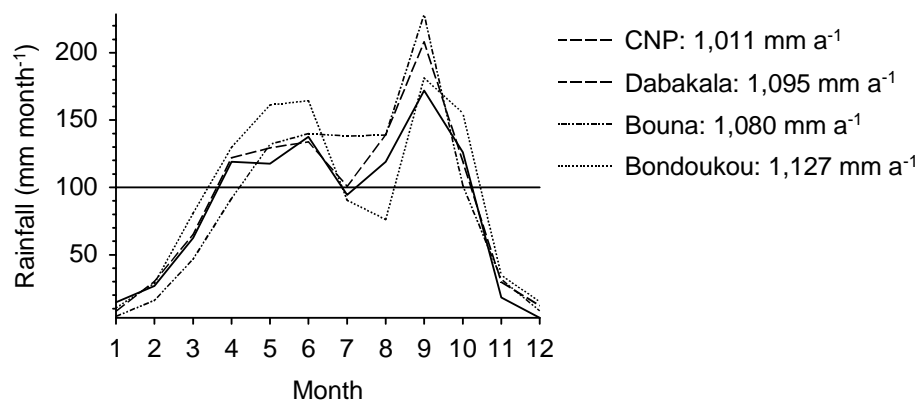


Fig. 2.2. Mean monthly and mean annual rainfall for three climate stations in northeastern Ivory Coast (compare Fig. 2.1) and for the climate station at the research camp of the University of Würzburg in the southern part of the CNP (Fischer *et al.* 2002). CNP: 1993-2001; Bondoukou: 1937-1980, 1984-1998; Bouna: 1921-1981, 1983-1987, 1990-1992, 1994, 1996-1997; Dabakala: 1923-1996. Data source for Bondoukou, Bouna, and Dabakala: Météorologie National, CI, FAO.

2.1.2 Geology and soils

The study area (about 220 m a.s.l.) is marked by a gently undulating relief with slope inclinations of normally less than 4%. According to Fölster (1983), this landscape type is a pediplain (compare Fig. 2.3). During the tertiary, ferricrests were formed in inland valleys, but as a result of their resistance against erosion, today, ferricrests can often be found on top hills (relief inversion, see Maignien 1966).

The study sites are located above Precambrian granites (Méagranite à biotite of the Rhyacien inférieur à moyen of the Birimien, Direction des Mines et de la Géologie 1995). According to Perraud (1969 in Poilecot *et al.* 1991), Ferralsols with a medium cation exchange capacity predominate in the southern part of the CNP, but also hydromorphic soil types occur especially in inland valleys (Poilecot *et al.* 1991).

Along three of the eight studied transects (T1, T4, and T7 in Fig. 2.1), soils samples were studied by Kersting (2003) with a focus on physical soil properties. In general, forest sites

were characterized by sandy loam with a higher pH of about 6.6 and higher organic content (1.9%) than sites in the savanna (sandy loam, pH of about 5.3, organic content of about 0.7%). Along the topographical gradient, forests were located on hilltops and savannas along slopes and in inland valleys (see Fig. 2.3). Forest sites were shallow with a soil depth of 30-60 cm above ferricrests (9.9% skeleton), whereas savanna sites mostly showed a soil depth of more than 200 cm (2.7% skeleton). But also at some locations shallow soils on ferricrests occurred in the savanna.

2.1.3 Vegetation

West Africa is characterized by a steep rainfall gradient from south to north with annual rainfall above 2,000 mm in the south (Abidjan, Ivory Coast: 2,144 mm; Monrovia, Liberia: 4,624 mm) and below 300 mm in the north (Goa, Mali: 270 mm) (Sträßer 1998). Along this climatic gradient a gradual change in the vegetation cover from evergreen rainforests to desert vegetation can be observed (Aubréville & Keay 1959, Keay 1959a, Eldin 1971, Guillaumet & Adjanohoun 1971, Knapp 1973, White 1983, Le Houérou 1989, Adjanohoun 1989). Regarding West Africa, vegetation maps and classifications provided by the above cited authors are mainly in accordance for the northern (Sahara, Sahel) and the southern zones (lowland rainforest). But in between, the classification is rather heterogeneous (see also Lawesson 1994 and Salzmann 1999). E.g., the study area in the southwestern part of the CNP is located in the 'sub-Sudanian sector' of the 'Sudanian domain' (Eldin 1971) and in the northern part of the 'Guineo-Congolian/Sudanian regional transition zone' (White 1983). This region is characterized by a mosaic of savannas and tropical deciduous and semi-deciduous forests. In addition, extra-zonal vegetation types can be found, e.g., on inselbergs and along rivers as gallery forests (Porembski 1991, Porembski 2001, Krieger *et al.* 2003). In the present thesis a nomenclature following Keay (1959a) is applied (northern and southern Sudanian zone, northern and southern Guinea zone), according to which the study area is located in the northern Guinea zone.

In terms of phytogeography, the study area is part of the African subkingdom of the Palaeotropical region, wherein Takhtajan (1986) classifies the study area as belonging to the 'Sudanian province' of the Sahelo-Sudanian subregion (Sudano-Zambezian region). Important genera of the Sudanian province include *Anogeissus* and *Terminalia* (Combretaceae), and *Andropogon* and *Hyparrhenia* (Poaceae).

As already stressed in Chapter 1.2, vegetation types from grass savanna to forest in the northern Guinea zone were often described to occur along topographical gradients (Spichiger & Pamard 1973, Menaut & César 1979, Fournier *et al.* 1982, Menaut & César 1982). Deciduous and semi-deciduous forest can often be found on hilltops that are influenced by ferricrests (Fig. 2.3, compare Chapter 2.1.2), also shown by soil studies in the CNP (Kersting 2003). The distribution pattern of vegetation types along the topographical gradient is

supposed to be caused by an interaction of factors such as soil-water availability, tree-grass competition, and fire as already discussed in Morison *et al.* (1948) for the Sudan. But also agricultural activities must be considered as a factor because sites on slopes are often more favorable for cultivation compared to sites on hilltop and in inland valleys (Hahn-Hadjali 1998, Neumann & Müller-Haude 1999).

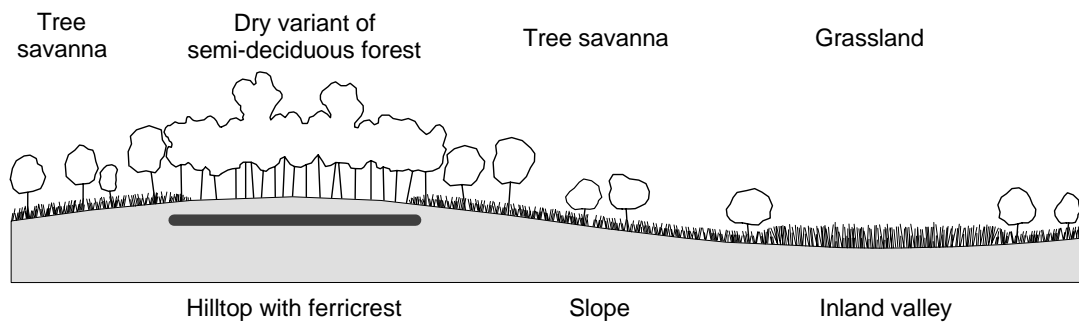


Fig. 2.3. Idealized model of the vegetation distribution along a topographical gradient of a pediplain according to soil studies in Kersting (2003).

The semi-natural forest-savanna mosaic of the southern CNP includes different savanna types (grass savanna, tree savanna, savanna woodland, woodland; 85% of the area), gallery forest (2.3%) and dense forest islands (8.4%) (FGU-Kronberg 1979, see Fig. 2.4). The savanna types are characterized by a continuous grass stratum that is typically absent from forest islands and gallery forests (C.S.A. 1956). In the study area, the size of the forest islands varies between less than 0.5 ha and up to 200 ha. A comparison of aerial photographs from 1954 and 1996 revealed that the borderlines of forest islands to the surrounding savanna remained mostly unchanged during this 42-year period and that the forest interior had a closed canopy also in 1954 (Goetze *et al.*, unpublished manuscript).

According to Poilecot *et al.* (1991) the forest islands in the southwestern part of the CNP can be classified as a less diverse variant of dense humid semi-deciduous forest of the *Celtis* spp. and *Triplochiton scleroxylon* type (Guillaumet & Adjanohoun 1971). Especially tree species of the upper tree layer of this forest type (e.g. *Ceiba pentandra*, *Celtis zenkeri*, *Cola cordifolia*, and *Milicia exelsa*) shed their leaves during the dry season whereas many tree species of the lower tree layer (e.g. *Diospyros abyssinica*, and *Drypetes floribunda*) stay foliated during the dry season. The forest islands are mostly surrounded by tree savannas that are characterized by tree species such as *Crossopteryx febrifuga*, *Daniellia oliveri*, *Detarium microcarpum*, *Lophira lanceolata*, and *Terminalia macroptera* (Poilecot *et al.* 1991).

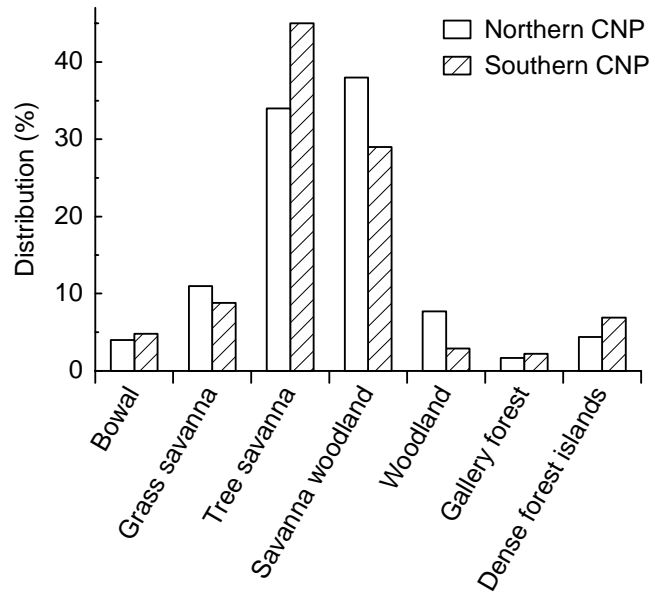


Fig. 2.4. Distribution of dominant vegetation types in the northern and southern part of the CNP. Data source: FGU-Kronberg 1979:68. Nomenclature of vegetation types follows C.S.A. (1956). Bowal = grass savanna on ferricrest.

2.1.4 Characteristics of *Anogeissus leiocarpus*

The genus *Anogeissus* (Combretaceae) with its eight species shows a paleotropical distribution (Mabberley 2000), whereas the family of the Combretaceae is pantropically distributed (Heywood 1998). In West and East Africa, *Anogeissus leiocarpus* colonizes the Guinea and Sudanian domain (Wickens 1976). White (1983) describes *A. leiocarpus* as a typical element of woodlands and savannas of the Sudanian regional center of endemism. From the northern Guinea zone up to the Sahelian zone, the deciduous species can be found in savannas, dry forests, and gallery forests (Couteron & Kokou 1997, Hahn-Hadjali 1998, Neumann & Müller-Haude 1999, Müller & Wittig 2002). It can grow up to a height of 15-18(-30) m (Arbonnier 2000). The crown is mostly sparse (Neumann & Müller-Haude 1999). Fruits of *A. leiocarpus* contain about 40 wind dispersed seeds of 10 mg each (Hovestadt *et al.* 1999) that germinate under high-light conditions, and a seed bank is absent (Orthmann *et al.*, *in prep.*). In accordance with Swaine & Whitmore (1988), *A. leiocarpus* is to be classified as a pioneer species. However, with up to 166 year (dbh of about 80 cm), the lifecycle of the individuals of *A. leiocarpus* appears to be comparatively long compared to other pioneer tree species (Schöngart *et al.*, *in prep.*), and tree individuals larger than 30 cm dbh show a significantly higher seed production than smaller ones (Orthmann *et al.*, *in prep.*).

2.2 Sampling design

In the study area in the southwestern part of the CNP, the borderlines of 68 forest islands were mapped with a hand-held GPS (GPS 12, GARMIN International, Inc., Kansas, USA) and the

data were entered in a geographic information system (ArcView GIS 3.2, see Fig. 2.1). Thirty-one of the mapped forest islands were classified as a dry variant of the semi-deciduous forest islands (compare tree inventories in Hovestadt *et al.* 1999). For transect analysis, seven large forest islands (number 34, 35, 37, 62, 66, 69, and 78 in Fig. 2.1, size of 21 – 146 ha) of this forest type were selected where the distance from the forest border to the forest interior was at least 200 m.

Perpendicularly to the forest border, eight transects (T1-T8) from the savanna towards the forest interior were installed, one transect at each forest island, except the largest forest island which had two (number 69 in Fig. 2.1). To assure standardized conditions, at both sides of the transects the forest border had to be as straight-lined as possible and distances between endpoints of different transects had to be at least 1 km. From those locations matching the criteria, transect positions were selected randomly. The northern and southern part of the largest forest island were treated as two islands (Transect T6 and T7, Fig. 2.1). The transect T4 was studied with a higher intensity than the other 7 transects and is named intensely studied transect (IST).

Each transect was divided into three sections: savanna, forest belt, and closed forest (Fig. 2.5). The borderline between savanna and forest belt was clearly demarcated by a higher cover of grasses in the savanna and a change in grass species composition. Distance measurements refer to this borderline (0 m). In direction of the forest interior, a second borderline was visible that was used to distinguish forest belt from closed forest. This borderline was demarcated by a higher density of shrubs in the forest interior. The width of the physiognomic forest belt differed between transects from 10 to 60 m (compare Table 3.4). The length of closed forest and savanna sections of the transects varied in dependence on the studied parameters from 105 to 200 m, and the transect width also varied from 10 to 50 m. Transects were sampled continuously or discontinuously (Fig. 2.5). Regarding the sampling scheme in Fig. 2.5 d, each transect was divided into five segments: savanna (Sav), savanna ecotone (S-Eco), belt ecotone (B-Eco), forest ecotone (F-Eco), and forest (For). To attain a higher resolution near the forest border, the transect segments S-Eco, B-Eco and F-Eco were subdivided into three sub-segments (Fig. 2.5 d).

In addition to the transects, one forest island with a monodominant upper tree layer built by *Anogeissus leiocarpus* (AS = *Anogeissus* stand, forest 75 in Fig. 2.1) was selected (compare Fig. 3.20). Within this 4-ha stand, remainders of old walls and broken pieces of crockery were found, indicating settlement before the CNP was established. According to local information, the settlement was an outpost of the village Kakpin 15 km towards the south and human population density had been very low. At 30 random sample points, the T-square procedure was applied to measure densities of different diameter classes of *A. leiocarpus* (see Chapter 2.3.2). To characterize this stand, environmental and structural vegetation data (see Chapter 2.3.1) were collected at 14 randomly chosen 4 m * 4 m plots (Fig. 3.20).

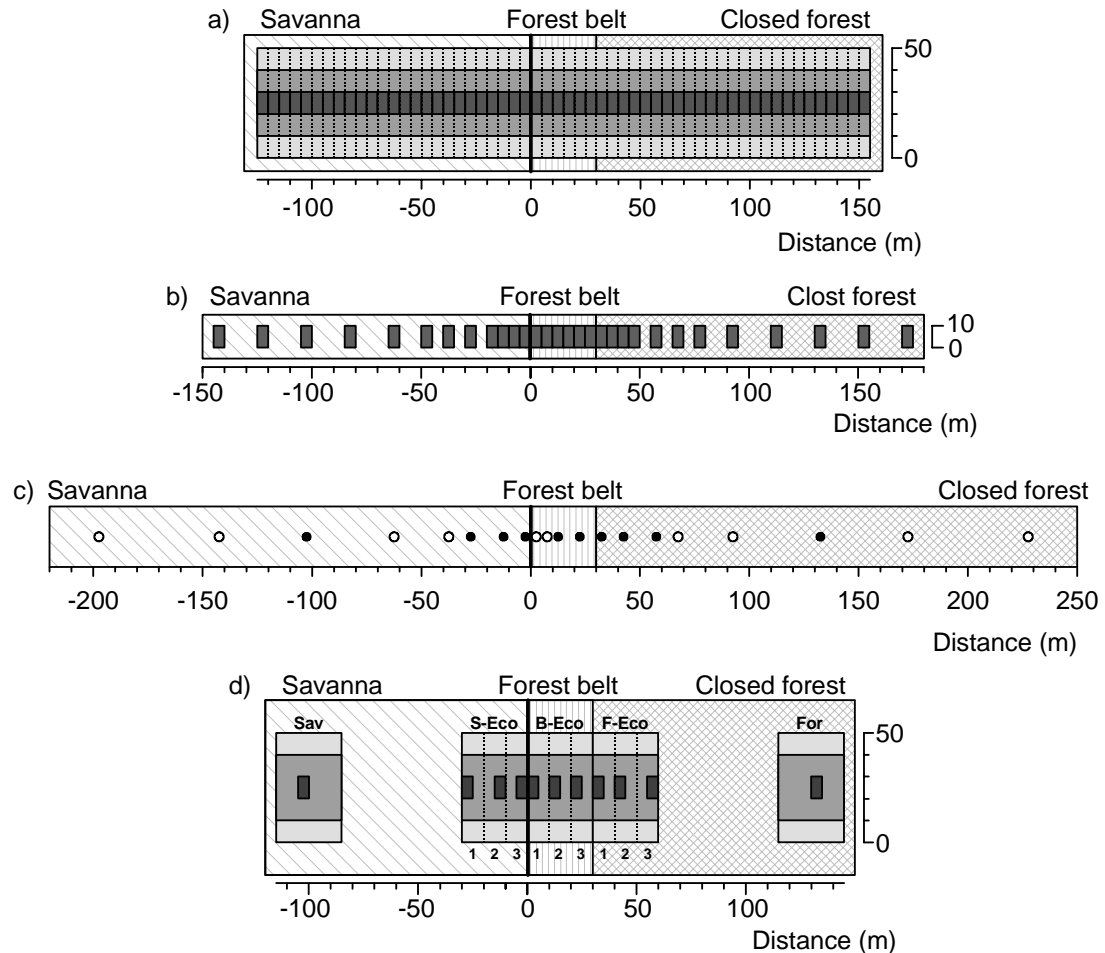


Fig. 2.5. Sampling designs along forest-savanna transects being adapted to the respective study parameters. a) Continuous sampling of vegetation data in 64 plots in 5 m steps (width of 10 m: relevés, trees and shrubs > 1 cm dbh; width of 30 m: trees and shrubs > 10 cm dbh; width of 50 m: trees > 20 cm dbh), b) discontinuous sampling (structural vegetation parameters, soil depth) c) discontinuous sampling of microclimatic parameters (compare Chapter 2.4.1), d) reduced sampling of vegetation data (width of 10 m: all tree and shrub individuals, structural vegetation parameters, soil depth; width of 30 m trees and shrubs > 10 cm dbh; width of 50 m: trees > 20 cm dbh); Sav = savanna segment, S-Eco = savanna-ecotone segment, B-Eco = belt-ecotone segment, F-Eco = forest-ecotone segment, and For = forest segment.

2.3 Sampling of vegetation

Plant species were determined according to Hutchinson *et al.* (1954-1972). Additional literature was Arbonnier (2000) for tree species and Poilecot (1995) for Poaceae. Nomenclature of species follows Lebrun & Storck (1991-1997).

2.3.1 Vegetation structure and composition

Structural vegetation parameters were recorded from September to October in the rainy season 2001. The vegetation was divided into five growth forms: grasses, herbs, shrubs, trees and woody climbers. According to BIOTA standards, total cover and the cover of seven vegetation strata (0-0.5 m, 0.5-1 m, 1-2 m, 2-5 m, 5-10 m, 10-20 m, and >20 m) were

estimated for each growth form as well as total cover of each vegetation stratum and total vegetation cover for a whole plot. Cover was estimated according to the decimal scale of Londo (Dierschke 1994), considering all leaves reaching into the plot. In addition, total cover of grass litter, herb litter, and leaf litter was estimated and the maximum height of grasses and herbs was measured.

The structural vegetation parameters were taken for all transect plots of 5 m * 10 m in size, (Fig. 2.5 a, b, and d) and for the 14 random plots (4 m * 4 m) in the *Anogeissus* stand (Fig. 3.20). Along the intensely studied transect (T4), cover of all species was estimated according to the decimal scale of Londo (Dierschke 1994) within 64 continuous relevé plots (5 m * 10 m each, Fig. 2.5 a).

2.3.2 Sampling of tree and shrub individuals

Tree data were collected from September 2001 to May 2002. Along the intensely studied transect (T4), all tree individuals larger than 20 cm dbh were mapped at a transect width of 50 m, tree and shrub individuals of 10-20 cm dbh were sampled at a transect width of 30 m, and tree and shrub individuals of 1-10 cm dbh at a transect width of 10 m (Fig. 2.5 a). Along the remaining seven transects, only all tree individuals larger than 20 cm dbh were also mapped continuously (Fig. 2.5 a), but the smaller size classes (10-20 cm dbh, 1-10 cm dbh) were sampled discontinuously as shown in Fig. 2.5 d. For all eight transects, tree and shrub individuals < 1 cm dbh were individually marked in the 5 m * 10 m plots in Fig. 2.5 d. Distances were measured with a range finder (VERTEX III, Haglöf, Inc., Finland, solution of 10 cm) and angles were investigated with a field compass (KB 14/400g, SUUNTO, Inc., Finland, solution of 0.5°). The diameter at breast height (dbh) was measured using a tape measure.

In the monodominant *Anogeissus* stand, four diameter classes (DC1: 0-1 cm dbh, DC2: 1-6 cm dbh, DC3: 6-30 cm dbh, DC4: > 30 cm dbh) were considered which were adjusted to growth of *A. leiocarpus*. Tree individuals of this species with a dbh of more than 1 cm are thought to be less vulnerable to fire than smaller individuals. Trees > 6 cm dbh reach the upper tree layer, and trees larger than 30 cm dbh show a significantly higher seed production than smaller tree individuals. In addition, dead trees larger than 30 cm dbh were recorded in the monodominant *A. leiocarpus* stand (DC5).

From this tree and shrub database, data were pooled for analyses in Chapter 3.4 and 3.6:

- 1) Border and ecotone detection by means of vegetation composition (Chapter 3.4). Transects were separated in 5 m stripes (Fig. 2.5 a). Data of the intensely studied transect (T4): tree individuals > 20 cm dbh, tree and shrub individuals of 10-20 cm dbh, and tree and shrub individuals of 1-10 cm dbh. tree individuals > 20 cm dbh.

- 2) Size-class distribution of tree species with a focus on *Anogeissus leiocarpus* (Chapter 3.6). For all eight transects, tree and shrub individuals were considered that were mapped according to the sampling scheme in Fig. 2.5 d. From these data, the diameter classes DC1 to DC4 were pooled. For the monodominant *Anogeissus* stand, only density measurements of the diameter classes (DC1-DC5) were considered (compare Chapter 2.3.3).

2.3.3 Density measurement of tree and shrub individuals

For transect plots, stripes, and segments, respectively, plot counts were used to record tree density (Fig. 2.5). In the monodominant *Anogeissus* stand, the T-square sampling procedure (Krebs 1999) was applied to measure density patterns of *A. leiocarpus* (see Chapter 2.6.6). For each diameter class, the T-square sampling procedure was carried out at 30 random points as suggested by Engeman *et al.* (1994).

Distances were measured with a range finder (VERTEX III, Haglöf, Inc., Finland). Calculations of tree density and random patterns revealed that individuals of all diameter classes were aggregated (compare Chapter 2.6.6). Thus, areas of aggregation were mapped for each diameter class by means of GPS-implement.

2.3.4 Sampling of surface biomass

In the vicinity of transects, 30 biomass-plots (size of 1 m * 1 m) were selected that included a wide range of different structural vegetation types occurring in the transect plots. The above described structural vegetation parameters were collected at the end of October, and non-woody biomass was harvested in these plots in November. The weight of the air-dried biomass was taken for the fractions grasses (including grass litter), herbs (including herb litter) and leaf litter. Leaf litter included all dead material of woody plants with a diameter smaller than 1 cm. At the end of dry season (beginning of March), the biomass of the 30 biomass-plots was sampled a second time to apprise leaf litter fall during this time period.

2.4 Sampling of abiotic parameters

2.4.1 Microclimatic parameters

Air temperature (T) and relative air humidity (H) were measured in 10-min intervals along the eight transects using 10 mini-data loggers (Tinytag Plus TGP-1500, Gemini Data Loggers, Ltd., UK). Data loggers at a height of 1 m being covered by an aluminum shield to avoid radiation errors were placed at positions corresponding to the filled dots in the sampling design of Fig. 2.5 c. The study period from 02/08 to 08/30/2002 (203 days) was divided into

five measurement periods (MP) of 8*5 days each (compare Fig. 3.10). Three days of the entire study period were needed to download data from the data loggers. During an MP, each transect was measured once over a five-day period due to a limitation in data loggers, i.e. each transect was sampled during 5 consecutive days every 40 days and transects were sampled temporarily staggered. Every 40 days 10 additional data loggers were available for five days. The transect T4 was therefore a more intensely studied transect (IST). There logger density (20 data loggers) and transect length was increased (460 m, filled and unfilled dots in Fig. 2.5 c). This transect was additionally sampled from 08/30 to 09/04/2002. During the whole study period, one data logger was placed at an open savanna site as reference. From air temperature and relative air humidity the vapor pressure deficit (VPD) was calculated following Arya (2001):

$$VPD = (6.107 \cdot 10^{((7.5 \cdot T)/(237+T))}) - ((6.107 \cdot 10^{((7.5 \cdot T)/(237+T))}) \cdot H/100)$$

As characteristic values for a single day, the mean, minimum, maximum, 5%- and 95%-quantil, and the amplitude of each measurement day were calculated for the three microclimatic parameters. Diurnal values were averaged over each five-day period. The five-day mean of diurnal mean air temperature (T_{mean}), of diurnal 5%-quantil of relative air humidity ($H_{5\text{-quantil}}$), and of diurnal amplitude of vapor pressure deficit ($VPD_{\text{ampl.}}$) showed most pronounced differences between savanna and closed forest. Therefore, they are supposed to be the most ecologically meaningful parameters, and they are presented in the present thesis (Chapter 3.3).

2.4.2 Fire occurrence, shading, and soil depth

At the end of the dry season (March 2002) the burned area was estimated for each transect-plot. Cover was estimated following the decimal scale of Londo (Dierschke 1994). Fire occurred along transects from 01/20 to 02/03/2002. As parameters representing light conditions, the cover above 1 m was calculated as the sum of the cover of each vegetation stratum above 1 m. Soil depth was determined by driving a steel rod with a diameter of 1 cm into the soil with 10 replications per plot (compare Hartge & Horn 1992).

2.5 Border-and-ecotone-detection analysis (BEDA) for univariate transect data

If two adjacent habitats can be distinguished from each other by differences in one variable, the gradient in that variable should be steeper in the ecotone than within each neighboring habitat (Cadenasso *et al.* 2003). A sigmoidal non-linear function according to the formula

$$f(x) = a + (c-a)/(1+\exp((x-b)/d)) \quad (1)$$

is an adequate mathematical model for this problem. The constant functions a and c represent the upper and lower asymptotes (Fig. 2.6), and approximate the mean conditions in two adjacent habitats. The coefficient b is the distance to the inflection point (B). B can be interpreted as the border between two habitats. The parameter d characterizes the steepness of the change of the quantity (Fig. 2.6).

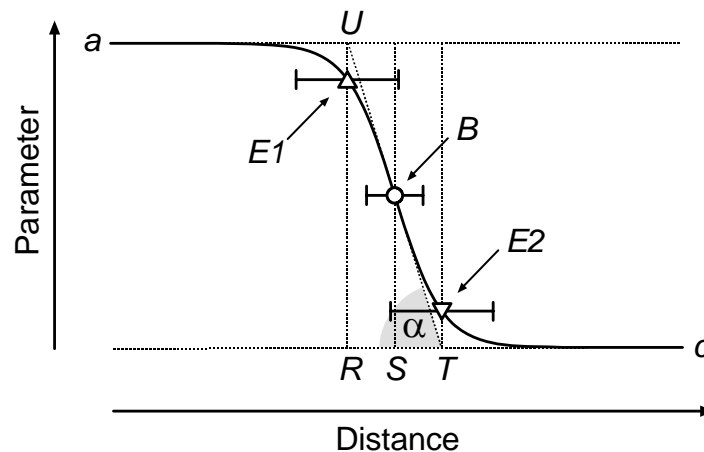


Fig. 2.6. Scheme of the border-and-ecotone detection analysis (BEDA, compare text). B = location of the border, $E1$ and $E2$ = locations of the ecotone limits. The angle α and the points R , S , T , and U were used for derivations of BEDA.

In the same manner like an ‘onset of light saturation’ was introduced in Talling (1957) an ‘onset of non-ecotone area’ can be defined by the points $E1$ and $E2$ on the left and right of a detected border B (Fig. 2.6). Accordingly, $E1$ and $E2$ confine the limits of the ecotone belonging to the border B , and they are equivalent to the DEI towards the two habitat interiors. These parameters can easily be computed from the coefficient estimates and their covariance matrix obtained by applying the sigmoidal regression model (see below).

Derivation of E1 and E2.

The x -coordinates of $E1$ and $E2$ can be calculate in the following way. The first derivative of $f(x)$ in (1) is

$$f'(x) = - (c - a) \left(\frac{e^{\left(\frac{x-b}{d}\right)}}{d \left(1 + e^{\left(\frac{x-b}{d}\right)}\right)^2} \right)$$

In the non-linear function, b reflects the x -coordinate of B (Fig. 2.6). The first derivative at b is:

$$f'(b) = (a-c) / (4*d) = \tan(\alpha) = -RU / RT$$

With RU being the difference between the two asymptotes, a and c , we get $RT = -4*d$.

Because the sigmoidal function is point-symmetric in B , $RS = ST = RT / 2 = -2*d$.

As x -coordinates of $E1$ and $E2$, $e1$ and $e2$, we get

$$e1 = b+2*d \text{ and } e2 = b-2*d.$$

The y -coordinates can simply be calculated as $f(e1)$ and $f(e2)$, respectively.

Let \hat{b} and \hat{d} denote the estimates for b and d . Then $e1$ and $e2$ can be estimated by

$$\hat{e}1 = \hat{b} + 2\hat{d} \quad \text{and} \quad \hat{e}2 = \hat{b} - 2\hat{d} \quad (2)$$

Derivation of confidence intervals for e1 and e2.

Next confidence intervals for the x -coordinates of $E1$ and $E2$, $e1$ and $e2$, are being derived (compare Lehmann 1999). Computing the variance by (2) we get

$$\text{var}(\hat{e}1) = \text{var}(\hat{b}) + 4*\text{var}(\hat{d}) + 4 * \text{covar}(\hat{b}, \hat{d});$$

$$\text{var}(\hat{e}2) = \text{var}(\hat{b}) + 4*\text{var}(\hat{d}) - 4 * \text{covar}(\hat{b}, \hat{d}).$$

Therefore, as estimate for standard deviations can be used

$$\hat{SD}(\hat{e}1) = \sqrt{\hat{\text{var}}(\hat{e}1)}, \quad \hat{SD}(\hat{e}2) = \sqrt{\hat{\text{var}}(\hat{e}2)}$$

Assuming a normal distribution for the distribution of \hat{b} and \hat{d} , which can be justified for sufficiently large sample sizes, a confidence interval for $e1$ and $e2$ can be constructed by

$$[\hat{e}1 - z_{1-\alpha/2} * \hat{SD}(\hat{e}1), \hat{e}1 + z_{1-\alpha/2} * \hat{SD}(\hat{e}1)] \text{ and}$$

$$[\hat{e}2 - z_{1-\alpha/2} * \hat{SD}(\hat{e}2), \hat{e}2 + z_{1-\alpha/2} * \hat{SD}(\hat{e}2)],$$

where $z_{1-\alpha/2}$ is the $(1-\alpha/2)$ -quantile of the standard normal distribution.

2.6 Statistical analysis

Statistical analyses were carried out using the software packages ArcView GIS 3.2a (Environmental Systems Research Institute, Inc.), Canoco for Windows 4.51 (Biometrics – Plant Research International, Wageningen, Netherlands), Exeter Software (package Ecological Methodology 6.1), GraphPad Prism 4.02 (PadGraph Software, Inc.), R 1.8.0 (2003), SPSS 11.0.1 (LEAD Technologies, Inc.), and SAS 8.02 (SAS Institute, Inc.). For clarity, the statistical procedures, that are applied in the six chapters in the result section of the present thesis, are described separately (Chapter 2.6.1 – 2.6.6).

2.6.1 General transect description

In Chapter 3.1, the border-and-ecotone-detection analysis (BEDA) on the basis of a non-linear regression model described in Chapter 2.5 was applied. As characteristic parameters the location of the border (B) and the limits of the associated ecotone ($E1$ and $E2$), both including confidence intervals, were computed. In addition, the conditions of the interior of the two habitats were supposed to be given by the asymptotes on the right and left side of the fit and their variability were appreciated by 95%-prediction bands.

To compute non-linear fits of BEDA, the nls-function (R package nls, Bates & Watts 1988) was used, and non-linear mixed effects models (nlme-function, R package nlme, Lindstrom & Bates 1990) were applied to incorporate the effect of transects in the models. Model selection was performed as described in Hastie *et al.* (2003). Prediction and confidence bands belonging to non-linear regressions were calculated in GraphPad Prism 4.02 (see Bates & Watts 1988). Given errors reflect the two-tailed 95%-confidence intervals and 95%-confidence and prediction bands. Q-Q plots and distribution of standardized residuals were satisfying for all analyses presented here.

Along the intensely studied transect cover of all species (64 relevés) was analyzed by detrended correspondence analysis (DCA, Canoco for Windows 4.51, detrending method: by segment, ter Braak & Smilauer 2002). In the analysis, species data were log-transformed ($\log(x+1)$).

2.6.2 Surface biomass and surface-fire probability

BEDA was applied as described in Chapter 2.6.1. In addition, non-parametric smoothing models were applied (loess-function, R package modreg, Cleveland *et al.* 1992). Binominal data were fitted with generalized linear models (glm-function, R package base, Hastie & Pregibon 1992) where the link-function logit was chosen. Model selection was performed as

described in Hastie *et al.* (2003). Q-Q plots and distribution of standardized residuals were satisfying for all analyses presented here.

2.6.3 Microclimate

Since transects were not sampled simultaneously but temporarily staggered, values for T_{mean} , $H_{5\%-\text{quantil}}$, and $VPD_{\text{ampl.}}$ were standardized to the reference value, i.e. calculated as the difference of the values for each logger and the values of the reference logger (e.g. $\text{stdVPD}_{\text{ampl.}}$, compare Fig. 3.13).

BEDA was applied as described in Chapter 2.6.1. During the analysis of the full data set containing the data of the 10 data loggers, for each single measurement period (MP), data of all transects were pooled. In a next step, a non-linear mixed effects model was applied to incorporate the effect of transects and measurement periods (MP) in the models. However, nlme-function failed due to the low number of 10 data loggers per transect. Therefore, a cubic model as an approximation for the sigmoidal model was chosen to be able to approximate transect effects (e.g. $\text{stdVPD}_{\text{ampl.}} \sim a1 * \text{Distance}^3 + a2 * \text{Distance}^2 + a3 * \text{Distance} + b0$; compare Fig. 3.13). The used linear mixed-effects models (lme-function, R package nlme, Lindstrom & Bates 1988) included MP and transect nested in MP as random factors, and, additionally, an autoregressive correlation structure of order 1 (Pinheiro & Bates 2000). Model selection was performed as described in Hastie *et al.* (2003). Q-Q plots and distribution of standardized residuals were satisfying for all analyses presented here.

2.6.4 Vegetation composition

To detect dissimilarities along the transects, the split-moving-window dissimilarity analysis was applied (SMWDA, Cornelius & Reynolds 1991). From a window split in two halves, the dissimilarity of species composition was calculated by Euclidean distance for each window-midpoint position. Depending on the type of vegetation data, different plot sizes were used: 5 m * 10 m for the species cover and number of tree and shrub individuals with a dbh of 1-10 cm, 5 m * 30 m for the number of tree and shrub individuals with a dbh of 10-20 cm, and 5 m * 50 m for the number of tree individuals with a dbh larger than 20 cm. In the analysis on the basis of tree and shrub species, the number of individuals of each species was considered. Concerning species cover, those species were included in the analysis that were mentioned at least three times in the relevés of the intensely studied transect. The latter data were log-transformed ($\log[x+1]$).

In the SMWDA window sizes from 2 to 20 plots (1 to 10 for each window half) were used. In Chapter 3.4, only the dissimilarity profiles of the average Z scores computed as the average of the z-transformed Euclidean distance of the different window sizes mentioned above are presented. According to Cornelius & Reynolds (1991), this pooled dissimilarity profile is

clearly less scale-dependent than profiles for an individual window size. For each data set, the standard deviation above the overall expected mean by a Monte Carlo procedure with 1000 replicates was computed (Cornelius & Reynolds 1991). The one-tailed 95%-confidence interval was used to detect significant peaks of the average Z score indicating borders along the transects.

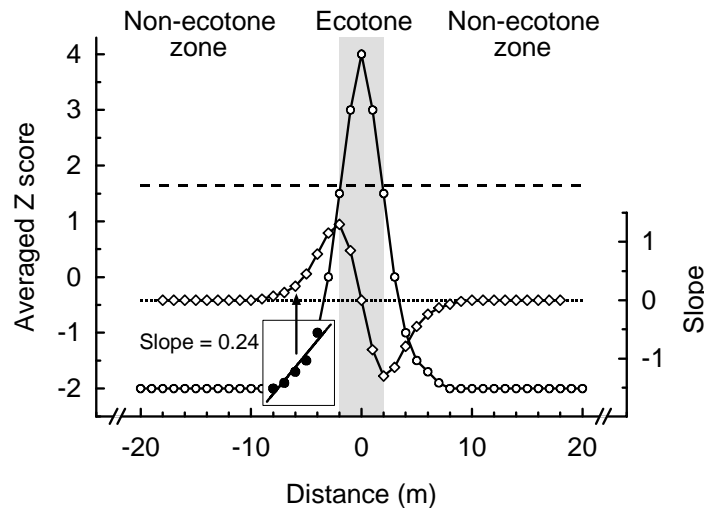


Fig. 2.7. Demonstration of the method to value the width of an ecotone at a significant border (peak above the one-tailed 95%-confidence interval, upper horizontal line) detected by the split-moving-window dissimilarity analysis (SMWDA). On the basis of average Z scores (circles), the slope of the linear least-square regression with a window size of $n = 5$ (moving-window regression analysis (MWRA), rectangle with black dots) was calculated at each midpoint position (diamonds). The lower horizontal line marks a slope of zero. The two borders between the ecotone and non-ecotone zones are given by a maximum and minimum of the slope calculated from MWRA. The ecotone is marked gray.

To determine the width of an ecotone, a moving-window regression analysis (MWRA) similar to Walker *et al.* (2003) was used. On the basis of average Z scores, the slope of the linear least-square regression with a window size of n was calculated at each midpoint position of the SMWDA. Window size was $n = 5$ (the score at the midpoint position and two scores on its left and right, compare Fig. 2.7). The slope at a window-midpoint position gives the degree of change of average Z scores. The maximum value above zero and the minimum value below zero of the MWRA between a detected border and the next change of sign (or hitting zero) of the slope on the left and right side of a detected border are interpreted as limits of the ecotone between two non-ecotone zones (Fig. 2.7). These statistic analyses were computed with the software package R 1.8.0.

2.6.5 Core-area analysis

Core-area analysis was carried out using the ArcView GIS extension Patch Analyst 2.2. The GPS mapping data of 31 semi-deciduous forest islands (Fig. 2.1) mentioned above were analyzed. Total area (TA) of the dry forest islands varied from 2.1 ha to 146.1 ha. After

subtracting a buffer zone from it, the relation between the TA and the remaining core area (CA) denoted the relative core area ($rCA = CA / TA$).

To estimate the size of a forest island that contains an rCA of at least 50%, the rCA was plotted versus the TA of the considered forest islands. A non-linear regression model was fitted on this data using the nls -function (R package nls , Bates & Watts 1988) and a 95%-confidence interval was constructed for the expected size of a forest island containing an rCA of 50% (Appendix A).

2.6.6 Size-class distribution of tree species

To detect differences in tree density and environmental parameters between the five transect segments along the eight transects (Fig. 2.5 d), a two-way ANOVA (UNIANOVA, SSTYPE(1), SPSS 11.0.1) was applied. The nested model was firstly specified by ‘transect’ as a random factor, and secondly by ‘transect segment’ within transects as a fixed factor. When significant differences ($\alpha < 0.05$) were detected between the five transect segments, a multiple range test (TUKEY, $\alpha = 0.05$, SPSS 11.0.1) was applied. Tree density data and structural vegetation data were log-transformed ($\log(x+1)$) to meet the assumptions of homoscedasticity and normality. Means and standard errors were back-transformed to the original scale for presentation. For regression analysis between abundance of tree offspring and environmental parameters Spearman’s rank correlation coefficient (r_s) was calculated (SPEARMAN TWOTAIL NOSIG, SPSS 11.0.1).

To ordinate the data set of the four diameter classes of *Anogeissus leiocarpus* as well as the structural vegetation data, to both the transect segments and the *Anogeissus* stand, a principal component analysis (PCA, Canoco for Windows 4.51) was applied. Detrended correspondence analysis (DCA, Canoco for Windows 4.51) revealed a linear response of the data (maximum length of gradient in standard deviation units (SD): 2.102 SD and 1.520 SD). Thus, calculation of PCA was suitable (ter Braak & Smilauer 2002). Data were log-transformed ($\log(x+1)$) and centered by species. Scaling was focused on ‘inter-sample distances’ and species scores were not post-transformed. Finally, confidence ellipses of sample scores of the first and second PCA axes were calculated using SAS/INSIGHT (8.02).

Concerning the T-square sampling (compare Chapter 2.3.3), firstly, the distance from a random sampling point to the closest individual is measured (R_i). Let l be the line from the random point to that closest individual. Then the line through the closest individual that is perpendicular to l splits the plane into two half-planes. Now T_i is the distance from the closest individual to its nearest neighbor that is located in the half-plane that does not contain the random sampling point. Several estimators can be based on R_i and T_i to estimate the density D (Diggle 1975, Byth 1982). Byth (1982) introduced the T-square estimator

$$D = n^2 / (2\sqrt{2} \sum_i R_i \sum_i T_i)$$

which showed a robust behavior even for moderately-clustered spatial patterns. In addition to the densities measurement it can be calculated whether the spatial distribution of individuals from a sampled population is random, uniform, or aggregated (Krebs 1999). Density and aggregation pattern were computed by Exeter Software (package Ecological Methodology 6.1).

No test exists to compare density data of plotless density estimators such as T-square and plot counts. Thus, the overlap of the 95%-confidence intervals was used to indicate whether density values measured by T-square and plot counts were significantly different or not.

3 Results

3.1 General transect description

For a general transect description, three structural parameters (cover above 1 m, cover of woody climbers, and cover of grasses and grass litter) and soil depth were selected (Fig. 3.1). Cover above 1 m along the transects was low in the savanna with values below 20% and high in the closed forest (values about 50%, Fig. 3.1 a). This parameter reflects the cover of shrubs and trees that increased in density towards the closed forests. Typical tree species in the savanna were *Detarium microcarpum*, *Crossopteryx febrifuga*, and *Vitellaria paradoxa*. *Anogeissus leiocarpus* and *Combretum nigricans* dominated the forest belt. Towards the forest interior *Diospyros abyssinica* and *Tapura fischeri* occurred with a high abundance in the lower tree layer, and *Ceiba pentandra*, *Diospyros mespiliformis*, *Dialium guineense*, and *Milicia exelsa* were found in upper tree layers. The distribution of woody climbers showed a pattern similar to tree and shrub species (Fig. 3.1 b). This growth form was absent from the savanna but occurred regularly in the forest belts and the closed forests.

Contrary to woody species, the cover of grasses and grass litter was high in the savanna (about 70%) and decreased towards the closed forest (Fig. 3.1 c). At some open sites in the forest belt and closed forest, however, rather high values of grass cover were observed. Soil depth as a parameter reflecting certain soil properties strongly differed between transects (Fig. 3.1 d). E.g., along transect T3, soil depth was frequently below 50 cm at savanna sites and more than 200 cm in the closed forest, but e.g. transect T4 showed the opposite pattern.

On the data presented in Fig. 3.1, the border-and-ecotone detection analysis (BEDA, Chapter 2.5) was applied. Fitting the soil depth data by non-linear regression failed due to the obvious heterogeneity of the data. The results concerning the three structural parameters assuming no transect effect are given in Table 3.1 (fixed model). In addition, the factor transect was included as random factor using the nlme-function (Chapter 2.6.1). Model selection within the latter analysis revealed, that significant random effects only occurred for the magnitude of the asymptotes (coefficient a and c , see Fig. A. 1 – Fig. A. 3 in the Appendix). As for the three structural parameters neither for the coefficient b (= location of the border) nor for the coefficient d (= slope of the sigmoidal model) a random effect was found. However, because BEDA is based on the coefficients b and d , it appears reasonable to ignore transect effects in regard to detect borders and ecotones for the considered structural parameters. This is supported by the visual comparison of the fixed model and the model including respective random effects (Fig. A. 1 - Fig. A. 3 in the appendix).

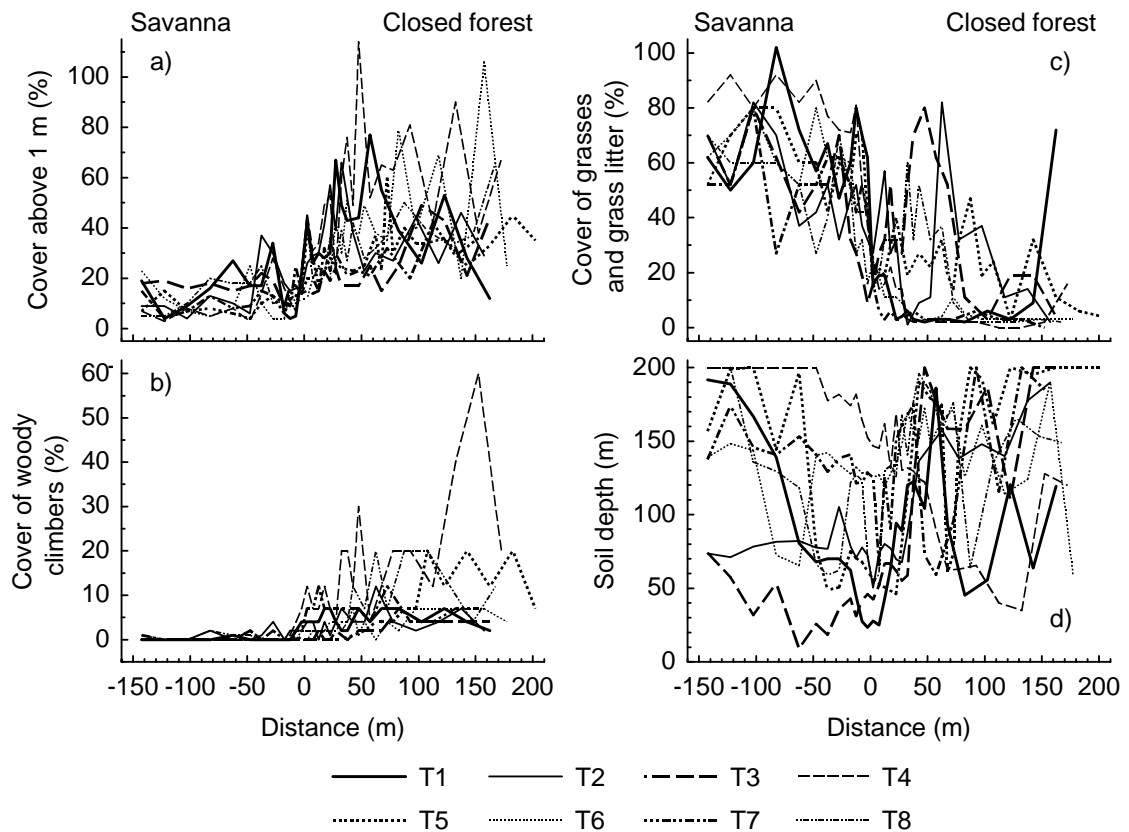


Fig. 3.1. Values of three structural parameters (a-c) and soil depth (d) sampled along the eight studied transects (T1-T8).

Table 3.1. Results of BEDA for three structural parameters assuming no random effect between transects (fixed model). The results of the respective models including significant random effects are presented in Fig. A. 1 - Fig. A. 3. *E1* = ecotone limits towards the savanna, *B* = border between forest and savanna, *E2* = ecotone limits towards the closed forest, Cover savanna = approximation of the asymptote towards the savanna, Cover forest = approximation of the asymptote towards the closed forest. Error represented 95%-confidence intervals and 95%-prediction bands, respectively. The border line between savanna and forest belt is 0 m. Negative values are located in direction of the savanna and positive values in direction of the closed forest.

Parameter	Border and ecotone detection				
	<i>B</i> (m)	<i>E1</i> (m)	<i>E2</i> (m)	Cover savanna (%)	Cover forest (%)
Cover of grasses and grass litter	-5.4 ±4.8	-22.2 ±9.8	11.4 ±9.8	63.5 ±34.2	15.4 ±34.1
Cover above 1 m	11.3 ±7.8	-9.3 ±15.5	32.0 ±15.5	12.2 ±28.0	41.4 ±28.0
Cover of woody climbers	45.4 ±30.5	-28.6 ±74.8	119.4 ±74.8	-0.3 ±11.4	11.9 ±11.6

On the basis of cover of grasses and grass litter, the detected border (*B*) between forest and savanna was located at 5.4 ± 4.8 m in direction of the savanna (Table 3.1). The width of the ecotone associated to this border was about 33.6 m. The ecotone limit *E2* that can be interpreted as the depth-of-edge influence (DEI) towards the closed forest was found at 11.4

± 9.8 m. Even though the cover of grasses was much higher in the savanna ($63.5 \pm 34.2\%$) than in the closed forest ($15.4 \pm 34.1\%$), the prediction bands of the asymptotes showed an overlap as a result of a high variability in both habitats (Table 3.1).

The detected border in regard to the cover above 1 m was located at 11.3 ± 7.8 m towards the closed forest and the DEI was 32.0 ± 15.5 m (Table 3.1). This divergence compared to the values for grass cover shows that the turn-over in grasses and trees and shrubs did not occur at the same location, but spatially shifted along the transects. This was additionally observed for the cover of woody climbers that showed a border at 45.4 ± 30.5 m and DEI of 119.4 ± 74.8 m (Table 3.1). However, the variability within the data of cover of woody climbers was rather high well visible in the large confidence intervals. Differences between the conditions in the closed forest and the savanna were also well visible for the cover above 1 m and the cover of woody climbers, but the overlap of the prediction bands of the two asymptotes was larger than for the grass data set (Table 3.1).

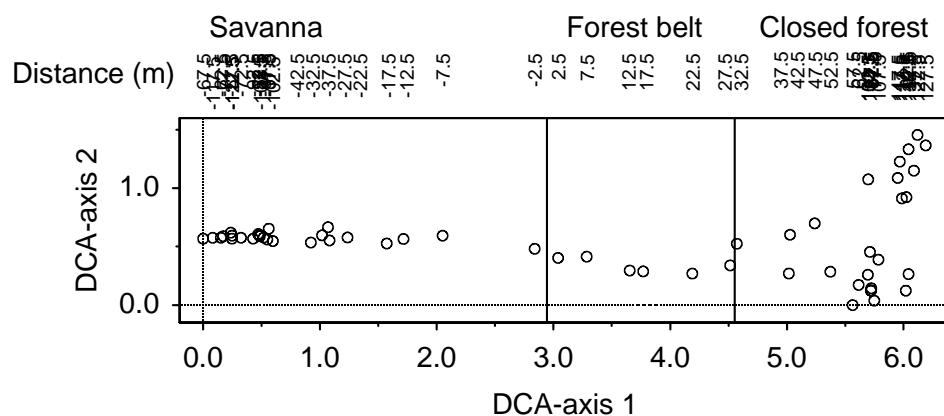


Fig. 3.2. Sample scores of the first and second DCA axes for the cover of all species along the intensely studied transect (T4). Data were log-transformed ($\log(x+1)$). The first DCA-axis explains 24.0% of the variance and the second DCA-axis 3.3%. Transect locations of each sample score are given on the top of the graph. Vertical lines mark the borderline between savanna and forest belt (0 m), and between forest belt and closed forest (30 m, compare Fig. 2.5).

In regard to species composition, DCA analysis for the cover of species of 64 relevés along the intensely studied transect (T4) revealed a length of gradient of 6.2 standard deviation units (*SD*) that marked a species turnover of one and a half times (ter Braak & Smilauer 2002). The first axis of DCA explained 24.0% of species data (Fig. 3.2). Each of the following axes accounted for less than 3.3%. This shows that the vegetation gradient along the intensely studied transect was very well reproduced by the first DCA-axis. Obviously, savanna plots were located on the left side of this DCA-axis and closed forest plots on the right side. In the transition between these two habitats from -42.5 m to 52.5 m, the plots were stringed together along the first axis (Fig. 3.2). This aspect stresses the gradual change in species composition across the forest-savanna ecotone.

3.2 Surface biomass and surface-fire probability

The amount of surface biomass harvested in the 30 biomass-plots is presented in Fig. 3.3. The dry mass of most savanna plots was dominated by grasses, whereas most plots in the closed forest and in the forest belt were characterized by a high amount of leaf litter. The mass of leaf litter at the beginning of the dry season showed a similar value to the mass of leaf litter sampled at the end of the dry season. The herb fraction was not of importance in the biomass plots. Biomass plots were not chosen randomly, but subjectively to sample a wide range of different structural vegetation types occurring in the transect plots (compare Chapter 2.3.4). Collected data do not reflect the mean conditions of the vegetation types and therefore, no statistic test is presented.

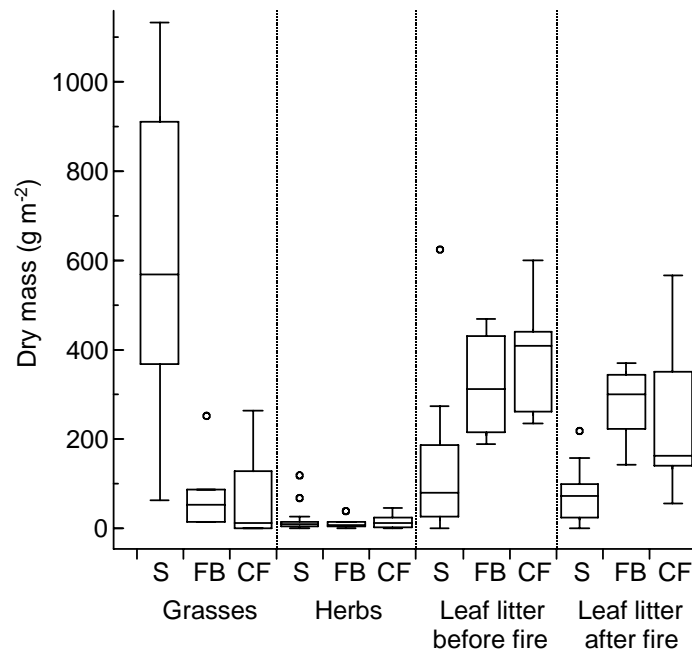


Fig. 3.3. Box-plot of dry mass of grasses (including grass litter), herbs (including herb litter), and leaf litter. Leaf litter was sampled before and after fire occurrence in the savanna. S = savanna (n = 16), FB = forest belt (n = 6), CF = closed forest (n = 8).

For the biomass plots, a strong relationship between dry mass of grasses and grass volume was found (Fig. 3.4). Grass volume was calculated as (maximum grass height) * (cover of grasses and grass litter). This relation was used to estimate the amount of dry mass of grass for each transect plot. For herbs and leaf litter, no satisfying relation between structural parameters and dry mass was found (data not shown).

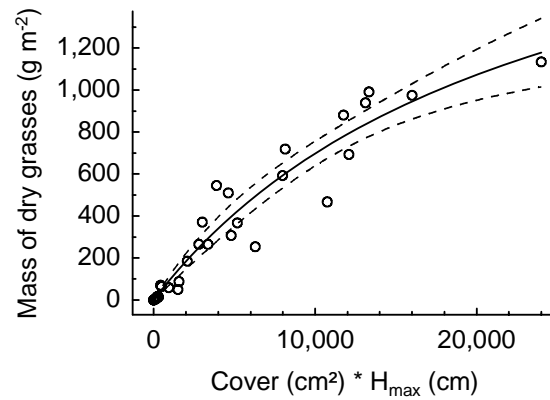


Fig. 3.4. Non-linear regression of grass volume (cover * maximum height) and mass of dry grasses. The shown fit is described by $f(x) = (2,319.5 * x) / (x + 23,250.2)$, $r = 0.955$, $P < 0.0001$. 95%-confidence bands of the models' mean are given by dashed lines.

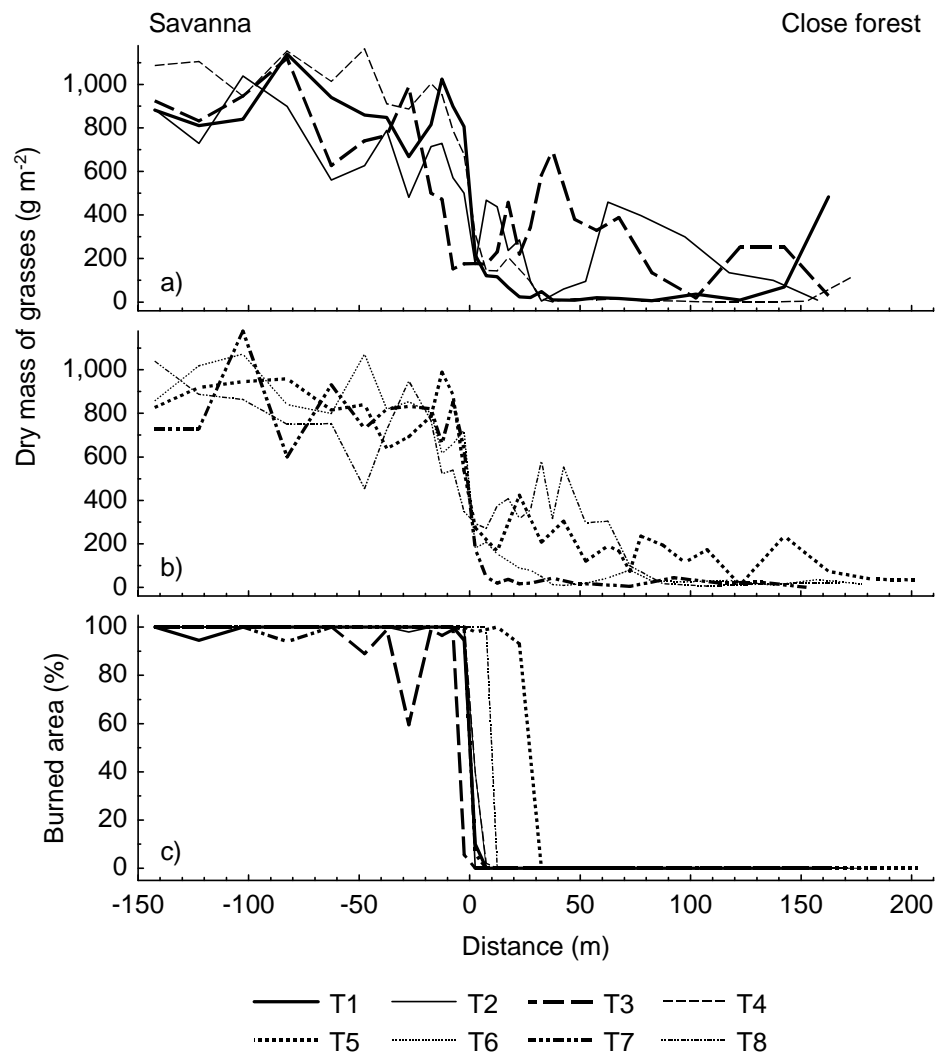


Fig. 3.5. Distribution of dry mass of grass (panel a and b) and burned area (panel c) along forest-savanna transects (T1-T8).

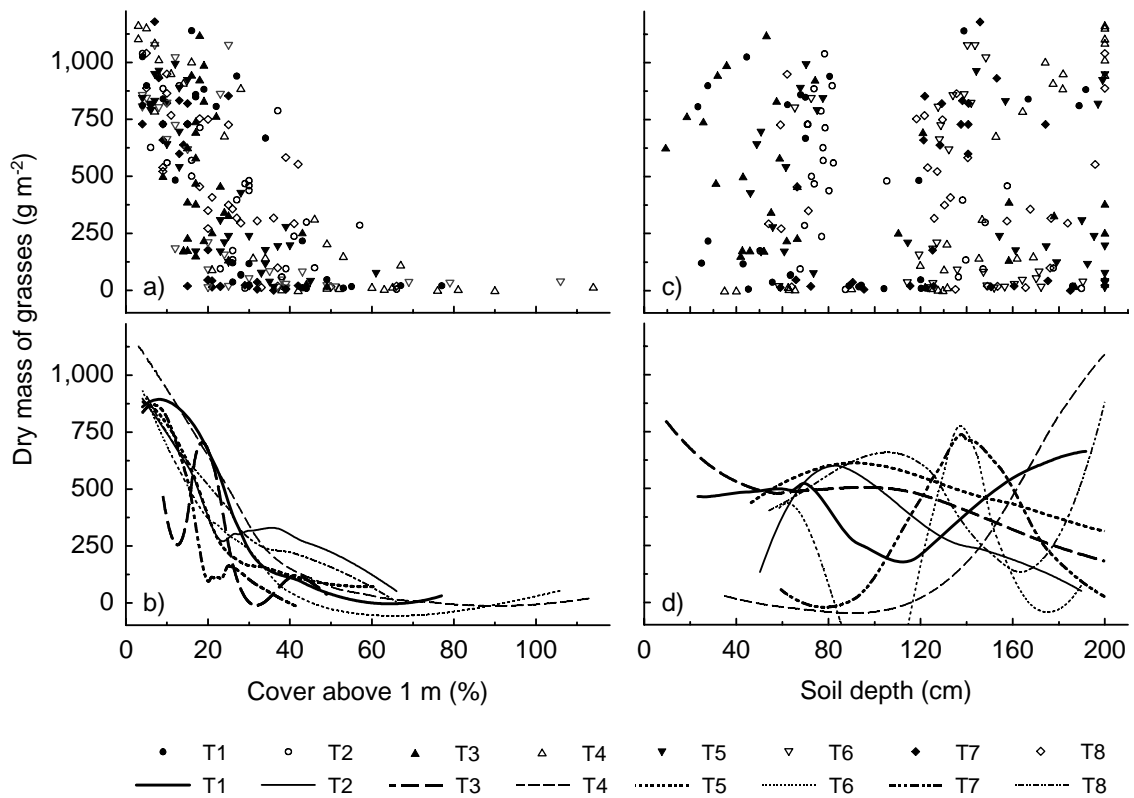


Fig. 3.6. Dry mass of grasses versus total vegetation cover above 1 m (panel a) and soil depth (panel c) along eight forest-savanna transects. Panel b and d show the results of the loess models that were applied to the data of each transect.

Fig. 3.5 a and b show the distribution of estimated dry mass of grasses along the eight forest-savanna transects. For all transects the amount of dry mass of grass in the savanna reached values of approximately 900 g m^{-2} . With the transition from savanna to forest belt, the amount of grass biomass dropped to values mostly below 400 g m^{-2} towards the forest interior.

The amount of dry mass of grasses versus the vegetation cover above 1 m and soil depth were plotted in Fig. 3.6 a and c, respectively. The applied loess-function yielded a strong negative correlation between the amount of grass biomass and the vegetation cover above 1 m (Fig. 3.6 b). All transects showed a similar tendency. In contrast, no directed relation between the soil depth and the amount of grass biomass was found (Fig. 3.6 c and d). This was also the case for savanna plots only (data not shown).

The results for the border and ecotone detection for the parameter 'dry mass of grasses' using a fixed model (transect effect ignored) are given in the last row of Table 3.2 (see also Fig. 3.7). However, model selection revealed a significant random effect for the coefficient d of the model function. This coefficient reflects the slope of the sigmoidal model and is used to compute $E1$ and $E2$ (compare Chapter 2.5). From the graphical comparison of the fixed model and the non-linear mixed effects model in Fig. 3.7 it is well visible that strong differences between transects in regard to BEDA should occur. Therefore, BEDA was also applied on each single transect (Table 3.2). For all transects detected borders were located from -2.5 to 2.4 m , that referred to the borderline between savanna and forest belt being well visible in the

field. Only transect T3 showed a border at -17.9 m, i.e. further towards the savanna. The width of associated ecotones marked by the detected ecotone limits, $E1$ and $E2$, ranged from 5.4 m to 46.5 m (compare Table 3.2). Transect T8 was exceptional with an ecotone width of 290.2 m. This transect was in general characterized by a very high variation resulting in large confidence intervals of B , $E1$, and $E2$.

The burned area of the transect plots was shown in Fig. 3.5 c. The burned area in savanna plots reached almost 100%, whereas plots in the closed forest remained unburned. For all transects the value for the burned area dropped abruptly near the border between savanna and forest belt. The surface fire entered up to about 30 m into the forest belt only in transect T5, which was characterized by a forest belt of 60 m (Table 3.2). Fires did not occur in the closed forests of any transect. The DEI detected for the mass of dry grasses reflected by $E2$ in BEDA, however, showed larger values than the limit of burned surface (Table 3.2).

Table 3.2. Results of BEDA for dry mass of grasses for each single transect. The last row gives the results for all transects assuming no random effect between transects (fixed model, compare Fig. 3.7). $E1$ = ecotone limits towards the savanna, B = border between forest and savanna, $E2$ = ecotone limits towards the closed forest, Savanna = approximation of the asymptote towards the savanna, Forest = approximation of the asymptote towards the closed forest. Error represented 95%-confidence intervals and 95%-prediction bands, respectively. The borderline between savanna and forest belt is 0 m. Negative values are located in direction of the savanna and positive values in direction of the closed forest. Looking from the savanna towards the forest interior, the limit of burned surface reflects the transect position where the burned area of the transect plots dropped from high values in the savanna below 50% (compare Fig. 3.5 c).

Transect	Width of forest belt (m)	Border and ecotone detection for dry biomass of grasses					Limit of burned surface (m)	
		B (m)	E 1 (m)	E 2 (m)	Savanna (g/m ²)	Forest (g/m ²)		
T1	0-20	0.5 ±2.5	-2.2 ±3.1	3.2 ±3.1	884.4 ±260.6	70.2 ±257.7		0
T2	0-15	-2.5 ±12.9	-25.8 ±25.7	20.7 ±25.7	783.3 ±356.9	169.6 ±350.9		0
T3	0-20	-17.9 ±6.6	-23.1 ±13.3	-12.7 ±13.3	867.8 ±383.1	281.8 ±370.4		-5
T4	0-30	-1.0 ±2.1	-12 ±4.2	10.0 ±4.2	1039.0 ±162.4	36.0 ±158.7		0
T5	0-60	-1.8 ±2.4	-5.6 ±5.8	2.0 ±5.8	846.7 ±234.1	164.3 ±229.9		27.5
T6	0-35	-1.9 ±3.5	-17.8 ±7.3	13.9 ±7.3	919.7 ±190.8	27.9 ±185.4		0
T7	0-10	-0.1 ±2.2	-3.7 ±3.7	3.6 ±3.7	808.2 ±227.8	22.4 ±226.3		0
T8	0-25	2.4 ±58.9	-142.7 ±176.9	147.6 ±176.9	965.7 ±353.1	-40.6 ±348.8		10
T1-T8 (fixed model)	-	-0.6 ±1.3	-28.5 ±22.0	27.2 ±22.0	887.6	76.7	-	-

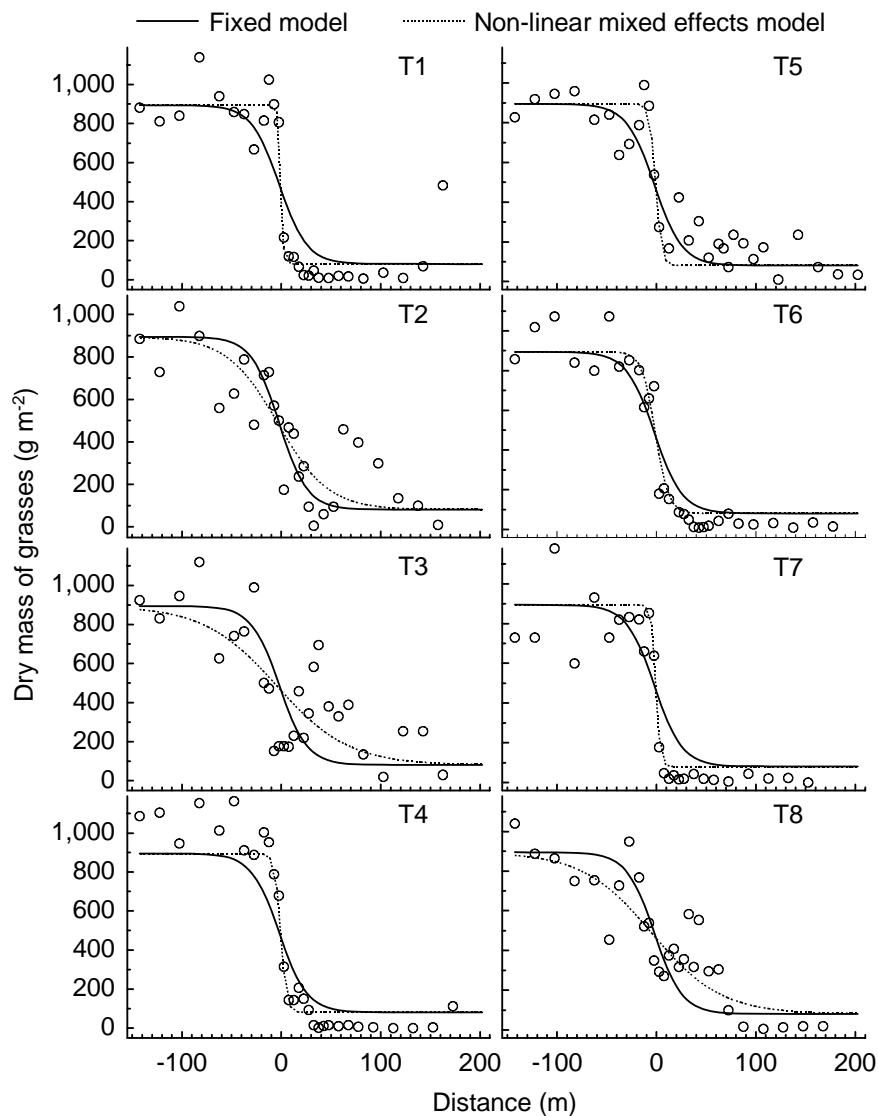


Fig. 3.7. Graphic comparison of the non-linear mixed effects model (significant random effect for the coefficient d representing the slope (see Chapter 2.5); dashed lines) and the fixed model (no transect effect; lines) for the parameter dry mass of grasses. Random transect effects for the coefficients a , b , and c were not significant. Dots = sample points, T1-T8 = transects (compare Fig. 2.1).

To assess the amount of dry mass of grasses that is necessary for ignition, the last burned and the first unburned plot of each transect were selected. Both plots had to be located directly side by side. As this was not the case with the respective plots in transect T5, they had to be excluded from the analysis. As surface fires stopped abruptly with each transect (see Fig. 3.5 c), it appeared reasonable to transform the parameter burned area to a binary variable, where all values larger than 50% were set to 1 and the others to 0. This binary variable was used as response variable, and dry mass of grasses was used as explanatory variables in fitting glm. The output of the models was interpreted as the ignition probability of a plot in the transition zone between forest and savanna in dependence on dry mass of grasses. Model selection revealed that the grouping factor transect did not significantly improve the model. Fig. 3.8 showed the ignition probability in dependence on dry mass of grasses. An ignition probability of 0.5 was given if a plot near the forest border line contained about 300 g m^{-2} of

dry mass of grass, but due to a low number of replicates ($n = 7$) the applied model was on the limit of statistical significance ($P = 0.056$).

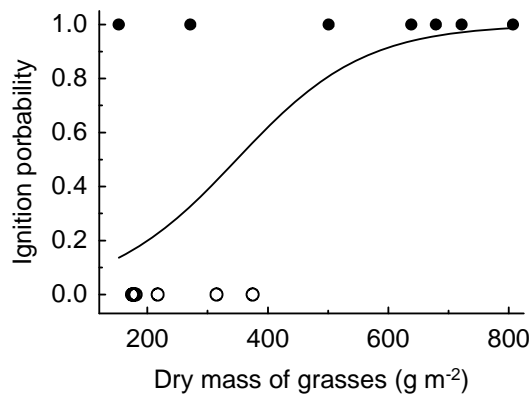


Fig. 3.8. Ignition probability in dependence on dry mass of grasses. Plots of seven transects that were directly located at the fire limit were selected (compare text). The parameter burned area was transformed to a binary variable, where all values larger than 50% were set to 1 (burned, filled dots, $n = 7$) and the other to 0 (unburned, open dots, $n = 7$). The line represented the result of glm (link-function = logit; $P = 0.056$). No transect effect occurred.

3.3 Seasonal variability in microclimatic borders and ecotones

The course of the microclimatic parameters followed diurnal oscillations during the dry and rainy season. At daytime, air temperature and vapor pressure deficit (VPD) were high and air humidity was low, and vice versa at nighttime. This is exemplarily shown for two five-day courses of VPD (dry and rainy season) measured along the intensely studied transect (T4, 20 data loggers, Fig. 3.9). VPD was lower during the rainy than during the dry season, especially towards the forest interior. But low values of VPD also occurred during nighttime in the dry season.

The courses of the three selected microclimate parameters (T_{mean} , $H_{5\%-\text{quantil}}$, and $VPD_{\text{ampl.}}$) measured at the reference site in the open savanna during the study period (February - September) are shown in Fig. 3.10. T_{mean} decreased from about 32°C in the dry season to about 25°C in the rainy season. $H_{5\%-\text{quantil}}$ increased during this period from about 7% to about 62%. $VPD_{\text{ampl.}}$, being computed from T_{mean} and $H_{5\%-\text{quantil}}$, showed an opposite course to $H_{5\%-\text{quantil}}$ (Fig. 3.10).

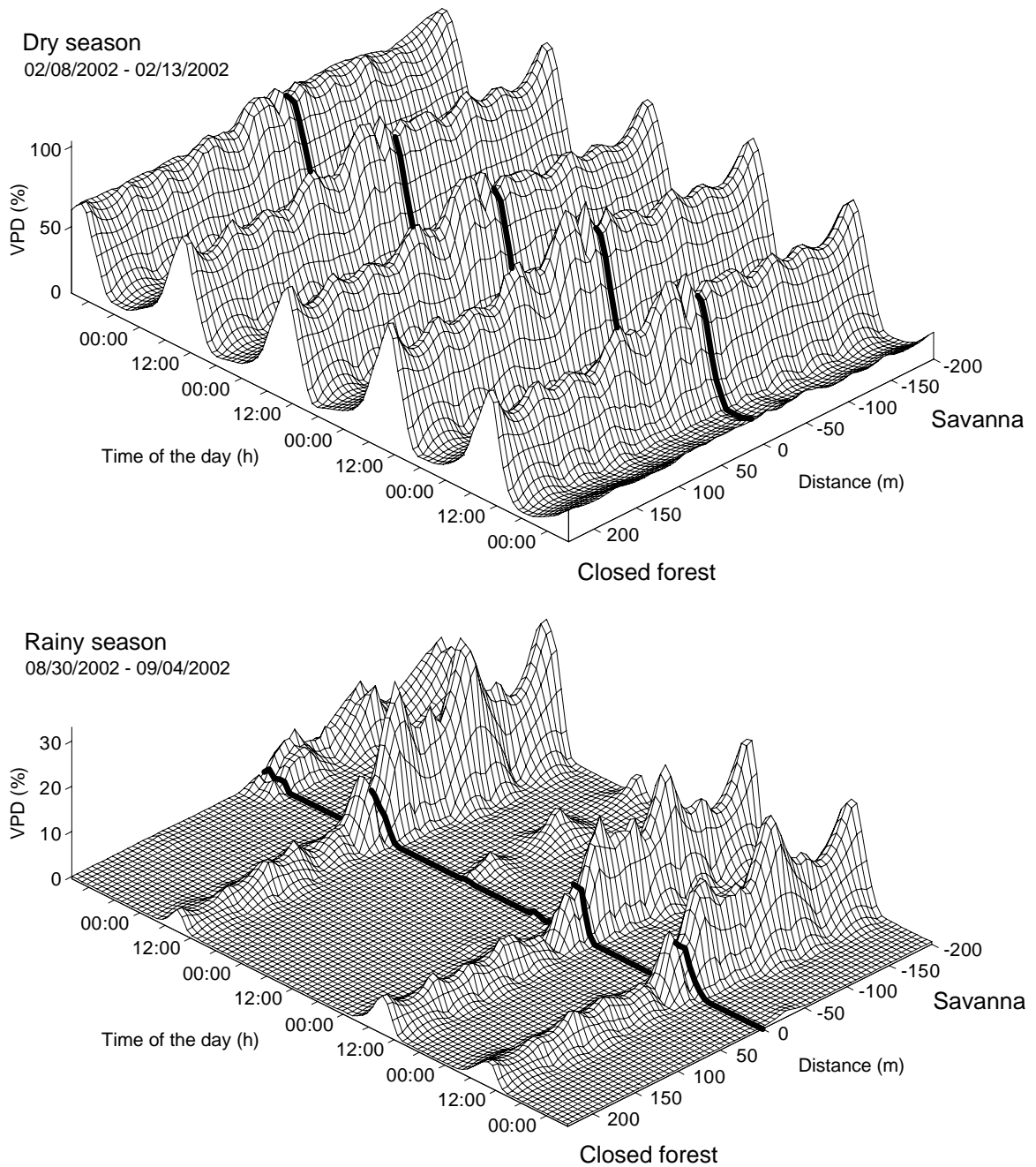


Fig. 3.9. 3D-presentation of two five-day courses of vapor pressure deficit (VPD) measured during the dry season (02/08/2002 - 02/13/2002) and rainy season (08/30/2002 - 09/04/2002) along the intensely studied transect T4 (20 data logger, sampling every 10 min). Data interpolation was computed with Surfer 7.04 (gridding method = kriging). The black line indicates the borderline between savanna and forest belt (0 m).

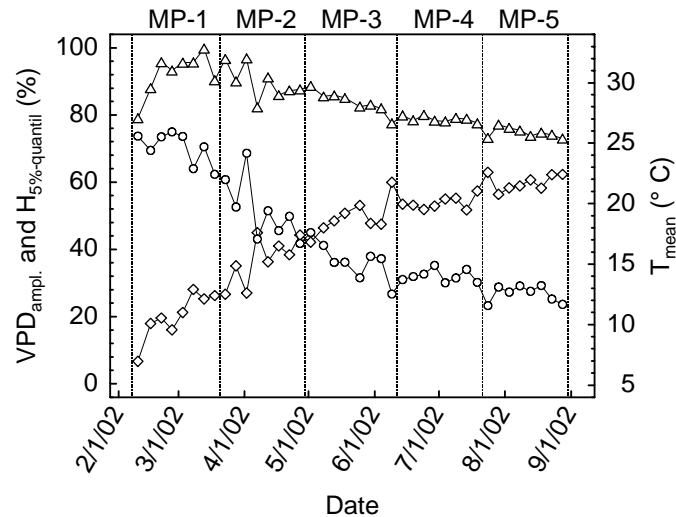


Fig. 3.10. Courses of three microclimatic parameters (T_{mean} (Δ) = five-day mean of diurnal mean air temperature, $H_{5\%-\text{quantil}}$ (\diamond) = five-day mean of diurnal 5%-quantil of air humidity, $VPD_{\text{ampl.}}$ (\circ) = five-day mean of diurnal amplitude of vapor pressure deficit) measured at the reference site in the open savanna in the Comoé National Park during the study period from 02/08/2002 to 08/30/2002. These values were used to standardize transect data.

Again exemplarily, $VPD_{\text{ampl.}}$ measured along the intensely studied transect for a five-day period during the rainy season is presented in Fig. 3.11. Border-and-ecotone detection analysis (BEDA) revealed a border between forest and savanna at -4.7 ± 10.5 m. The associated ecotone had a width of 34.9 m and the DEI towards the forest interior was 12.7 ± 18.9 m (Fig. 3.11). Conditions for $VPD_{\text{ampl.}}$ in the savanna and closed forest were $20.7 \pm 7.7\%$ and $5.2 \pm 7.5\%$, respectively.

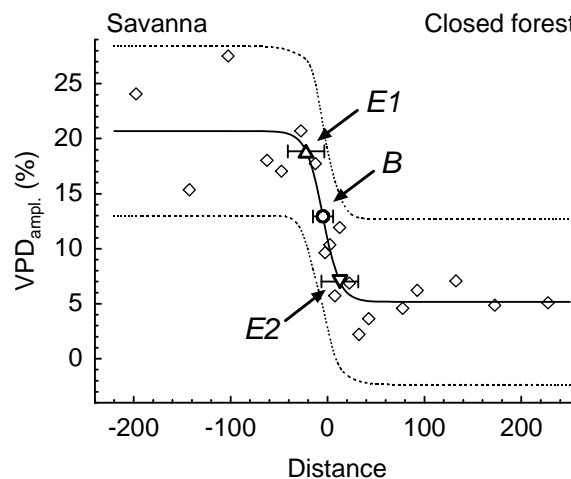


Fig. 3.11. Five-day mean of diurnal amplitude of vapor pressure deficit ($VPD_{\text{ampl.}}$) measured along the intensely studied transect from 08/30/2002 to 09/04/2002. The sigmoidal non-linear model (solid line) and its 95%-prediction bands (dashed lines) were presented. The asymptotes of the model were interpreted as the conditions in savanna and closed forest. Their variability was approximated by the 95%-prediction bands (savanna: $20.7 \pm 7.7\%$, closed forest: $5.2 \pm 7.5\%$). The magnitude of the effect between forest and savanna was given by the difference of the two asymptotes (15.5%). Border-and-ecotone-detection analysis (BEDA) revealed that the border (B \circ) was located at -4.7 ± 10.5 m. The associated ecotone ranged from -22.2 ± 18.9 m on the savanna side ($E1$ \triangle) to 12.7 ± 18.9 m ($E2$ ∇) towards the forest interior. $E2$ reflected the depth-of-edge influence (DEI) towards the forest interior.

Border and ecotone detection for the five MP for $\text{stdT}_{\text{mean}}$, $\text{stdH}_{5\%-\text{quantil}}$, and $\text{stdVPD}_{\text{ampl}}$. (data of the eight transects pooled within each MP) revealed borders mostly located near the borderlines between savanna and forest belt (0 m) that were well visible in the field (Fig. 3.12). The largest divergence of about 40 m occurred for $\text{stdT}_{\text{mean}}$ in MP-1, other values range between -14.5 m and 25.4 m (Fig. 3.12). For the three parameters, the border between forest and savanna was located further towards the forest during the dry season and further towards the savanna during the rainy season. The width of the associated ecotones varied from 31 m ($\text{stdH}_{5\%-\text{quantil}}$ in MP-2) to 192 m ($\text{stdT}_{\text{mean}}$ in MP-1). In general, the ecotones for $\text{stdT}_{\text{mean}}$ were wider than for $\text{stdH}_{5\%-\text{quantil}}$ and $\text{stdVPD}_{\text{ampl}}$. (Fig. 3.12). Values for DEI of all parameters in direction of the forest interior marked by the positions of *E2* were higher during the dry than the rainy season. E.g., for $\text{stdT}_{\text{mean}}$, a maximum value of 137.3 ± 138.3 m occurred in the dry season (MP-1) and a minimal value of 39.1 ± 36.3 m was detected in the rainy season (MP-5). The mean value of DEI for all microclimate parameters was 50.5 m. The difference between forest and savanna was more pronounced during the rainy season than during the dry season (Fig. 3.12 b, d, and f). In addition, the confidence intervals of the estimated parameters *E1*, *B*, *E2*, and the prediction bands were much narrower during the rainy than during the dry season. This reflected the more distinct edge effects during the rainy season (Fig. 3.12).

A cubic model was used in the linear mixed effects model as an approximation of the sigmoidal non-linear model (see VPD_{ampl} in Fig. 3.13 as an example). The mean of the cubic model was mostly located within the 95%-confidence bands of the sigmoidal model (see Fig. 3.13). Only for MP-4 and MP-5, where the confidence bands were rather narrow, the mean of the cubic model was beyond the 95%-confidence, especially in the asymptotic part of the non-linear model. However, the cubic approximation was still satisfying. This was also the case for T_{mean} and $\text{H}_{5\%-\text{quantil}}$.

For the parameter $\text{stdVPD}_{\text{ampl}}$, model selection revealed that transects being nested in MP as random factor did not significantly improve the model (Table 3.3). About half of the remaining standard deviation was explained by MP as random effect. For $\text{stdH}_{5\%-\text{quantil}}$, transects being nested in MP significantly improved the model, but only a small amount of standard deviation accorded to this random factor. For $\text{stdT}_{\text{mean}}$, about 1/3 of the standard deviation was explained by the significant random factor transect being nested in MP (Table 3.3).

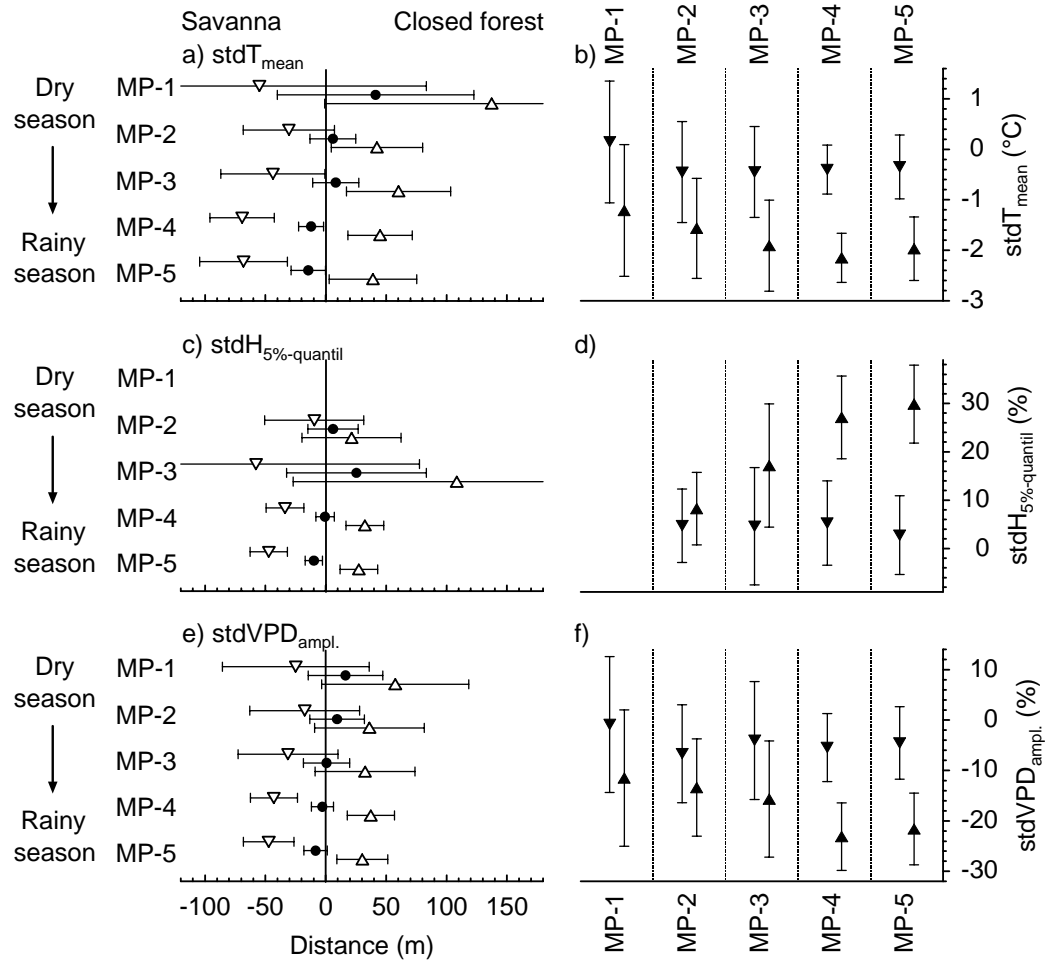


Fig. 3.12. Borders and ecotones detected by BEDA for three standardized microclimatic parameters for the five measuring periods (MP-1 to MP-5, compare Fig. 3.10). $\text{stdT}_{\text{mean}}$ = standardized five-day mean of diurnal mean air temperature, $\text{stdH}_{5\%-\text{quantil}}$ = standardized five-day mean of diurnal 5%-quantil of air humidity, $\text{stdVPD}_{\text{ampl.}}$ = standardized five-day mean of diurnal amplitude of vapor pressure deficit, E1 = ecotone limit towards the savanna ($E1$), B = border between forest and savanna (B), E2 = ecotone limit towards the closed forest ($E2$), ∇ = approximation of the asymptote towards the savanna, \blacktriangle = approximation of the asymptote towards the closed forest. Error bars represented 95%-confidence intervals and 95%-prediction bands, respectively. Transect effects were ignored in the models. For $\text{H}_{5\%-\text{quantil}}$ and MP-1 fitting, the non-linear model failed.

Table 3.3. Results of random effects of linear mixed effects models with a cubic term computed as approximations of sigmoidal non-linear models for three microclimatic parameters being standardized by the values of the reference data logger at an open savanna site ($\text{stdT}_{\text{mean}}$ = standardized five-day mean of diurnal mean air temperature, $\text{stdH}_{5\%-\text{quantil}}$ = standardized five-day mean of diurnal 5%-quantil of air humidity, $\text{stdVPD}_{\text{ampl.}}$ = standardized five-day mean of diurnal amplitude of vapor pressure deficit). StdDev = standard deviation, MP = measurement period, AR1 = autoregressive correlation structure of order 1.

Parameter	AR1 (Phi)	MP (StdDev)	Transect nested in MP (StdDev)	Residuals (StdDev)
$\text{stdT}_{\text{mean}}$	0.252	2.391	1.124	0.358
$\text{stdH}_{5\%-\text{quantil}}$	0.896	21.530	0.304	9.004
$\text{stdVPD}_{\text{ampl.}}$	0.355	4.092	-	5.097

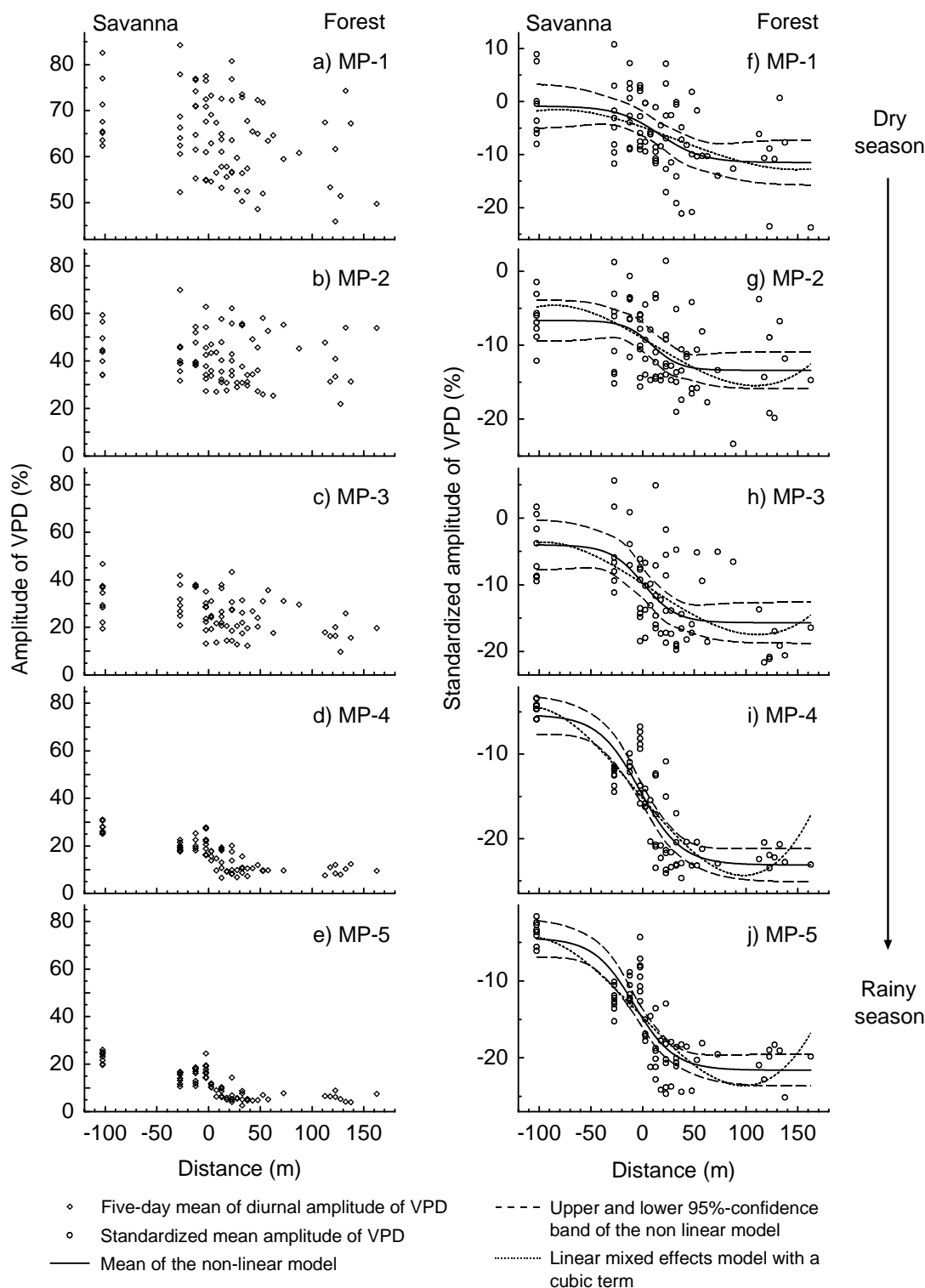


Fig. 3.13. Panel a-e represented the five-day mean of diurnal amplitude of vapor pressure deficit ($VPD_{ampl.}$) for the five measurement periods (MP-1 to MP-5). Panel f-j showed the standardized values ($stdVPD_{ampl.}$, compare Chapter 2.4.1). The data of each measurement period (MP) were fitted by a sigmoidal model where transect effects were ignored. A linear mixed effects model with a cubic term ($stdVPD_{ampl.} \sim a1 * Distance^3 + a2 * Distance^2 + a3 * Distance + b0$) was used as an approximation of the sigmoidal model. This linear mixed effects model comprised MP and transect nested in MP as random factor and, additionally, an autoregressive correlation structure of order 1. In the case of $stdVPD_{ampl.}$, no transect effect occurred (see Table 3.3). The quality of the cubic approximation could be appreciated from its location between the upper and lower 95%-confidence band of the sigmoidal non-linear model. Results of BEDA carried out for the five MPs are presented in Fig. 3.12 e and f.

3.4 Border and ecotone detection by means of vegetation composition

Along the intensely studied transect, the dissimilarity profile computed on the basis of the cover of all species in the 64 relevés showed a clear and significant peak of dissimilarity (Fig. 3.14 a). The location of the borderline between savanna and forest belt observed in the field was in good accordance with the one detected by the split-moving-window dissimilarity analysis (SMWDA) using the cover of all species. Moving-window regression analysis (MWRA) showed an ecotone width of 125 m, i.e., 50 m into the savanna and 75 m into the forest (Fig. 3.14 a). Thus, according to the cover of all species the depth-of-edge influence (DEI) was 75 m.

The dissimilarity profiles presented in Fig. 3.14 b and c were computed from the cover of grasses and herbs, respectively. Both profiles showed a single border, but for the grass-data set, both the position of the maximum of dissimilarity and the location of the ecotone, were indicated further in the savanna than for the herb-data set. For herbs, ecotone detection was somewhat fuzzy with a second peak at 5 m on the savanna that could not be separated as a border of its own (Fig. 3.14 c). The observed pattern was a result of a continuous species turnover, particularly involving the abundant grasses *Andropogon gayanus* and *Panicum phragmitoides* (savanna), *Setaria barbata* (forest belt/closed forest), and *Sporobolus pyramidalis* (forest belt), as well as the characteristic herbs *Blepharis maderaspatensis* and *Geophila repens* (closed forest), *Justicia insularis* (savanna/forest belt), and *Mitracarpus villosus* (savanna).

The dissimilarity profile computed for the cover of woody climbers (Fig. 3.14 d) showed a significant border at 25 m which was in good accordance with the border between closed forest and forest belt visible in the field. The associated ecotone of 30 m was rather narrow. This distinct pattern was caused by a regular appearance of woody climbers such as *Campylostemon warneckeanum*, *Motandra guineensis*, *Salacia baumannii*, and *Saba comorensis* in forest plots and their missing in savanna plots.

The cover of trees and shrubs revealed an ecotone of 100 m in width (window midpoint position from 20 m into the savanna to 80 m into the forest, Fig. 3.14 e), wherein several significant peaks were detected. In addition, a border with a very narrow ecotone (15 m) occurred at 115 m. The observed change in tree- and shrub-species composition between savanna and forest belt was associated with an increase in stem density and tree and shrub cover towards the forest interior (compare Fig. 3.1 a).

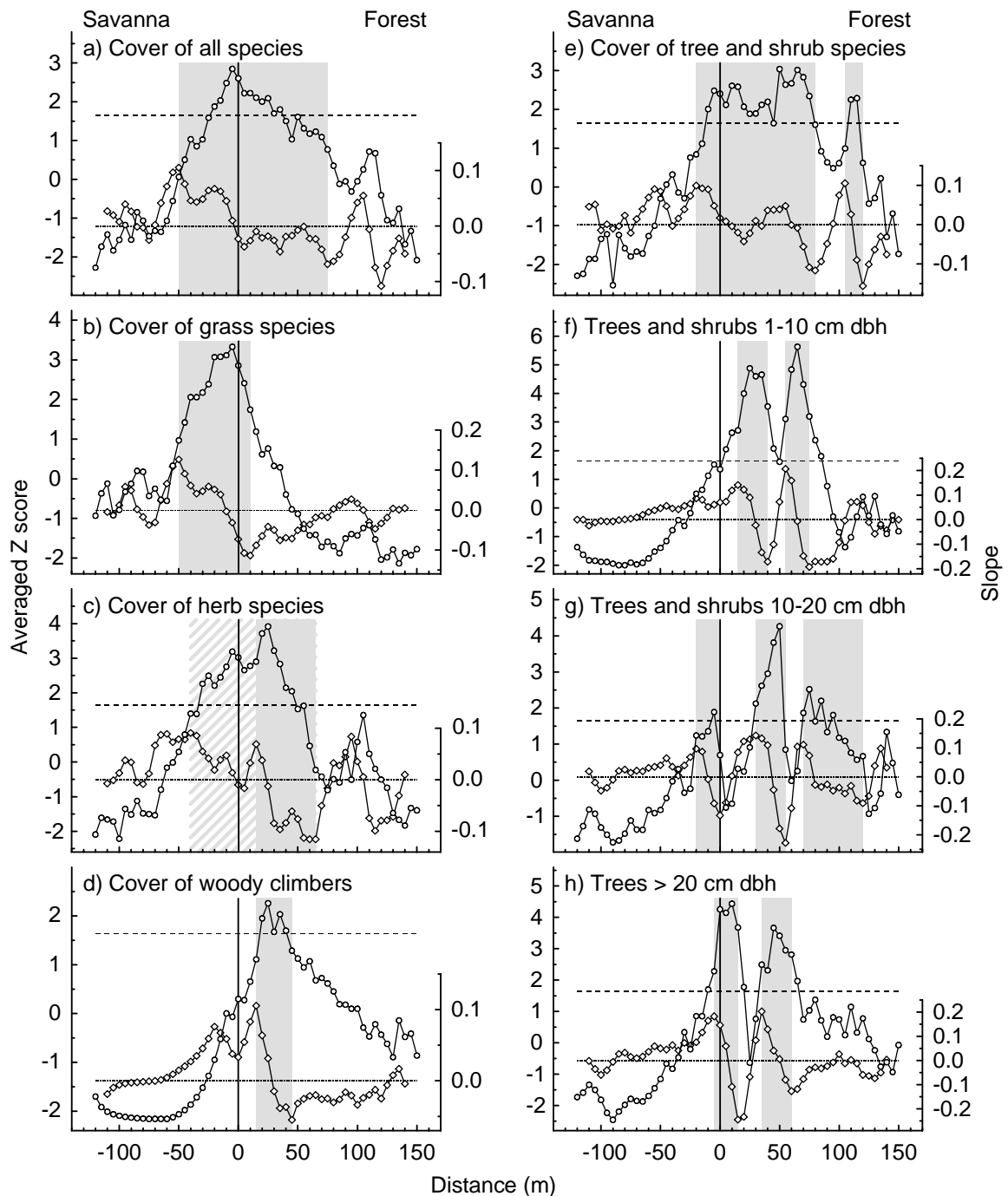


Fig. 3.14. Pooled average Z scores (circles) computed by the split-moving-window dissimilarity analysis (SMWDA, window sizes from 2 to 20 were included) and slopes calculated by the moving-window regression analysis (MWRA, diamonds) for the intensely studied transect for cover of all species (a, 133 species), grasses (b, 22 species), herbs (c, 45 species), woody climbers (d, 14 species), and for counted tree and shrub individuals of different size classes (f, 18 species; g, 11 species; h, 12 species). The upper horizontal line marks the one-tailed 95%-confidence interval that is used as a significance level of the SMWDA to detect borders. The lower horizontal line reflects the zero-baseline of slopes of the MWRA. The borderline between savanna and forest belt being visible in the field is placed at a distance of zero meters (vertical line). Ecotones are marked gray (fuzzy detected ecotones: dashed gray).

The rather imprecise border detection by cover of tree and shrub species could be clarified by examining the pattern of tree- and shrub-size classes (Fig. 3.14 f-h). The dissimilarity profile computed for trees and shrubs of 1-10 cm dbh along the intensely studied transect showed

two significant borders (Fig. 3.14 f). The first border at 25 m and its associated ecotone were congruent with the detected border and ecotone for woody climbers and, as mentioned above, reflected the location of the border between closed forest and forest belt that was visually identified in the field. Between the two detected ecotones with a width of 25 m and 15 m, a non-ecotone zone of 15 m occurred (Fig. 3.14 f). It was characterized by a high density of shrubs, mainly *Croton membranaceus* and *Mallotus oppositifolius*. The DEI could be marked at 75 m, that was the same as detected for the cover of all species (Fig. 3.14 a).

The dissimilarity profile computed for tree and shrub species of 10-20 cm dbh showed three significant borders (Fig. 3.14 g). Near the stratified border between savanna and forest belt (window midpoint position of -5 m), a peak of the averaged Z score occurred that was just above the significance level (ecotone width of 20 m, Fig. 3.14 g). A second significant border was detected at the window midpoint position of 50 m (ecotone from 30 m to 55 m). Between these two borders, the tree species *Anogeissus leiocarpus* showed a high abundance. At the window midpoint position of 75 m a third significant peak of dissimilarity occurred. Between the second and third border, *Diospyros abyssinica* was dominant. Further to the forest interior, *Tapura fischeri* became the most abundant species besides *D. abyssinica*. The ecotone associated with the third border took a width of 60 m and reached up to 120 m into the forest interior (Fig. 3.14 g).

Table 3.4. Width of the forest belt visible in the field, depth-of-edge influence (DEI) detected for tree species larger than 20 cm dbh along eight forest-savanna transects and number of species involved in the analysis. Correlation (Pearson) between width of forest belt and DEI: $r = 0.852$, $P = 0.015$. IST = intensely studied transect; n.s. = not significant.

Transect	Width of forest belt (m)	DEI for tree individuals > 20 cm dbh (m)	Number of species > 20 cm dbh
T1	20	35	5
T2	15	50	5
T3	20	45	8
T4 (IST)	30	60	12
T5	60	100	8
T6	35	55	8
T7	10	55	8
T8	25	n.s.	7
Median	22.5	55	

SMWDA for tree species larger than 20 cm dbh revealed two significant borders. Between them, *Anogeissus leiocarpus* showed a high abundance (Fig. 3.14 h). Detected ecotones at the first and second border had a width of 20 m and 25 m, respectively. For this tree-size class, the DEI was 60 m.

Seven of the eight transect replicates showed significant borders for tree individuals larger than 20 cm dbh using SMWDA and confirmed the results from the intensely studied transect. For these transects, the associated ecotones and the DEI were detected by MWRA. The median of the DEI values is 55 m with a maximum of 100 m and a minimum of 35 m (Table 3.4). The width of the forest belt visually stratified in the field showed a high linear correlation with DEI detected by SMWDA and MWRA for tree individuals larger than 20 cm dbh (Pearson: $r = 0.852$, $P = 0.015$), but values of the former reach only about half of the values of the latter (Table 3.4).

3.5 Core-area analysis

The detected DEI along the studied forest-savanna transects regarding vegetation composition, microclimate, structural parameters, grass biomass, and fire were summarized in the Table A. 1. The lowest DEI was 0 m for the median of DEI of fire. The highest DEI of 137.3 m occurred for air temperature during the dry season. Most detected DEI ranged from 20 m to 60 m (see Table A. 1 in the Appendix).

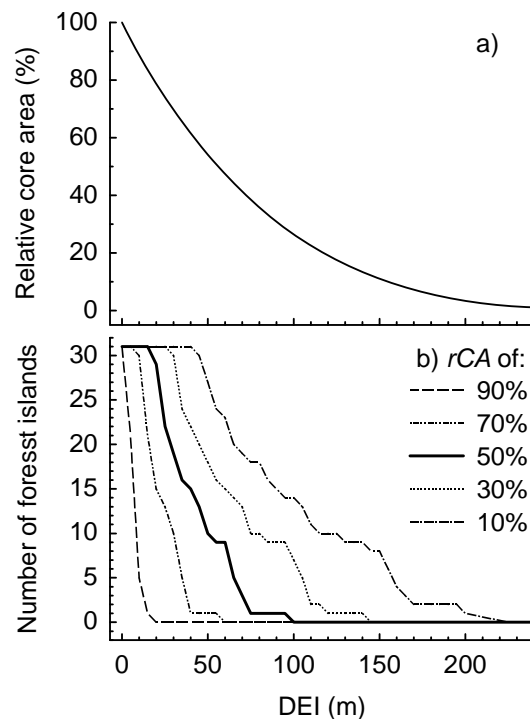


Fig. 3.15. a) Sum of relative core area (rCA) for 31 studied semi-deciduous forest islands in dependence on depth-of-edge influence (DEI). b) Number of forest islands that contained a rCA of 90 - 10% in dependence on DEI.

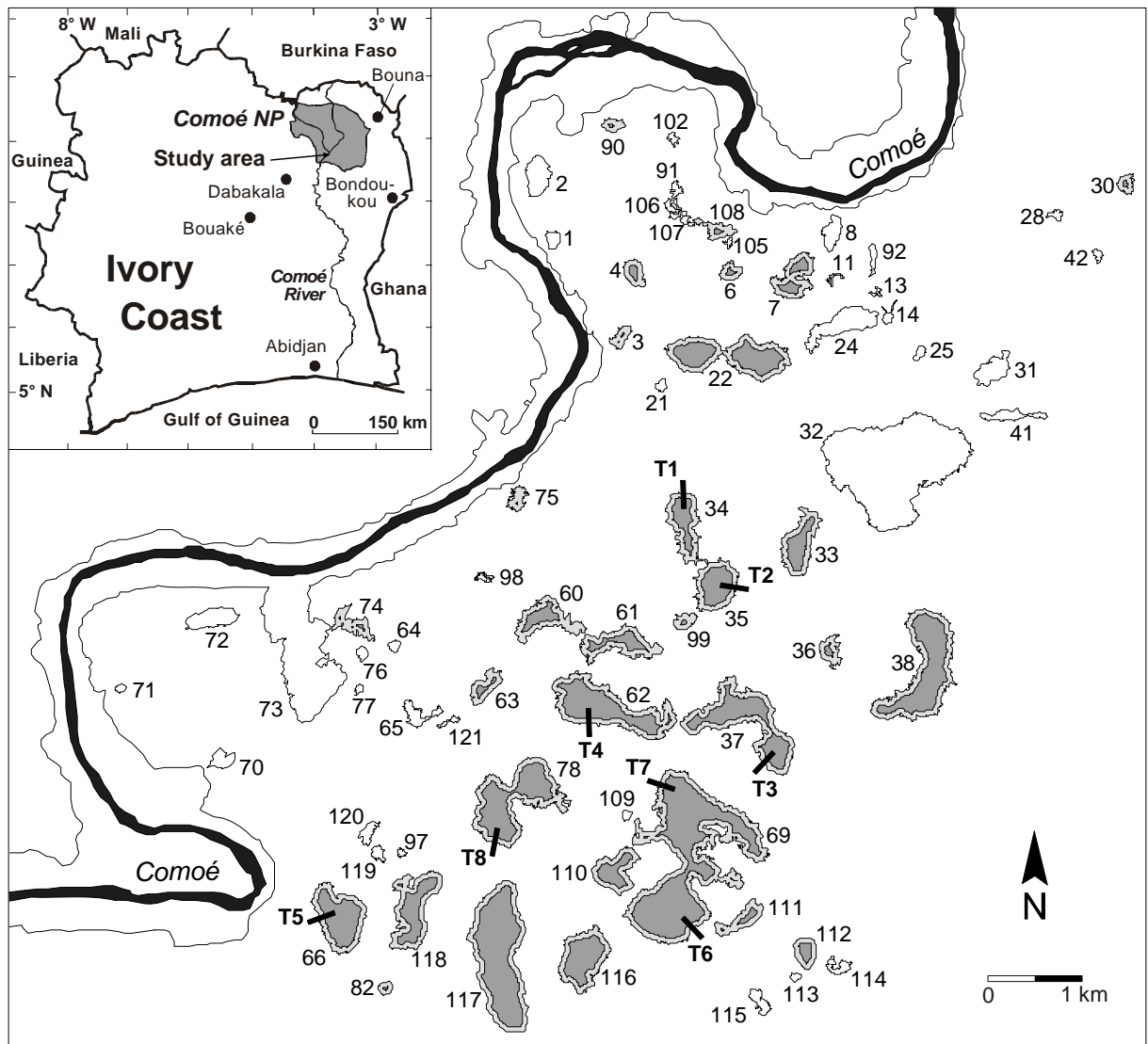


Fig. 3.16. Map of the study area in the southwestern part of the Comoé National Park (CNP). Presented are forest islands > 0.5 ha that were mapped with a handheld GPS. The location of the Comoé river (black) and the borderline of the gallery forest were digitized from a satellite image (Landsat ETM+ image from December 2002). Gallery forest and forest islands that did not belong to the studied type of semi-deciduous forest are displayed white. Studied forest islands were colored light-gray. The dark-gray area inside of each studied forest island represented the remaining core area (CA) assuming a depth-of-edge influence (DEI) of 55 m. Locations of the eight forest-savanna transects (T1-T8) are marked with black bars.

On the basis of 31 GPS-mapped semi-deciduous forest islands, core-area analysis was carried out by subtracting a buffer zone of 5 m to 250 m (5 m steps). The sum of relative core area (rCA) of these forest islands was plotted versus the DEI in Fig. 3.15 a. The number of forest islands that contained a specific rCA in relation to DEI is given in Fig. 3.15 b. A rCA of 50% regarding all forest islands occurred for a DEI of about 55 m (Fig. 3.15 a), but only nine forest islands of 31 (29%) still contained a rCA of at least 50% (Fig. 3.15 b). This situation is illustrated in Fig. 3.16. For a DEI of 75 m, only one forest island was left that contained a rCA of 50% (Fig. 3.15 b), but the sum of rCA was still about 38% (Fig. 3.15 c).

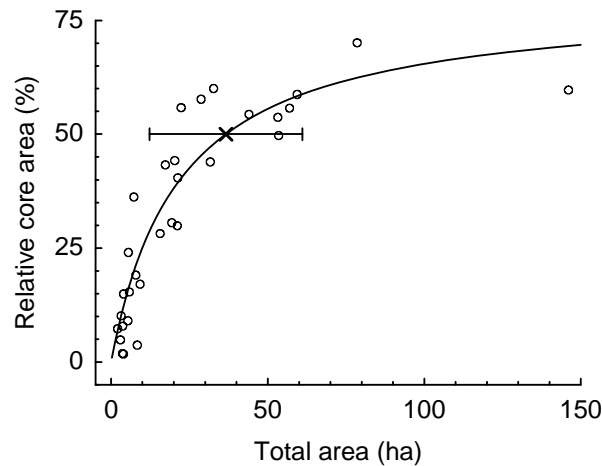


Fig. 3.17. Relative core area (rCA) and total area (TA) of semi-deciduous forest islands. In the non-linear regression analysis forest islands were considered that still contained a core area after subtracting a buffer of 55 m. Non-linear fit ($n = 31$): $rCA = (a * TA) / (TA + b)$; $P < 0.001$, $r^2 = 0.855$, $a = 79.784 \pm 7.581$, $b = 21.823 \pm 5.038$, $Corr_{a,b} = 0.909$. $TA_{(rCA = 50\%)} = 36.6$ ha (cross), the error bar reflects the 95% confidence interval ($CI_{TA(rCA = 50\%), 0.025, 0.975} = 12.3$ ha, 61.0 ha; compare Appendix A).

Fig. 3.17 shows the relation between the rCA for a buffer size of 55 m and the total area of forest islands ($n = 31$). The applied non-linear model revealed that for this buffer size an rCA of 50% could be expected for forest islands with a size of 36.6 ± 24.4 ha). This analysis was computed for buffer sizes of 5 m to 250 m (5 m steps, Fig. 3.18). The size of forest islands being required to guarantee that a forest island contained a rCA of 50% increased with increasing DEI. The quality of the estimates decreased with increasing DEI well visible from the 95%-confidence intervals (Fig. 3.18), but the distribution of standardized residuals and Q-Q plots were still satisfying.

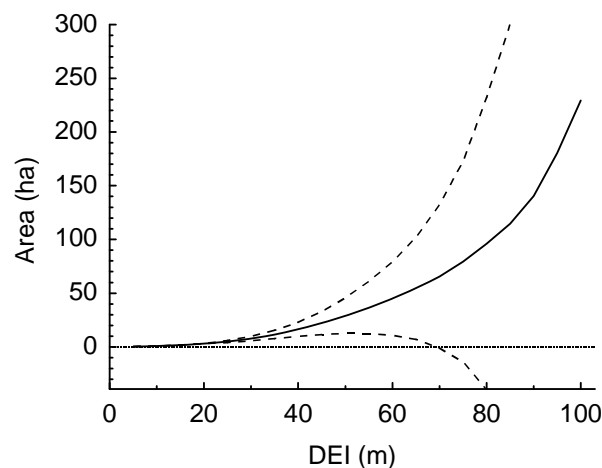


Fig. 3.18. Size of forest islands required to guarantee that a forest island contains a relative core area (rCA) of 50% in dependence on depth-of-edge influence (DEI). Shown are $TA_{(rCA = 50\%)}$ (line) and $CI_{TA(rCA = 50\%), 0.025, 0.975}$ (dashed lines) calculated for 5 m steps (compare Fig. 3.17 and Appendix A). At DEI of 100 m, 19 of 31 the studied forest islands contained a core area.

3.6 Size-class distribution of tree species with a focus on *Anogeissus leiocarpus*

Structures of tree populations

The population structure of *Anogeissus leiocarpus* and of all trees showed a typical age pyramid, with high densities of smaller diameter classes (DC1: up to 8000 individuals/ha) and lower densities of larger diameter classes (DC4: up to 65 individuals/ha; Fig. 3.19, see also Table 3.5). Except for the smallest diameter class, which was randomly distributed along the transects (Fig. 3.19 a), density values for all trees were significantly higher in the forest (For) and lower in the savanna (Sav), with a gradual change being observed at the S-Eco, B-Eco, and F-Eco segment (Fig. 3.19 b-d).

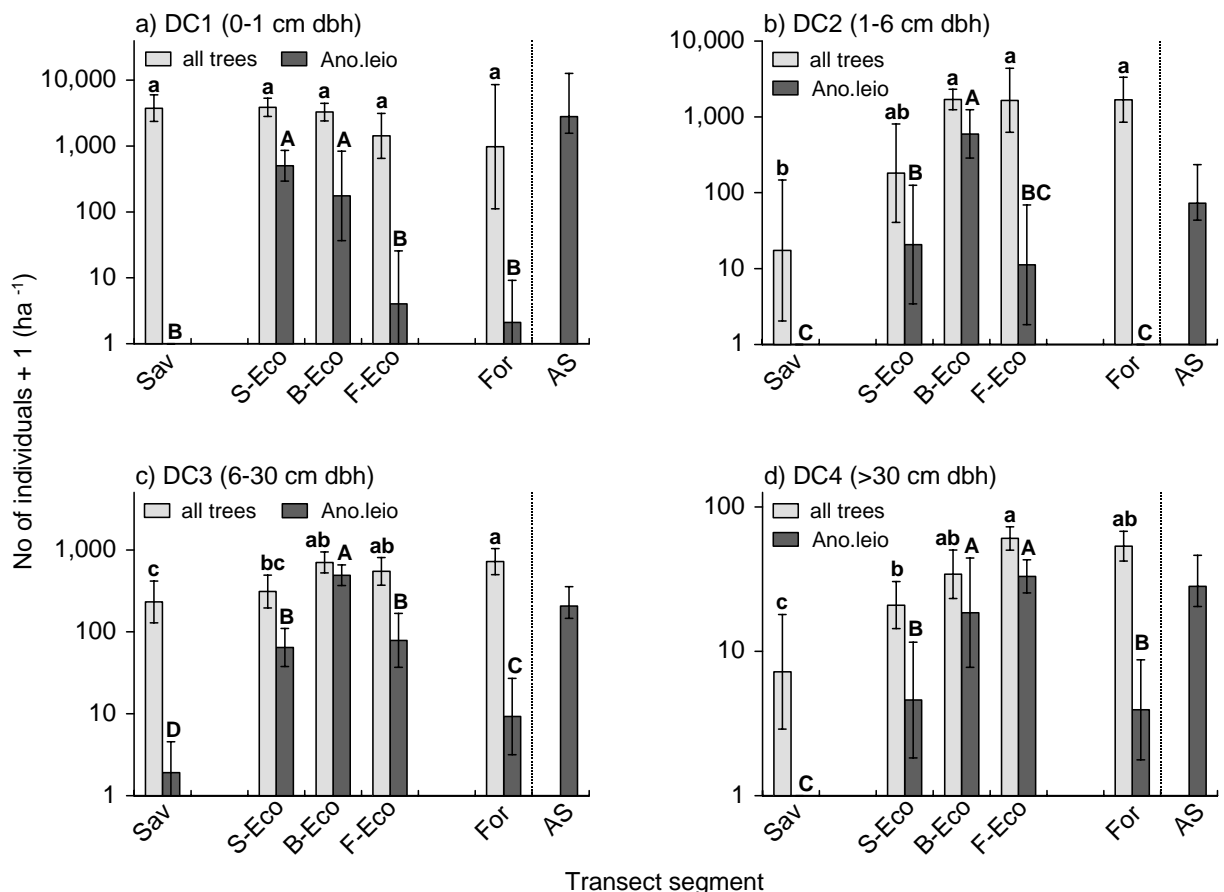


Fig. 3.19. Mean abundance and 95%-confidence intervals of four diameter classes (DC1-DC4) of *Anogeissus leiocarpus* and of all trees (including *A. leiocarpus*) along eight forest-savanna transects (transect segments: Sav, S-Eco, B-Eco, F-Eco, For; compare Fig. 2.5 d) and a human-influenced monodominant *A. leiocarpus* stand (AS) in the CNP. Different letters (small letters: all trees; capital letters: *A. leiocarpus*) indicate statistically significant differences between transect segments (multiple range test ($\alpha = 0.05$, TUKEY, SPSS 11.0) subsequent to a two-way ANOVA). No differences between transects and no interaction effects occurred. The *Anogeissus* stand was not included in the analysis.

Anogeissus leiocarpus itself was almost completely absent from the forest and savanna segment (For, Sav; Fig. 3.19). All diameter classes occurred with high-density values near the forest border (S-Eco, B-Eco, F-Eco). There, the diameter class composition of *A. leiocarpus* indicated a gradual change with the smallest diameter class (DC1) being most abundant towards the savanna-ecotone segment (S-Eco, B-Eco; Fig. 3.19 a), the two middle diameter classes (DC2 and DC3) in the belt-ecotone segment (B-Eco; Fig. 3.19 b and c) and the largest trees (DC4) towards the forest-ecotone segment (B-Eco, F-Eco; Fig. 3.19 d). For the whole data set presented in Fig. 3.19, neither significant differences between transects nor combination effects between transects and transect segments were observed.

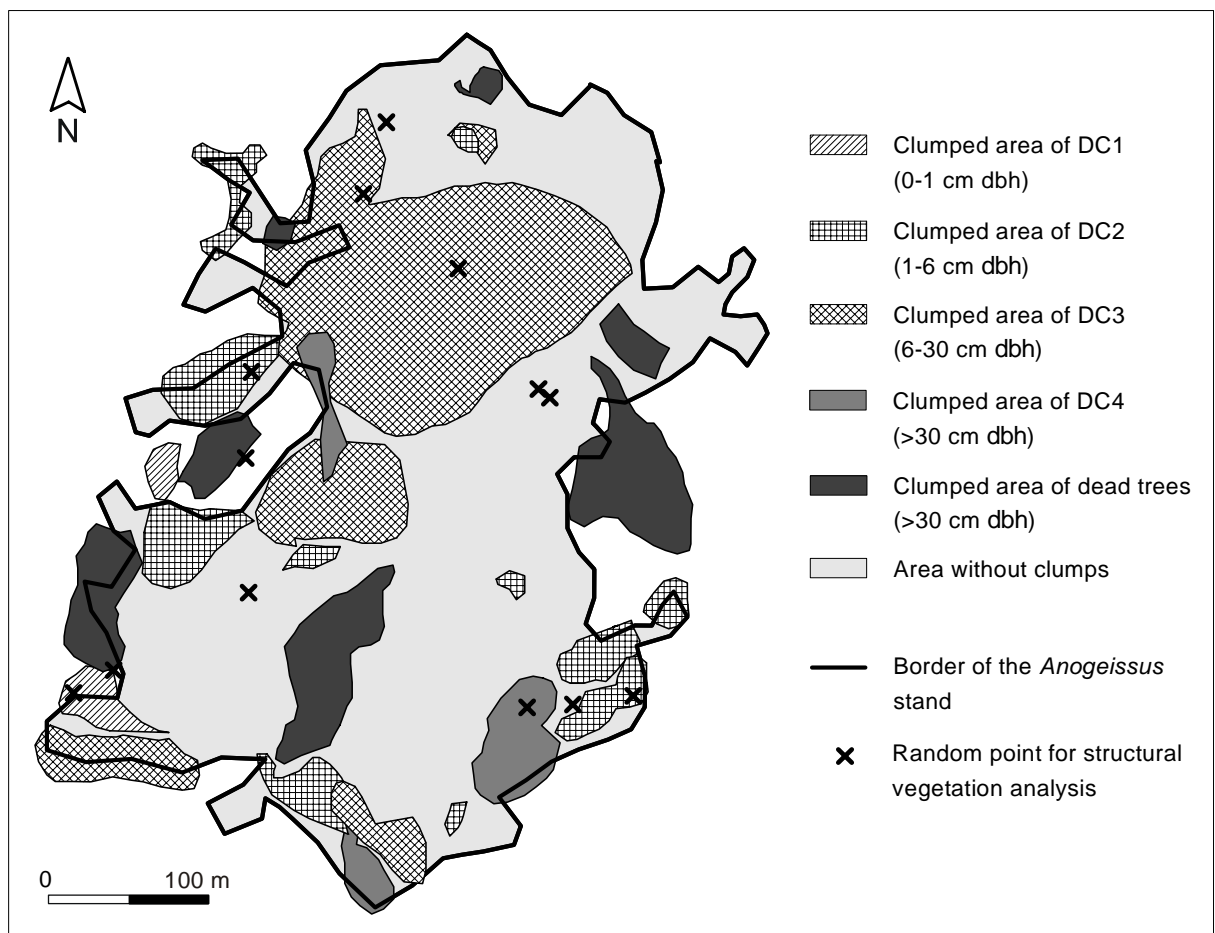


Fig. 3.20. Map of clumped occurrence of the different diameter classes (DC1-DC5) in a human-influenced monodominant stand of *Anogeissus leiocarpus* (about 3.9 ha; forest number in Fig. 2.1: 75).

Hines' test statistic from randomness of T-square data (Krebs 1999) revealed a clumped spatial pattern for all diameter classes in the monodominant *Anogeissus* stand. Fig. 3.20 illustrates aggregated areas mapped with a hand held GPS for the five diameter classes of *A. leiocarpus*. Aggregations of the two smaller diameter classes (DC1 and DC2) were mainly located near the forest border whereas areas with clumps of diameter class DC3 were found more to the forest center. Clumps of diameter class DC4 were rarely mapped because density of DC4 was low. Patchy dieback events of *A. leiocarpus* were found in the forest interior as

well as at the forest border (DC5 in Fig. 3.20). In addition, the *Anogeissus* stand was characterized by a frayed borderline.

In the *Anogeissus* stand, the density of the smallest diameter class (DC1) was more than three times higher than that in the transect segments, being significantly different from all transect segments (Fig. 3.19 a). In contrast, the low density of the diameter class DC2 found in the *Anogeissus* stand was similar to the density in the S-Eco and F-Eco segments (Fig. 3.19 b). With about 200 individuals/ha in the *Anogeissus* stand, density of diameter class DC3 took a medium position between the density in the B-Eco segment and in the F-Eco and S-Eco segments (Fig. 3.19 c), whereas density data of the largest diameter class (DC4) were similar to those of the B-Eco and F-Eco segment (Fig. 3.19 d).

On the basis of the heterogeneous results for each diameter class of *A. leiocarpus* (Fig. 3.19), a clear similarity between transect segments and the *Anogeissus* stand (AS) is not evident. Therefore a PCA was computed for the complete density data set of *A. leiocarpus*, where diameter classes were handled as species. Fig. 3.21 a shows the first two axes of the four-dimensional space explaining 87.3% of the variance of the data set. Three clearly distinct clusters, which are marked by their 80% confidence ellipses (cluster 1-3, Fig. 3.21 a) were separated along the two axes. The scores of the *Anogeissus* stand (AS) were not considered when calculating the confidence ellipses. Within this PCA diagram, the *Anogeissus* stand (AS) is located next to the 80% confidence ellipse of the third cluster containing seven B-Eco and five S-Eco segments. The S-Eco segments are plotted in direct contiguity to the *Anogeissus* stand (AS). Thus, on the basis of the diameter class composition of *A. leiocarpus* the patchy *Anogeissus* stand (AS) was most similar to the S-Eco and B-Eco segments.

With regard to structural vegetation data, the first PCA axis explains 55.6% of the variance (Fig. 3.21 b), reflecting the ecological gradient along the studied transects. Plots of the savanna and the closed forest are clearly separated along the first axis of the PCA diagram. S-Eco, B-Eco, and F-Eco plots show a gradual change from savanna (Sav) to closed-forest plots (For). The 80% confidence ellipse for the structural vegetation data of the *Anogeissus* stand (AS) was used to characterize which transect segment is most similar to the *Anogeissus* stand with respect to structural vegetation data (Fig. 3.21 b). Within the area of the confidence ellipse, 50% of Sav, 42% of B-Eco, and 33% of S-Eco plots are located, but only 13% of F-Eco and 0% of For plots. Hence on the basis of structural vegetation data, the *Anogeissus* stand was clearly most similar to savanna, savanna-ecotone and belt-ecotone segments.

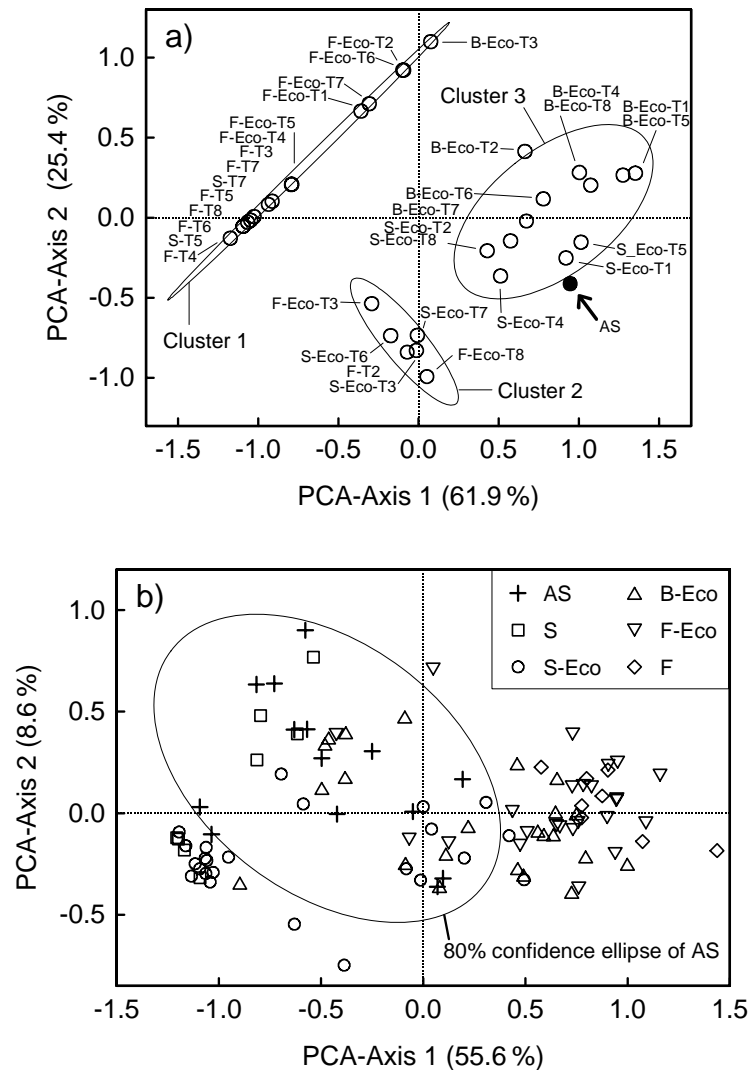


Fig. 3.21. a) Sample scores of the first and second PCA axes for the abundance of four diameter classes from the transect segments (Sav, S-Eco, B-Eco, F-Eco, For; compare Fig. 2.5 d) of eight transects (T1-T8) and the *Anogeissus* stand (AS). The first two PCA-axes explain 87.3% of the variance. Three distinct clusters are symbolized by 80% confidence ellipses (AS scores excluded). b) Sample scores of the first and second PCA axes for structural vegetation data from the *Anogeissus* stand and five transect segments. 64.2% of the variance is explained by the first two PCA-axes. 80% confidence ellipse is given for the sample scores of the *Anogeissus* stand (AS). The following portions of plot types are located in the area of the 80% confidence ellipse of the *Anogeissus* stand (AS): AS = 13/14; Sav = 4/8; S-Eco = 8/24; B-Eco = 10/24; F-Eco = 3/24; For = 0/24.

Table 3.5. (next page) Mean abundance of four diameter classes (DC1-DC4) of 10 dominant tree species in transect segments with high abundance of *A. leiocarpus* (S-Eco, B-Eco, and F-Eco; compare Fig. 2.5 d). Each transect segment is divided in three sub-segments (Sub1-Sub3). Different letters indicate statistically significant differences between sub-segments (multiple range test ($\alpha = 0.05$, TUKEY, SPSS 11.0) subsequent to a two-way ANOVA; P-tran = significance level of transects, P-plot = significance level of sub-segments; a.v. = assumptions of ANOVA violated; n = number of replicates per sub-segment).

Table 3.5.

Species	Abundance (individuals/ha)									P-tran	P-plot
	S-Eco			B-Eco			F-Eco				
	Sub1 (n=8)	Sub2 (n=8)	Sub3 (n=8)	Sub1 (n=8)	Sub2 (n=7)	Sub3 (n=8)	Sub1 (n=8)	Sub2 (n=8)	Sub3 (n=8)		
<i>Manilkara multinervis</i>											
DC1	0.9	-	3.1	19.6	5.6	3.1	0.9	1.4	7.7	0.056	0.311
DC2	-	-	-	-	-	-	-	-	-	a.v.	a.v.
DC3	-	-	-	-	-	-	-	-	-	a.v.	a.v.
DC4	-	-	0.5	0.6	-	-	-	0.5	-	a.v.	a.v.
<i>Dialium guineense</i>											
DC1	- ^a	- ^a	- ^a	3.3 ^a	3.6 ^a	17.4 ^a	7.0 ^a	4.5 ^a	11.0 ^a	0.001	0.034
DC2	-	-	-	-	-	-	3.3	3.5	-	a.v.	a.v.
DC3	-	-	-	-	-	-	-	0.6	1.8	a.v.	a.v.
DC4	-	-	-	-	-	-	0.5	1.1	0.5	a.v.	a.v.
<i>Diospyros abyssinica</i>											
DC1	- ^c	- ^c	0.9 ^{bc}	3.7 ^{abc}	6.6 ^{abc}	11.6 ^{abc}	80.6 ^{ab}	51.1 ^{ab}	112.7 ^a	0.018	0.001
DC2	- ^b	- ^b	- ^b	0.9 ^b	- ^b	14.5 ^{ab}	21.2 ^{ab}	23.8 ^{ab}	105.4 ^a	0.055	0.001
DC3	- ^c	- ^c	0.5 ^c	1.0 ^{bc}	- ^c	5.1 ^{cb}	14.4 ^b	167.1 ^a	277.5 ^a	0.001	0.001
DC4	-	-	-	-	-	-	-	0.5	-	a.v.	a.v.
<i>Diospyros mespiliformis</i>											
DC1	1.6 ^{cd}	7.4 ^{bcd}	0.9 ^d	125.5 ^{ab}	499.2 ^a	288.9 ^{ab}	799.5 ^a	77.8 ^{abc}	10.6 ^{bcd}	0.001	0.001
DC2	- ^a	- ^a	0.9 ^a	0.9 ^a	1.4 ^a	7.7 ^a	9.3 ^a	15.3 ^a	7.7 ^a	0.001	0.023
DC3	-	-	-	-	-	0.9	0.6	1.3	1.3	0.762	0.465
DC4	- ^b	- ^b	- ^b	- ^b	- ^b	- ^b	- ^b	1.1 ^{ab}	4.0 ^a	0.087	0.001
<i>Combretum nigricans</i>											
DC1	- ^c	1.3 ^{bc}	1.7 ^{abc}	101.0 ^a	46.9 ^{ab}	14.2 ^{abc}	4.1 ^{abc}	3.1 ^{abc}	1.1 ^{bc}	0.001	0.003
DC2	-	-	0.9	2.8	4.3	8.5	1.2	-	-	0.303	0.160
DC3	-	-	-	2.1	4.6	6.0	10.3	0.9	-	0.026	0.024
DC4	-	-	-	-	0.7	0.5	0.5	-	-	a.v.	a.v.
<i>Anogeissus leiocarpus</i>											
DC1	103.3 ^{ab}	110.2 ^{ab}	84.5 ^{ab}	340.4 ^a	13.7 ^{ab}	0.9 ^b	4.2 ^{ab}	1.1 ^b	0.9 ^b	0.055	0.001
DC2	- ^c	3.3 ^c	18.3 ^{abc}	275.1 ^{ab}	487.0 ^a	312.5 ^{ab}	9.9 ^{abc}	7.0 ^{bc}	0.9 ^c	0.202	0.001
DC3	4.8 ^b	40.5 ^{ab}	69.6 ^{ab}	520.2 ^a	418.2 ^a	416.3 ^a	35.0 ^{ab}	57.2 ^{ab}	23.2 ^b	0.740	0.001
DC4	1.3 ^b	0.5 ^b	2.7 ^{ab}	6.9 ^{ab}	6.6 ^{ab}	14.3 ^{ab}	41.3 ^a	12.3 ^{ab}	13.9 ^{ab}	0.147	0.001
<i>Detarium microcarpum</i>											
DC1	26.6 ^a	30.8 ^a	12.4 ^a	14.3 ^a	7.3 ^a	1.2 ^a	- ^a	- ^a	- ^a	0.001	0.007
DC2	0.9	1.1	1.1	7.0	-	-	-	-	-	0.279	0.113
DC3	4.0	1.2	10.1	2.3	1.1	-	-	-	-	0.025	0.028
DC4	-	-	0.5	-	-	-	-	-	-	a.v.	a.v.
<i>Pseudocecrela kotschy</i>											
DC1	4.6	4.1	4.4	-	-	-	0.9	-	0.9	a.v.	a.v.
DC2	-	-	-	-	-	-	-	-	-	a.v.	a.v.
DC3	-	0.6	-	-	0.7	-	-	-	-	a.v.	a.v.
DC4	-	-	-	-	-	-	-	-	-	a.v.	a.v.
<i>Crossopteryx febrifuga</i>											
DC1	16.7 ^a	17.4 ^a	18.7 ^a	9.6 ^a	4.0 ^a	- ^a	- ^a	- ^a	- ^a	0.261	0.006
DC2	-	-	0.9	-	-	-	-	-	-	a.v.	a.v.
DC3	6.1 ^{ab}	27.6 ^a	2.4 ^b	2.9 ^{ab}	0.7 ^b	- ^b	- ^b	- ^b	- ^b	0.171	0.001
DC4	2.4	2.1	1.1	0.5	-	0.5	-	-	-	0.410	0.083
<i>Vitellaria paradoxa</i>											
DC1	51.4 ^{ab}	78.3 ^a	8.3 ^{abc}	14.5 ^{abc}	1.1 ^{bc}	- ^c	- ^c	- ^c	- ^c	0.126	0.001
DC2	-	-	-	0.9	-	-	-	-	-	a.v.	a.v.
DC3	-	-	-	-	-	-	-	-	-	a.v.	a.v.
DC4	-	-	-	-	0.5	-	-	-	-	a.v.	a.v.

Regeneration of tree species

Concerning the regeneration of tree species in the shade of *A. leiocarpus*, data of tree species from the sub-segments of S-Eco, B-Eco, and F-Eco (in total 9 sub-segments) were considered, where *A. leiocarpus* was dominant. Table 3.5 summarizes distribution patterns of the four diameter classes of the 10 tree species that were most frequent in diameter class DC1 in the transect plots. Although statistical analysis was limited by a generally low number of individuals, a clear sequential species turnover from sub-segments towards the savanna (S-Eco-1) to sub-segments towards the closed forest (F-Eco-3) could be observed along the nine sub-segments (Table 3.5). *Detarium microcarpum*, *Crossopteryx febrifuga*, and *Vitellaria paradoxa* occurred more frequently in sub-segments towards the savanna. *Anogeissus leiocarpus*, *Combretum nigricans*, *Diospyros mespiliformis*, *D. abyssinica*, and *Dialium guineense* showed a distribution sequence towards the closed forest in this order. *Manilkara multinervis* was equally distributed and for *Pseudocedrela kotschy* a classification was statistically not possible. Moreover, focusing on particular tree species, a sequence in the distribution of diameter classes – as described above for *A. leiocarpus* – could also be observed, especially for *Diospyros mespiliformis* and *D. abyssinica*. The general tendency is that offspring of tree species which occurred more towards the closed forest showed a higher abundance of smaller diameter classes in sub-segments towards the savanna than larger diameter classes. However, in the shade of large individuals of *A. leiocarpus* (DC3 and DC4), mainly tree species regenerated that occurred with a high abundance in sub-segments towards the closed forest (Table 3.5).

Table 3.6. Regression analysis of diameter class DC1 of 10 dominant tree species and three environmental parameters (n = 87). r_s = Spearman's rank correlation coefficient; significant correlations (2-tailed, test wise error rate with Bonferoni correction): * P < 0,017; ** P < 0.003; *** P < 0.0003.

Species	Dry mass of grasses	Cover above 1 m	Soil depth
<i>Manilkara multinervis</i>	-0.33**	-0.01	-0.16
<i>Dialium guineense</i>	-0.53***	0.46***	-0.11
<i>Diospyros abyssinica</i>	-0.54***	0.32**	0.20
<i>Diospyros mespiliformis</i>	-0.48***	0.49***	-0.12
<i>Combretum nigricans</i>	0.06	0.13	-0.17
<i>Anogeissus leiocarpus</i>	0.25*	-0.04	-0.29*
<i>Detarium microcarpum</i>	0.36**	-0.29*	-0.31*
<i>Pseudocedrela kotschy</i>	0.26*	-0.18	0.01
<i>Crossopteryx febrifuga</i>	0.36**	-0.38***	-0.04
<i>Vitellaria paradoxa</i>	0.57***	-0.40***	-0.01

Correlation analysis of density values of diameter class DC1 and environmental parameters resulted in high correlation coefficients with values up to 0.57 (Table 3.6). Within the analysis, two species groups could be separated: firstly *Detarium microcarpum*, *Crossopteryx febrifuga*, and *Vitellaria paradoxa* that regenerated in a savanna environment (high dry mass of grasses, low cover above 1 m), and secondly *Diospyros mespiliformis*, *D. abyssinica*, and *Dialium guineense* that regenerated in a forest environment (low dry mass of grasses, high cover above 1 m, Table 3.6). As expected, this result corresponds to the distribution pattern of diameter class DC1 in Table 3.5. Regeneration of *A. leiocarpus* coincides with a high dry mass of grasses, stressing the potential of this species to regenerate at savanna sites. *Manilkara multinervis*, showing an indifferent distribution along the sub-segments in Table 3.5, was negatively correlated with dry mass of grasses but was independent of cover above 1 m. Soil depth was only correlated with *A. leiocarpus* and *Detarium microcarpum*, with both species regenerating on more shallow soils.

4 Discussion

4.1 Border and ecotone detection

4.1.1 Border-and-ecotone detection analysis (BEDA) for univariate transect data

The proposed border-and-ecotone-detection analysis (BEDA) based on sigmoidal non-linear regression analysis was successfully applied to univariate data along forest savanna transects in the CNP (Chapter 3.1 – 3.3). Sigmoidal models similar to the non-linear regression model used in BEDA are commonly applied to describe ecological gradients between two adjacent habitats (Chen *et al.* 1996, Saunders *et al.* 1999, Farnsworth & Anderson 2001, Cadenasso *et al.* 2003). However, Williams-Linera *et al.* (1998) criticized that especially in forest-edge-effect studies often only the forest-edge half of the boundaries was sampled, while the adjacent habitat received less attention.

For a univariate parameter, the border between two habitats can objectively be defined as the locality where the magnitude of change of the variable is greatest (Fagan *et al.* 2003). Consequently, the inflection point of the sigmoidal non-linear model was used in BEDA to determine borders (see Chapter 2.5). Chen *et al.* (1996) stated that the selection of a criterion to define the borders of an ecotone is a subjective decision as ecotones are continuous by nature. In BEDA, the criterion used to define ecotone borders was adopted from the onset of light saturation (Talling 1957), a parameter clearly defined and commonly used in physiological studies. The calculation of the border and the limits of the associated ecotone in BEDA was directly connected to the applied non-linear regression model by using the coefficient estimates and their covariance matrix (Chapter 2.5). Therefore, in contrast to, e.g., Saunders *et al.* (1999), it was possible to construct confidence intervals for locating the border and the two ecotone limits. In addition, the magnitude of the effect between two habitats and its relevance can be approximated by the difference of the two asymptotes and the prediction bands of the sigmoidal non-linear regression model. Thus, it has to be stressed that for ecological gradients following a sigmoidal course, the BEDA provides the parameters of interest including their confidence intervals.

Piecewise regression recently enhanced by Toms & Lesperance (2003) has a similar potential. Compared to BEDA, an advantage of piecewise regression is that conditions in adjacent habitats are not assumed to be constant, but may also follow own gradients. The main disadvantage of this approach is the need of a sufficiently high number of sampling points in

each regression section to guarantee adequate modeling. This requires a good knowledge of the expected location of a studied border and the width of the associated ecotone. BEDA, instead, is more robust against this aspect due to stricter model assumptions. In addition, software is available for BEDA to compute random effects that occur between sampled transects by applying mixed effects models (Pinheiro & Bates 2000). This analysis was successfully carried out for structural vegetation data and mass of dry grasses for about 30 sample points at each single transect (Chapter 3.1 and 3.2). Instead, on the basis of microclimatic data (10 sample points per transect, Chapter 3.3) the application of non-linear mixed effects models was limited.

In concern to the power of BEDA and piecewise regression in gradient analysis it would be worthwhile to compare these two methods along simulated gradients of different steepness, variability, and magnitude of effects that were sampled with different intensities. However, in addition to a sigmoidal pattern, univariate parameters may also show other patterns along an ecotone such as a bell-shaped curve and a combination of a sigmoidal and a bell-shaped curve (Chen *et al.* 1996, Saunders *et al.* 1999, Davies-Colley *et al.* 2000). Therefore it would be reasonable to expand the proposed BEDA by incorporating additional model functions.

4.1.2 SMWDA and MWRA for multivariate transect data

The discrimination between borders and associated ecotones that are real features of a landscape, and those arising from random chance is of paramount importance in all ecotone studies (Cornelius & Reynolds 1991, Fagan *et al.* 2003), because a reliable detection of borders is the basis for core-area models (Laurance & Yensen 1991, Fernandez *et al.* 2002). Walker *et al.* (2003) used the scores of the first axis of a detrended correspondence analysis (DCA) of multivariate vegetation data along continuous transects followed by two MWRA to detect borders and the width of ecotones. The main disadvantage of this approach is that a criterion is missing to decide whether a detected border is significant or not, but for SMWDA a Monte Carlo randomization test is available (Cornelius & Reynolds 1991). In ecology, SMWDA is frequently employed to detect vegetation boundaries (e.g. Beals 1969, Ludwig & Cornelius 1987, Nishimura & Kohyama 2002). Instead, the application of SMWDA in combination with the Monte Carlo permutation was found only in Kemp *et al.* (1994) who analyzed a climatic time series, and in Zalatnai & Körmöczi (2004) who studied species composition in an alkaline grassland, though the method is specially designed for transect-like analyses and easy to compute. The combination of SMWDA and MWRA applied to multivariate vegetation data (Chapter 3.4) proved to provide a coherent set of analyses for reliably detecting borders and more objectively characterizing the width of associated ecotones and, furthermore, making studies more comparable.

A simulation study by Brunt & Conley (1990) on the quality of SMWDA using squared Euclidean distance (SED) as distance metric revealed that SMWDA worked well, but

increasing background noise and increasing levels of border and patch complexity reduced the quality of border detection. Direct comparisons of different border-detection methods are rare. As an example, Harper & Macdonald (2001) computed rather similar profiles with SMWDA and wavelet analysis of riparian ecotones at lakeshore edges in Canada. As already stressed for univariate methods in Chapter 4.1.1, it is strongly recommended that in future simulation studies different gradient types, sampling designs (continuous vs. discontinuous transects), and methods of analysis such as wobbling-methods (e.g. Fortin 1994) and wavelet analysis (e.g. Csillag & Kabos 2002) should be considered in addition to DCA, MWRA and SMWDA.

4.2 Relation of surface biomass and surface fire

The amount of grass biomass being investigated along transects in the CNP ranged from low values at the forest sites ($0\text{-}600\text{ g m}^{-2}$) to high values at savanna sites ($500\text{-}1,100\text{ g m}^{-2}$). Annual leaf litter fall was about $600\text{ g m}^{-2}\text{ a}^{-1}$ at forest sites and about $150\text{ g m}^{-2}\text{ a}^{-1}$ at savanna sites (see Chapter 3.2).

At savanna sites in northeastern Ivory Coast (Ouango-Fitini, annual rainfall of $1,050\text{ mm a}^{-1}$) biomass of the herb layer varied from 400 to $1,200\text{ g m}^{-2}$ in dependence on topographical locations (Fournier *et al.* 1982). The highest value occurred at an inland valley. For several sites in Ivory Coast, Fournier (1991) measured a maximal biomass of the herb layer of $1,400\text{ g m}^{-2}$ at a wooded savanna at the lowest part of a slope (Lamto, central Ivory Coast). Savannas in Ivory Coast with a similar species composition and vegetation structure compared to those studied in the CNP had a biomass of the herb layer of about 400 to $1,100\text{ g m}^{-2}$ (see Menaut & César 1979, Villecourt *et al.* 1979, Villecourt *et al.* 1980, César 1981, Fournier *et al.* 1982, Fournier 1991). For semi-deciduous forests in Ivory Coast (Lamto) the weight of annual leaf litter fall varied from $510\text{ g m}^{-2}\text{ a}^{-1}$ to $810\text{ g m}^{-2}\text{ a}^{-1}$ (Devineau 1976). Biomass values measured in the CNP were in a similar range to the values of both the herb layer and the leaf litter in the aforementioned studies. Nevertheless, it must be taken into account that the material weighed in the present study was air-dried and not oven-dried, so that values may be slightly overestimated.

Grass growth in savannas and thus, the amount of biomass, is influenced by a complex interaction of biotic and abiotic parameters (Scholes & Archer 1997, Higgins *et al.* 2000). Scholes & Archer (1997) pointed out that in general an increase in woody plant cover or density results in a dramatic decline of grass production. This is mainly a consequence of competition between trees and grasses for resources (e.g. light, soil-water, and nutrients). Along forest-savanna transects in the CNP, also a negative relation between the cover above 1 m and grass biomass was found (Fig. 3.6), that may be interpreted as suppression of grasses by woody species (Mordelet & Menaut 1995). Grass biomass showed no directed relation to

soil depth. This may indicate that in the studied forest-savanna system the interaction between grasses and trees is of higher importance than soil conditions.

Border-and-ecotone detection analysis (BEDA) along the studied transects with regard to grass biomass revealed that the calculated borders were located near the borderline between savanna and forest belt approving the applied habitat stratification. For the detected border no transect effect was observed, but the slope of the sigmoidal model used in BEDA varied significantly between transects. In consequence, the depth-of-edge influence (DEI) varied between transects as well. For the DEI towards the forest interior values below 21 m were calculated except for one transect that showed a DEI of about 150 m. For the studied year, the DEI of grass biomass was not related to fire occurrence. Thus, the DEI computed for dry mass of grasses is limited to represent fire occurrence in forest-core-area analysis.

Along the studied transects, fire occurred mainly in savanna plots. At one transect, surface fire entered almost 30 m into the forest belt, but fires were absent from plots in closed forest (Table 3.2). The ignition probability of plots in the transition zone between forest and savanna was correlated with the amount of grass biomass whereupon an ignition probability of 0.5 was given for a dry mass of grasses of about 300 g m^{-2} (Fig. 3.8).

In his review on the combustion in tropical biomass fires Stott (2000) pointed out that, along with litter, grasses represent the most important combustible material in most tropical ecosystems, especially as grasses play a vital role in ignition. Beside the presence of sufficient oxygen and heat, the moisture content of the respective fuel mainly determines its ignitability (Biddulph & Kellman 1998, DeBano *et al.* 1998, Stott 2000). In a field experiment at savanna-gallery forest boundaries in Venezuela, Biddulph & Kellman (1998) revealed that ignitability of grasses, un-decomposed litter and root-mat material was achieved at a moisture content of about 80-100% being independent from the material, but the drying behavior of the surface fuels was strongly related to the type of the organic material and the microclimate at a site. After a raining event, grasses in the savanna dried up to ignitability within one day, whereas at a forest site ignitability occurred after 2-3 days. Leaf litter and root mat showed an ignitable moisture content after 7 days at a savanna site and almost after 4 weeks at a forest site. The authors argue that in their study fires occur rarely in gallery forest because savannas tend to burn earlier in the dry season before forest fuels become ignitable (Biddulph & Kellman 1998).

Savanna sites at the studied transects in the CNP burned from 01/20 to 02/03/2002. Monthly rainfall measured at the research camp of the University of Würzburg was 65 mm, 11 mm, and 0 mm in October, November, and December 2001. In January 2002, one single rainfall event of 5 mm occurred on 01/06/2002. Though the amount of rain was low, it is conceivable that differences in the fuel moisture content at savanna and forest sites as described by

Biddulph & Kellman (1998) may have promoted the extinction of fire at the borderline between savanna and forest belt at the studied transects in the CNP.

Another aspect is that fires usually start and spread in fine fuels with its low ignition temperature as a result of a large surface-area-to-volume ratio (Anderson 1982). Therefore, leaf litter with its more compact structure may need a higher ignition temperature than grasses. This may also reduce ignitability of forest-belt plots if the grassy component of the fuel load drops below a specific value. If fires occurred at the end of the dry season, fuels would be drier and, especially at forest-belt and closed-forest sites, a higher amount of leaf litter would be available as fuel (compare Fig. 3.3). This might raise ignitability of respective sites and, therefore, the probability of fires to enter the forest interior could increase as well. Such fire events were recently described by Cochrane & Laurance (2002) and Laurance (2003) for Brazilian lowland rainforest, where the fire risk especially increased during dry years. However, the analysis of the ignitability of different surface biomass fractions in combination with manipulation experiments concerning surface biomass along forest-savanna boundaries would be required for a final proof of these aspects.

As already outlined above, fire penetration into the forest belt was related to threshold values of fuel conditions, i.e. the amount of grass biomass. Grass biomass production is known to be related to annual rainfall. Breman & Dewit (1983), e.g., confirmed this relation for pasture sites along a rainfall gradient from the Sahel to the Sudanian zone. In their study, grass growth was stronger limited by nutrient availability than by annual rainfall. But annual variations in grass-biomass production without fertilization mainly depend on annual rainfall conditions (e.g. César 1981, Sturm 1993, van de Vijver 1999). In the CNP, such a relation was also found for the inter-annual variation of the maximum height of a single grass tuft (compare Fig. 4.1). Biomass data presented in this study were collected in 2001, a year characterized by low annual rainfall of 680 mm (Fig. 4.1). As a consequence of a higher grass production in wetter years, a generally higher fire probability and intensity can be expected in wetter years (compare van Langevelde *et al.* 2003). In addition, a higher grass production in wetter years that should also occur at forest-belt and closed-forest sites should enhance fires to enter more deeply into island forests. Regarding tree regeneration, juveniles that are suppressed by fire should be able to escape the 'burn back zone' with a higher probability in drier years, especially at unburned sites that may occur more frequently at savanna sites near the borderline between savanna and forest belt than in the open savanna (compare Higgins *et al.* 2000).

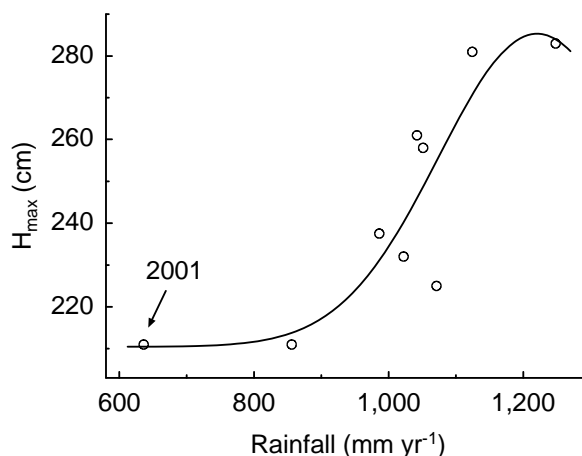


Fig. 4.1. Maximum height of a grass tuft of *Hyparrhenia* sp. versus annual rainfall from 1993 to 2001. Maximum grass height, a parameter reflecting grass biomass (Fournier 1991), was sampled at a location in the open savanna. In its direct vicinity, daily rainfall was measured with a manual rain gage at the climate station of the research camp of the University of Würzburg. The line represents the mean of the non-linear model of the formula $[210.43+74.89*\exp(-((x-1220.39)/206.47)^2)]$; $n = 9$; $r = 0.8752$; $P = 0.0104$. Data source: Frauke Fischer and Koffi Kouadio.

Another aspect is that grass biomass distribution as well as fire occurrence was very regular at the studied savanna sites (Fig. 3.5). This situation may be explained by a dramatic decrease of larger herbivores in the CNP during the last decade due to poaching (Fischer & Linsenmair 2001). Especially large herbivores are known to cause a patchy reduction of grassy biomass in savannas (Adler *et al.* 2001), that can also lead to a patchy occurrence of fire (Fuls 1992). Even though Keesing (1998, 2000) documented in an exclusion experiment in a tropical savanna of central Kenya that an increase of small mammals could compensate the surface-biomass consumption of excluded ungulates, it is questionable if also the patchiness of biomass reduction by large herbivores and its consequences for the coexistence of grasses and trees at savanna sites (e.g. Jeltsch *et al.* 2000, see also Chapter 4.6) can be compensated by small mammals.

4.3 Seasonal variability in microclimatic borders and ecotones

Microclimatic data measured along forest-savanna transects in the CNP revealed that the location of the forest border with respect to air temperature, relative air humidity and vapor pressure deficit shifted over the year. Detected borders were located further towards the forest interior during the dry season and further towards the savanna during the rainy season. In general, microclimate followed the course of macroclimate (Fig. 3.10 and panel a-e in Fig. 3.13), but differences along the studied transects cannot be explained by macroclimate. It is well known that microclimatic parameters usually depend on vegetation structure along forest boundaries (e.g. Matlack 1993). Also in the present study, microclimatic parameters measured during the rainy season in 2002 were significantly correlated with structural vegetation parameters from 2001. As sampling of structural vegetation parameters in 2002

was not possible, correlations are not presented in detail. In addition, the changes in foliation patterns of tree species over the year may be of importance. In Chapter 3.4 and 3.6 it was shown that the forest belt of the studied forest islands was dominated by deciduous tree species, especially *Anogeissus leiocarpus*, that shed their leaves during the dry season, whereas several tree species of the closed forest such as *Diospyros abyssinica* and *Dialium guineense* stay foliated during the whole year. In consequence, microclimatic conditions of the forest belt were more similar to the closed forest during the rainy season when the forest belt was foliated, and microclimatic borders shifted towards the savanna. Microclimate of the forest belt was more similar to the savanna during the dry season when trees of the forest belt were leafless, and the microclimatic borders shifted towards the closed forest. Also Young & Mitchell (1994) reported an annual change in DEI for microclimatic parameters along transects from pasture to evergreen broadleaf forest in New Zealand. In summer (March), they found pronounced microclimate gradients with a DEI of about 50 m for air temperature and VPD. But effects were indistinct in winter (September) because microclimatic differences between the two adjacent habitats were low. Along the studied transects in the CNP, less pronounced gradients were observed during the dry season than during the rainy season. Accordingly, the difference between forest and savanna was smaller in the dry season, and the predictions from BEDA showed a higher variability.

With regard to DEI, in the CNP a minimal DEI towards the forest interior of 27.4 ± 15.5 m was computed for air humidity in the rainy season. A maximal DEI of 137.3 ± 138.3 m occurred for air temperature in the dry season. The average of DEI for all microclimatic parameters was 50.5 m. These values are in accordance with values given in the literature for both tropical and temperate forest boundaries (see overview in Baker & Dillon 2000). In the CNP, high DEI values for microclimatic parameters were found during the dry season, but differences between savanna and closed forest were rather low and prediction bands of the two habitat types showed a wide overlap. In contrast, DEI observed during the rainy season were much more pronounced (compare Fig. 3.12 and 3.13).

Concerning the variability between transects, for vapor pressure deficit no transect effect and for air humidity a rather small one were found, whereas a pronounced transect effect was computed for air temperature. These differences between transects might be a sampling effect as sun-facing edges often show the deepest DEI (Baker & Dillon 2000). However, these effects on forest boundaries can be expected to be small in the tropics due to the low distance to the equator. More presumably, differences in vegetation structure between the transects may explain the transect effect observed in the CNP. Didham & Lawton (1999) showed that the character of the forest border can be of importance with regard to the DEI of microclimatic parameters. Along two forest edges with a closed character, the authors determined for air temperature a DEI of 6.5 m at a continuous forest and of 19.5 m at a 100-ha forest fragment. For two forest edges with an open character, the calculated values of DEI

were 101 m (continuous forest) and 184 m (100-ha fragment). Didham & Lawton (1999) stress that the open character of forest edges can enhance air convection and, thus, lead to high DEI for microclimatic parameters (see also Chen *et al.* 1995). Comparing a closed forest edge with an experimentally thinned one, Cadenasso & Pickett (2000, 2001) showed similar relations for herbivore damage and the flux of species into forest interiors. Along the studied transects in the CNP, it appears that the DEI concerning microclimate may predominantly be determined by the vegetation composition and changes in foliation patterns over the year. Foliation patterns may also change the openness of the forest border for air convection, that should especially strengthen the DEI towards the forest interior with regard to microclimate during the dry season (compare Kapos 1989 and Camargo & Kapos 1995, Chen *et al.* 1995, Didham & Lawton 1999).

4.4 Border and ecotone detection by means of vegetation composition

Ecotone detection along the eight forest-savanna transects on the basis of trees larger than 20 cm dbh revealed a DEI of 35 to 100 m (median = 55 m). Along the intensely studied transect, ecotone detection by means of cover of all species revealed an ecotone with a width of 125 m, running 50 m in direction of the savanna and 75 m towards the forest interior. It comprised a continuous species turnover as a result of an interlocked sequence of ecotones for different life forms. A maximal DEI of 120 m occurred for species composition of trees and shrub with a size of 10-20 cm dbh.

Extreme DEI for vegetation parameters were recorded along clear-cut edges, e.g. for the mortality rate of large trees near Manaus, Brazil (up to 300 m, Laurance *et al.* 1998, 2000) and for seedlings of *Tsuga heterophylla* in the western United States (137 m, Chen *et al.* 1992), but for most vegetation parameters the DEI is below 60 m (Baker & Dillon 2000). This is also the case for species composition along forest boundaries. For vegetation composition, e.g. Palik & Murphy (1990) detected a DEI of 5-20 m along deciduous forest-cropland borders in Michigan (USA), and Fraver (1994) determined a DEI of 60 m along hardwood forest-cropland borders in North Carolina (USA). For tropical forests, no data on DEI regarding vegetation composition are available in the literature. However, the DEI values determined in the present study for tropical semi-deciduous forest islands based on species composition were in a similar order to the values mentioned for temperate forests.

Along the eight studied transects, a boundary formation dominated by the semi-fire resistant tree species *Anogeissus leiocarpus* occurred (Chapter 3.6). This species was already described as a typical tree species of boundaries of semi-deciduous forests in the northern Guinea and southern Sudanian zone (MacKay 1936, Clayton 1958, Jones 1963, Poilecot *et al.* 1991). Fagan *et al.* (2003) point out that the occurrence of ecotones can be interpreted as a result of

gradients in environmental variables. In the CNP, grass-species composition changed near the forest border from tall savanna grasses to small forest grasses (Fig. 3.14 b). This change, that was clearly visible in the field, might be an effect of competition between trees and grasses that results in a lower grass biomass, thus a lower highly ignitable fuel load, at forest sites (Chapter 3.2 and 4.2). In consequence, fire-sensitive species would establish more towards the forest interior. This may explain the change of species composition of grasses, herbs, and woody climbers near the borderline between savanna and forest belt along the intensely studied transect, but not the interlocked sequence of shrubs and small trees, trees of medium size, and large trees (Fig. 3.14). The latter pattern supports the presumption of that forests encroach into adjacent savanna by sequential succession. This aspect is discussed in detail in Chapter 4.6 (see also Hennenberg *et al. in press*).

4.5 Core-area analysis

In the present thesis, the depth-of-edge influence (DEI) was computed for several biotic and abiotic data sets (see Table A 1 in the Appendix). Values of DEI ranged from 0 m (e.g. for the occurrence of fire) to more than 140 m (e.g. dry mass of grasses, Table 3.2). Most DEI values were detected between 20 and 60 m. For the comparison of the DEI of different parameters, it is to be stressed that they were rarely related with each other. This was even true for correlated parameters. E.g., the parameters cover of grasses and cover above 1 m were negatively correlated, but DEI differed with values of 11.4 ± 9.8 for cover of grasses and 32.0 ± 15.5 for cover above 1 m. Another example is the occurrence of fire and the DEI of mass of dry grasses (compare Table 3.2). Therefore, it was not possible to use a generalized DEI for the application in core-area analysis, and, in consequence, the dependence on core area at the considered 31 semi-deciduous forest islands (2.1 to 146.1 ha) in the CNP was computed in 5 m steps for a DEI of 5 to 250 m (see Fig. 3.15 and 3.18). Data showed that the forest area that is required to allow for a relative core area (*rCA*) of 50% increased exponentially with increasing DEI (Fig. 3.18). Given the detected DEI of 55 m, computed as median for tree-species composition of trees larger than 20 cm dbh, only 9 of the considered forest 31 islands contained an *rCA* larger than 50% though the total core area still amounted to half of the total forest area. Under these conditions an *rCA* of 50% can be expected for forest islands with a size of 36.6 ± 24.4 ha. For a DEI of 120 m (e.g. cover of woody climbers and species composition of trees and shrubs, see Table A 1), only 1 forest island contained an *rCA* larger than 50%, total core area was less than 20%, and to allow for a forest-core area of 50% forest islands must be larger than 250 ha (compare Fig. 3.15 and Fig. 3.18).

Examples on core-area analysis are rare in the literature. Core-area analysis at fragments of old-growth coastal redwood forest in California (USA) revealed for a DEI of 200 m that 47% of the old-growth was not effected by edge effects (Russell & Jones 2001). Even though

Russell & Jones (2001) determined a DEI of 200 m for sub-canopy height and cover, solar radiation and species richness, this high DEI value is questionable, because the number of sampling points per transect ($n = 9$) was low and especially the criterion to detect the DEI was quite cryptic. An analysis of remote sensing data from Atlantic rainforest fragments in Brazil revealed that with a supposed DEI of 60 m into the forest, 50% of the forested area could be considered as forest-core area (Ranta *et al.* 1998). Moreover, its proportion rapidly declined with increasing DEI. These findings of Ranta *et al.* (1998), however, were not validated in the field. The results obtained at forest islands in the CNP were more similar to the results of Ranta *et al.* (1998) than to those from Russell & Jones (2001). This was probably due to geometric properties and patch sizes.

In accordance with the theory of island biogeography (MacArthur & Wilson 1967), Hovestadt *et al.* (*in press*) found for the study area of the present thesis an increase in woody species with an increasing size of forest islands. From the data base of Hovestadt *et al.* (*in press*), semi-deciduous forest islands ($n = 20$) considered in the present thesis were extracted. These data were used to compute logistic regressions on the basis of presence/absence data of single woody species in dependence on the size of forest islands. Especially forest interior species such as *Antiaris africana* and *Majidea fosteri* occur with a higher probability in larger forest islands (Fig. 4.2). Also in fragmented forests in Ghana, the occurrence of rare forest-interior species was correlated positively with forest size and slightly positively with forest irregularity and shape (Hill & Curran 2001, 2003). The latter parameters can be interpreted as parameters reflecting edge effects and, thus, enforce the area effect.

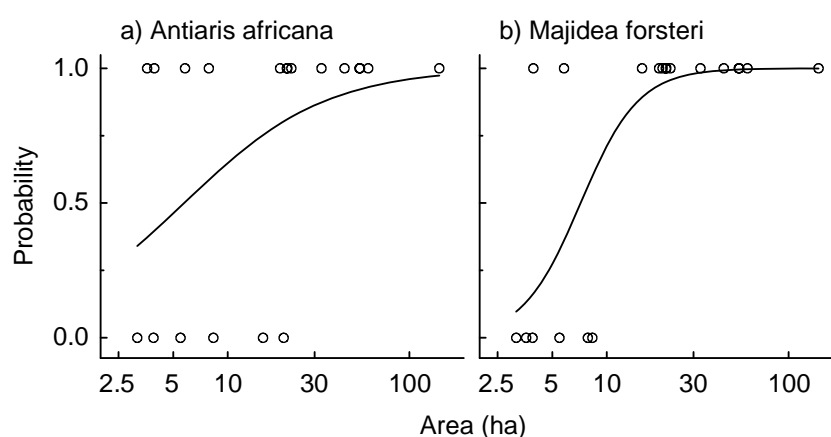


Fig. 4.2. Occurrence probability of (a) *Antiaris africana* and (b) *Majidea fosteri* in dependence on the area of forest islands (dry variant of semi-deciduous forest only) computed on the basis of presence/absence data (circles, data source: Hovestadt *et al.* *in press*). The line represented the result of glm (link-function = logit (see Chapter 2.6.2); a) $P = 0.0658$; b) $P = 0.0235$; $n = 20$; area was log-transformed).

If forest-interior species are the conservation target, Gascon *et al.* (2000) advise – beside protecting forest edges against damage and minimizing the harshness from the surrounding matrix – to protect larger forest patches rather than small ones (minimization of

area/perimeter relation). In accordance with this advice, Bender *et al.* (1998) concluded from a meta-analysis of 25 studies testing relationships between patch size and population density, that for interior species, the decline in population size associated with habitat fragmentation per se will be greater than that predicted from pure habitat loss alone. On the other hand Turner & Cortlett (1996) stress the value of small forest fragments that may become the last refuges of many forest-interior species (see also ‘single large or several small’ (SLOSS) debate, Simberloff 1988). However, in this context no standard solution is available (Lomolino 1994), but knowledge on core area is necessary for management concepts such as population viability analysis (Henle *et al.* 2004) that aim to optimize the conservation of forest interior species (Baskent 1997, Clemens *et al.* 1999, Putz *et al.* 2001).

Outside the CNP, strong deforestation took place during the last two decades (Goetze *et al.*, *unpublished manuscript*). It has especially to be stressed that as a consequence of the current land-use practice of cultivating cashew (*Anacardium occidentale* L.) in association with field crops, which leads to a subsequent conversion of fields into cashew plantations, shifting-cultivation cycles are interrupted. This leads to a progressive reduction of areas suited for cultivating crops and, therefore, an increasing land-use pressure on forests. For the protection of forest interior species in forest islands outside the CNP – and other regions of the northern Guinea and southern Sudanian zone where undisturbed references are absent –, the findings of the presented core-area analysis may be of high importance for forest protection plans.

Using a GIS-based approach to detect areas of edge influence across a patchy landscape (Chequamegon National Forest, USA), Zheng & Chen (2000) showed that edge effects were not symmetrically distributed in all directions around clear cuts, and that multiple edge effects occurred across the landscape. With regard to such aspects, Fernandez *et al.* (2002) have developed a model to compute complex edge effect in habitat patches following the theory of electric fields. This approach is a ‘formal realization of the multiplicity, simultaneousness and additivity’ of an influence exerting across a patch border (Fernandez *et al.* 2002, Malcolm 1994). This model can deal with different edge functions and varying DEI along borderlines, but the method is not yet implemented to analyze GIS data. The non-additive core-area model applied in the present thesis that subtracts a homogeneous buffer to determine the core area is the current pragmatic method (F. López, *personal communication*). The core-area model of Laurance & Yensen (1991), however, can be seen as an oversimplification that tends to underestimate core areas (Ranta *et al.* 1998).

4.6 Dynamics of forest-savanna ecotones and the role of *Anogeissus leiocarpus*

Do forest islands spread into savanna by sequential succession?

In the CNP, an ecotone between forest and savanna dominated by *Anogeissus leiocarpus* occurs. Detailed distribution data of *A. leiocarpus* along forest-savanna transects reveal a spatial sequence of size classes (Chapter 3.6). In the border zone, larger individuals were located towards the forest interior whereas smaller individuals were mainly encountered in direction of the savanna, which can be interpreted as a sign of progression of *A. leiocarpus* into the savanna. The distribution pattern of dominant tree species in the understorey of *A. leiocarpus* stands near the forest border supports this assumption. A clear spatial sequence of the tree species *A. leiocarpus*, *Combretum nigricans*, *Diospyros mespiliformis*, *D. abyssinica*, and *Dialium guineense* from the forest border towards the forest interior was found. To some extent, also a spatial sequence of diameter classes was observed for these species, with younger individuals being more frequent towards the savanna.

For the northern Guinea zone the existence of forest boundaries dominated by *A. leiocarpus* has already been described by several authors for forest islands as well as for gallery forests (MacKay 1936, Clayton 1958, Jones 1963, Letouzey 1969, Sobey 1978, Hall & Swaine 1981, Poilecot *et al.* 1991, Porembski 2001). Letouzey (1969) and Poilecot *et al.* (1991) assume this transition formation to encroach into the savanna. In general, succession is characterized by a sequential turnover of species in time, that was not only shown in long-term studies (e.g. Sheil *et al.* 2000) or chronosequences (e.g. Cain & Shelton 2001) but also in modeling approaches (Huston & Smith 1987, Hovestadt *et al.* 2000, Favier *et al.* 2004). The results presented in Chapter 3.6 indicate that in the CNP the forest-border zone may encroach into the adjacent savanna by sequential succession.

The contrary assumption that savanna formations encroach into forests by continual regression is to be rejected for two reasons: firstly, no sequential patterns could be found for tree species dominating plots towards the savanna as it was found for species of the forest belt and the closed forest and, secondly, at the belt-ecotone segment the parameter dry mass of grasses reflecting savanna conditions was clearly similar to forest and not to savanna segments. Thus, the results presented here support the assumption of Hovestadt *et al.* (1999) that forest decline should occur by sudden events like, e.g., drought periods with increased tree mortality (Swaine *et al.* 1992, Condit *et al.* 1995, Gascon *et al.* 2000). However, only time series can give a final proof of this assumption.

An interesting aspect in this context is the time scale of successional processes. In 3,000 year-old isolated savannas, which are today enclosed by forest (Mayombe mountain, Congo,

rainfall of 1,200-2,000 mm), Schwartz *et al.* (1996) concluded from the determination of the mean residence time of soil organic matter by ^{14}C dating and a change of the isotope characteristic of soil organic matter ($\delta^{13}\text{C}$) a growth rate of forest borders of about 20-50 m per century. In this case, a high frequency of savanna fires, but also drier climate conditions and a lower soil fertility, may slow down forest encroachment into savanna (Favier *et al.* 2004). In the CNP, tree ring analyses of *A. leiocarpus* (Schöngart *et al.*, *in prep.*) revealed a maximum age of 166 years. Old individuals of *A. leiocarpus* are mainly located at a distance of about 30 m from the forest border. Thus, assuming a successional process at forest borders in the CNP, forests with *A. leiocarpus* borders might expand at a similar or even longer time scale as demonstrated by Schwartz *et al.* (1996).

Can monodominant Anogeissus leiocarpus stands be interpreted as a successional stage in the succession from savanna to forest?

Final-successional forest stands can be dominated by single tree species in temperate zones as well as in the tropics (Connell & Lowman 1989, Hart *et al.* 1989). Torti *et al.* (2001) point out that traits of both, adult and juvenile stages of monodominant tree species, are of importance for the occurrence of such stands. Adult individuals of a monodominant tree species alter the understorey environment in a way that makes it difficult for other tree species to regenerate, but their own juveniles are adapted to these conditions (Torti *et al.* 2001). In the CNP, however, several forest tree species regenerate well in the understorey of old *A. leiocarpus* trees, and juveniles of *A. leiocarpus* show a regeneration peak in open areas less influenced by older *A. leiocarpus* individuals. Thus, *A. leiocarpus* is not a species that typically builds up final-successional monodominant stands.

PCA analysis of diameter class composition of *A. leiocarpus* and vegetation structure revealed that the analyzed monodominant *Anogeissus* stand was most similar to transect segments directly adjacent to the forest border, where a sequential succession from savanna to forest might proceed. In accordance with the observation that monodominant *Anogeissus* stands colonize abandoned village sites in northwestern Ghana (Sobey 1978), the monodominant *Anogeissus* stand can be interpreted as a successional stage towards closed forest.

Such a development is only possible if tree species of the subsequent successional stages are present. In the northern Guinea zone, this is the case in combination with the occurrence of effective dispersal vectors (Hovestadt *et al.* 1997, 1999), but further to the north those tree species are mostly restricted to gallery forests or are completely absent as a result of climate conditions (White 1983). Thus, in the Sudanian zone the persistence of monodominant *Anogeissus* stands is determined by the lack of late-successional tree species rather than unsuitable abiotic conditions in the understorey of *A. leiocarpus*. Monodominant *A. leiocarpus* forests in the Sudanian region (Guinko 1985, Hahn-Hadjali 1998) are in accordance with this assumption, with *A. leiocarpus* forests in southwestern Burkina Faso

(Neumann & Müller-Haude 1999) more likely representing degenerated, formerly denser forests that still include some typical Guinean elements such as *Cola cordifolia* and *Milicia excelsa*.

What are favorable regeneration sites for Anogeissus leiocarpus?

The correlation analysis for the density of young *A. leiocarpus* individuals and selected environmental parameters (dry mass of grasses, cover above 1 m, and soil depth) showed that offspring of *A. leiocarpus* was slightly positively correlated with the amount of inflammable material and shallow soils. In western Nigeria, Letouzey (1969) observed a high recruitment rate of *A. leiocarpus* in savannas adjacent to island-forest borders dominated by *A. leiocarpus*. Sobey (1978) points out that a regeneration of *A. leiocarpus* seems to be favored at sites with reduced fire intensity or frequency (northwestern Ghana). Soil conditions at *A. leiocarpus* sites were more beneficial than in the open savanna, but this might be due to positive effects of *A. leiocarpus* on soil fertility (Sobey 1978). In southern Burkina Faso, *A. leiocarpus* was frequent at locations with shallow, poor soils, unfavorable for agriculture (Neumann & Müller-Haude 1999). It is concluded that in the CNP, *A. leiocarpus* seems to be able to regenerate well and build up stands with a closed canopy at sites characterized by a moderate fire intensity and shallow soils.

The potential role of Anogeissus leiocarpus in the forest-savanna mosaic

Equilibrium concepts (Huntley *et al.* 1982, Walter 1979) and non-equilibrium concepts (review in Scholes & Archer 1997) aim to explain the coexistence of trees and grasses in savannas. However, factors maintaining savannas are complex and may be unique for each savanna (Furley *et al.* 1992, Scholes & Archer 1997, Higgins *et al.* 2000, van Langevelde *et al.* 2003). Looking for general patterns, Jeltsch *et al.* (2000) have identified two groups of 'buffering mechanisms' that reduce the probability of a shift either from savannas to forest (e.g. buffered by fire, elephants, or seed predators) or from savanna to grassland without trees (e.g. buffered by microsites favoring tree establishment or grazers), and thus lead to a grass-tree coexistence.

Fire as a prominent buffering mechanism (Jeltsch *et al.* 2000) is of paramount importance for the distinctive physiognomy of humid savannas in West Africa (see Chapter 1.2 and 4.2). A reduced fire intensity and frequency can occur on termite mounds of the genus *Macrotermes* (Harris 1971, Bloesch 2002), at abandoned village sites (Lawson *et al.* 1968, Sobey 1978), and in the shade of trees (Mordelet 1993, Mordelet & Menaut 1995, San Jose & Montes 1997). Also random pattern of fire frequency and the date of fire are of importance (Bloesch 2002, Louppe *et al.* 1995). In this context, the relevance of the topographical position of a site in the pediplain is to be stressed. As outlined in Chapter 1.2 and 2.1.3, drier conditions on hilltops may favor tree establishment as a consequence of low grass productivity. This is

especially in accordance with site conditions that were found to be favorable for the establishment of *A. leiocarpus* as discussed above.

Among the tree species sampled along the studied transects, *A. leiocarpus* has the highest potential to break through the buffering mechanism fire by regenerating in savanna sites, by being medium-fire resistant (see Hall & Swaine 1981), and shading out grass effectively (see Irvine 1961). *Combretum nigricans*, that shows a regeneration peak directly at the borderline of the forests, did not regenerate in savanna plots and was not correlated with dry mass of grasses. Savanna trees such as *Crossopteryx febrifuga* and *Detarium microcarpum* may also suppress grasses at a growth location, but their abundance, however, appears to be too low to initialize a succession from savanna to forest. On the other hand, forest-tree species clearly reduced grass biomass in the forest interior (Chapter 3.2), but regenerated at shady sites with a low dry mass of grasses including sites in the understorey of *A. leiocarpus* and not in the savanna.

By modeling succession by life-history traits, Huston & Smith (1987) showed that the removal of an early species in a succession sequence can lead to a strong change in vegetation development. Such effects were rarely tested in field experiments. Ernest & Brown (2001) concluded from an exclusion experiment of kangaroo rats from a desert ecosystem in the United States for 20 years that other species of the original community were unable to compensate the excluded species. The results of the present study suggest that *A. leiocarpus* may act as an important pioneer species which plays a significant role in the succession from savanna to forest and, thus, in the dynamics of the studied forest-savanna mosaic, but a final proof can only be given by an exclusion experiment or adequate modeling (compare Favier *et al.* 2004). In the study region, however, not all forest borders are fringed by *A. leiocarpus* (Poilecot *et al.* 1991). Also tree inventories in Hovestadt *et al.* (1999) show that *A. leiocarpus* is absent from some small forest islands. This underlines that the successional pathway (Gibson 1996) proposed here is only one possibility in forest succession at forest-savanna ecotones in West Africa.

5 Conclusions

The first topic of the present thesis deals with a methodological lack of statistical analyses of transect data along ecotones. Regarding univariate transect data, a new border-and-ecotone detection analysis was developed and confidence intervals were derived for the respective parameters that describe border and ecotone properties. For the analysis of multivariate data, two existing methods were combined to determine significant borders and the width of ecotones. For both the uni- and multivariate case, transect data sampled along forest-savanna transects were successfully analyzed using these methods. These sets of analyses may hopefully contribute to facilitating future studies along ecological boundaries. However, it would be worthwhile to compare the power of these techniques with those of other boundary-detection methods using simulation studies.

Within the second topic of the present thesis, the methods outlined in the first topic were applied to analyze transect data sampled along forest-savanna transects in the CNP. For the African continent, measurements on the depth-of-edge influence (DEI) towards the interior of forests carried out with a comparable intensity are missing in the literature for both forest islands and forest fragments. Concerning the parameters studied in the CNP (vegetation structure and composition, grass biomass as fuel, and microclimate) a similar magnitude of DEI values was detected in studies along forest boundaries of tropical and temperate regions of other continents. For most parameters studied worldwide, DEI towards the forest interior was below 60 m (Baker & Dillon 2000). But also DEI of several kilometers were observed that were mostly related to complex mechanisms such as slow fire movement on the floor of tropical forests (Laurance 2003) and plant-animal interactions (Curran *et al.* 1999, Laurance 2000). Large distance edge effects are often hard to study and those that are documented were found somewhat accidentally. A demand for future research on DEI should firstly call for developing an understanding of key processes that may act at insular forests and for identifying those parameters and processes that have the potential to cause large distance DEI. Secondly, these parameters and processes should be studied in the field.

The third topic treated the calculation of core areas of forest islands in the studied area in the CNP. A GIS-based non-additive core-area model was applied that is currently the state of the art. A new approach incorporating additive effects along forest boundaries is under development (Fernandez *et al.* 2002, F. López, *personal communication*). With this approach also varying DEI due to changes in the character of the border can be considered. Even though this type of analysis may improve core-area analysis, the quality of ground data will still determine the quality of core-area analysis. In particular, knowledge on changes of the

character of the forest borders along the borderline, and linking this knowledge to specific DEI appears rather exhausting – if it will ever be realizable. In this study, transects were selected to provide standardized conditions at straight-lined forest borders. In a second step, the obtained data on DEI were used for core-area analysis. Another approach to achieve a realistic core-area analysis might be the use of remote sensing data to detect DEI across forest patches and then to select locations for intensive field studies to validate the calculated results. However, it is questionable to which extent remote sensing can detect parameters of ecological interest that could represent, e.g., the distribution of tree-size classes or the survival of seedlings.

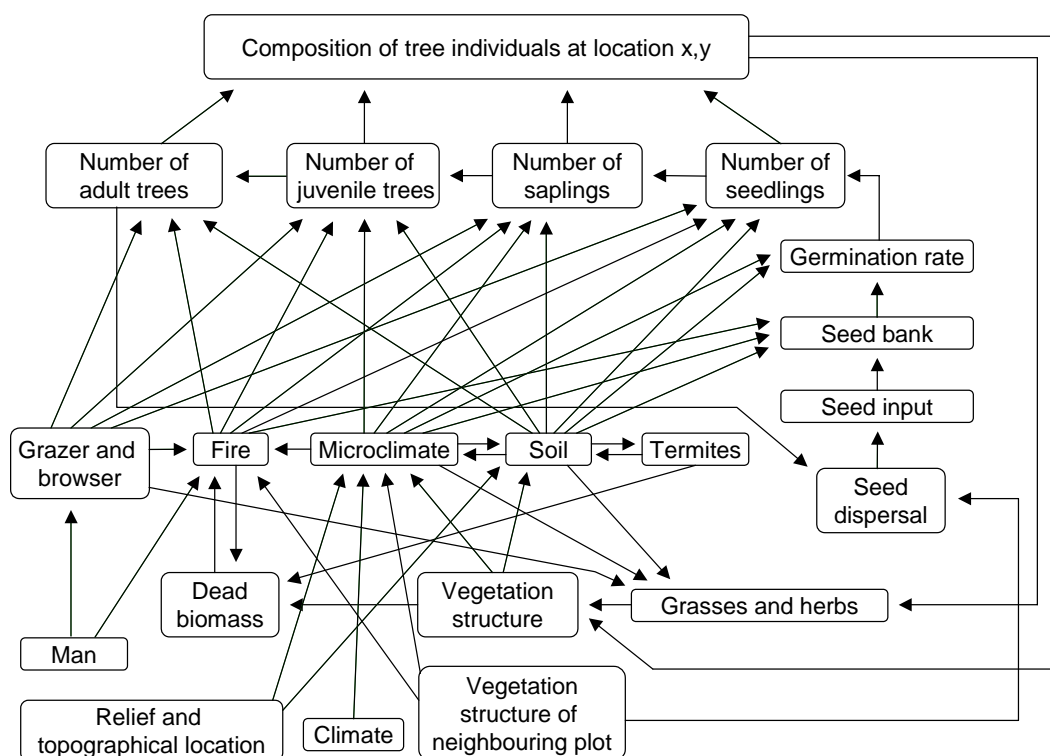


Fig. 5.1. Modeling approach for the planned forest boundary model (cooperation with the team of F. Jeltsch, University of Potsdam, BIOTA S09). A central question to be answered shall be: ‘How does the composition of tree individuals change in time at locations across the forest-savanna boundary?’ The cell size of a spatially-explicit model shall be 5 m * 5 m in an area of 20 km². The time steps shall be 1 year. Tree species shall be modeled as functional groups, e.g. species of the closed forest, savanna species, and species of the forest belt. To this model, additional questions could be addressed such as ‘How does the forest border react if a dominate species of the forest belt is absent?’ or ‘How does the location of the forest-savanna boundary change with regard to a reduction of the annual rainfall of 30%?’.

The fourth topic of the present thesis addressed successional processes at the forest-savanna boundary. The analysis of the distribution of tree-size classes along the studied transects in combination with selected environmental parameters revealed sequential series of both species and tree size classes. The results suggest that the studied forests spread into savanna by sequential succession. It was stressed that the pioneer-tree species *Anogeissus leiocarpus*

may play an important role in the succession from savanna to forest. These assumptions ought to be verified by long term studies. In addition, spatially explicit modeling could be very helpful to learn about processes and mechanisms that act along the studied forest-savanna boundary and to test the importance of single parameters, such as the topographical location. The design of the field work of the present thesis was strictly directed towards data acquisition for the subsequent development of a forest boundary model. During modeling workshops within the BIOTA framework, a first modeling approach was already developed (Fig. 5.1). Additional data, e.g. dendrochronological data of selected tree species for calibrating the temporal accuracy of modeling, were collected that are not presented here (Schöngart *et al.*, *in prep.*). With the work of the present thesis, an profound basis exists for both long-term studies on the dynamics of forest savanna boundaries in the CNP and respective modeling.

References

- Achard, F., H. D. Eva, H. J. Stibig, P. Mayaux, J. Gallego, T. Richards, and J. P. Malingreau. 2002. Determination of deforestation rates of the world's humid tropical forests. *Science* 297:999-1002.
- Adam P. 1990. Saltmarsh ecology. Cambridge University Press, Cambridge.
- Adjanohoun E. J. 1989. Contribution aux études ethnobotaniques et floristiques en République populaire du Bénin. Agence de Coopération Culturelle et Technique, Paris.
- Adler, P. B., D. A. Raff, and W. K. Lauenroth. 2001. The effect of grazing on the spatial heterogeneity of vegetation. *Oecologia* 128:465-479.
- Anderson H.E. 1982. Aids to determining fuel models for estimating fire behavior. USDA Forest Service general technical Report, INT-122, United States Department of Agriculture, Ogden, Utah.
- Anhuf, D. 1994. Zeitlicher Vegetations- und Klimawandel in Cote d'Ivoire. Pages 7-299 in *Veränderung der Vegetationsbedeckung in Cote d'Ivoire*. Steiner, Stuttgart.
- Anhuf, D., and P. Frankenberg. 1991. Die naturnahen Vegetationszonen Westafrikas. *Die Erde* 122:243-265.
- Arbonnier M. 2000. Arbres, arbustes et lianes des zones sèches d'Afrique de l'Ouest. CIRAD, MNHN, UICN, Montpellier, Paris.
- Arnould M. 1961. Etudes géologiques des migmatites et des granites précambriens du nord-est de la Côte d'Ivoire et de la Haute-Volta méridionale. Ed. Technip, Paris.
- Arya P. S. P. 2001. Introduction to micrometeorology. 2nd edition. Academic Press, San Diego.
- Aubréville A. 1949. Climats, forêts et désertification de l'Afrique tropicale. Société d'Éditions Géographiques, Maritimes et Coloniales.
- Aubréville A., and R.W.J. Keay 1959. Vegetation map of Africa south of the tropic of cancer. Oxford, Oxford University Press.
- Augustine, D. J. 2003. Spatial heterogeneity in the herbaceous layer of a semi-arid savanna ecosystem. *Plant Ecology* 167:319-332.
- Baker, W. L., and G. K. Dillon. 2000. Plant and vegetation responses to edges in the southern Rocky Mountains. Pages 221-245 in R. L. Knight, F. W. Smith, S. W. Buskirk, W. H. Romme, and W. L. Baker editors. *Forest fragmentation in the southern Rocky Mountains*. University Press of Colorado, Colorado.
- Baskent, E. Z. 1997. Assessment of structural dynamics in forest landscape management. *Canadian Journal of Forest Research* 27:1675-1684.
- Bates D. M., and D. G. Watts. 1988. Nonlinear regression analysis and its applications. John Wiley and Sons, New York.

- Beals, E. W. 1969. Vegetational change along altitudinal gradients. *Science* 165:981-985.
- Bender, D. J., T. A. Contreras, and L. Fahrig. 1998. Habitat loss and population decline: a meta-analysis of the patch size effect. *Ecology* 79:517-533.
- Biddulph, J., and M. Kellman. 1998. Fuels and fire at savanna gallery forest boundaries in southeastern Venezuela. *Journal of Tropical Ecology* 14:445-461.
- BIOTA West Africa. 2003. Towards sustainable use of biodiversity. Project proposal for the second phase, Volume I, BMBF.
- Bloesch U. 2002. The dynamics of thicket clumps in the Kagera savanna landscape, East Africa. Shaker, Aachen.
- Bourlière F. (ed.) 1983. Tropical savannas. Elsevier, Amsterdam.
- Bradshaw, G. A., and T. A. Spies. 1992. Characterizing canopy gap structure in forests using wavelet analysis. *Journal of Ecology* 80:205-215.
- Brand, L. A., and T. L. George. 2001. Response of passerine birds to forest edge in coast redwood forest fragments. *Auk* 118:678-686.
- Breman, H., and C. T. Dewit. 1983. Rangeland productivity and exploitation in the Sahel. *Science* 221:1341-1347.
- Brooks, T., A. Balmford, N. Burgess, J. Fjeldsa, L. A. Hansen, J. Moore, C. Rahbek, and P. Williams. 2001. Toward a blueprint for conservation in Africa. *Bioscience* 51:613-624.
- Brunt, J. W., and W. Conley. 1990. Behavior of a multivariate algorithm for ecological edge detection. *Ecological Modelling* 49:179-203.
- Byth, K. 1982. On robust distance-based intensity estimators. *Biometrics* 38:127-135.
- C.S.A. 1956. Specialist meeting on phytogeography, Yangambi. Scientific Council for Africa South of the Sahara 53:1-33.
- Cadenasso, M. L., and S. T. A. Pickett. 2000. Linking forest edge structure to edge function: mediation of herbivore damage. *Journal of Ecology* 88:31-44.
- Cadenasso, M. L., and S. T. A. Pickett. 2001. Effect of edge structure on the flux of species into forest interiors. *Conservation Biology* 15:91-97.
- Cadenasso, M. L., S. T. A. Pickett, K. C. Weathers, and C. G. Jones. 2003. A framework for a theory of ecological boundaries. *Bioscience* 53:750-758.
- Cain, M. D., and M. G. Shelton. 2001. Secondary forest succession following reproduction cutting on the Upper Coastal Plain of southeastern Arkansas, USA. *Forest Ecology and Management* 146:223-238.
- Camargo, J. L. C., and V. Kapos. 1995. Complex edge effects on soil moisture and microclimate in central Amazonian forest. *Journal of Tropical Ecology* 11:205-221.
- Cantrell, R. S., C. Cosner, and W. F. Fagan. 2001. How predator incursions affect critical patch size: the role of the functional response. *American Naturalist* 158:368-375.
- César, J. 1981. Cycles de la biomasse et des repousses après coupe en savane de Côte-d'Ivoire. *Revue D Elevage et de Medecine Veterinaire des Pays Tropicaux* 34:73-81.

- Chatelain, C., L. Gautier, and R. Spichiger. 1996a. A recent history of forest fragmentation in southwestern Ivory Coast. *Biodiversity and Conservation* 5:37-53.
- Chatelain, C., L. Gautier, and R. Spichiger. 1996b. Deforestation in southern Côte d'Ivoire: a high-resolution remote sensing approach. Pages 259-266 *in* L. J. G. van der Maesen, and et al. editors. *The Biodiversity of African Plants - Proceedings XIVth AETFAT Congress*. Kluwer Academic Publishers.
- Chen, J. Q., J. F. Franklin, and J. S. Lowe. 1996. Comparison of abiotic and structurally defined patch patterns in a hypothetical forest landscape. *Conservation Biology* 10:854-862.
- Chen, J. Q., J. F. Franklin, and T. A. Spies. 1992. Vegetation responses to edge environments in old-growth Douglas-fir forests. *Ecological Applications* 2:387-396.
- Chen, J. Q., J. F. Franklin, and T. A. Spies. 1995. Growing-season microclimatic gradients from clearcut edges into old-growth Douglas-fir forests. *Ecological Applications* 5:74-86.
- Chevalier A. 1951. Sur l'existence d'une forêt vierge sèche sur de grandes étendues aux confins des bassins de l'Oubangui, du Haut-Chari et du Nil (Bahr-el Ghazal). *Revue internationale de botanique appliquée et d'agriculture tropicale* 31, 135-136.
- Clayton, G. 1958. Secondary vegetation and the transition to savanna near Ibadan, Nigeria. *Journal of Ecology* 46:217-238.
- Clemens, M. A., C. S. ReVelle, and J. C. Williams. 1999. Reserve design for species preservation. *European Journal of Operational Research* 112:273-283.
- Clements F. E. 1905. *Research methods in ecology*. University of Nebraska Publishing Company, Lincoln.
- Cleveland, W. S., E. Grosse, and W. M. Shyu. 1992. Local regression models. Page 312-376 *in* J. M. Chambers, and T. J. Hastie editors. *Statistical Models in S*. Wadsworth & Brooks/Cole, Wadsworth.
- Cochrane, M. A., and W. F. Laurance. 2002. Fire as a large-scale edge effect in Amazonian forests. *Journal of Tropical Ecology* 18:311-325.
- Collins, S. L., S. M. Glenn, and D. W. Roberts. 1993. The hierarchical continuum concept. *Journal of Vegetation Science* 4:149-156.
- Condit, R., S. P. Hubbell, and R. B. Foster. 1995. Mortality rates of 205 neotropical tree and shrub species and the impact of a severe drought. *Ecological Monographs* 65:419-439.
- Connell, J. H., and M. D. Lowman. 1989. Low-diversity tropical rain forests: some possible mechanisms for their existence. *American Naturalist* 134:88-119.
- Cornelius, J. M., and J. F. Reynolds. 1991. On determining the statistical significance of discontinuities within ordered ecological data. *Ecology* 72:2057-2070.
- Couteron, P., and K. Kokou. 1997. Woody vegetation spatial patterns in a semi-arid savanna of Burkina Faso, West Africa. *Plant Ecology* 132:211-227.
- Crawley, M. J. 1997. The structure of plant communities. Pages 475-531 *in* M. Crawley editor. *Plant ecology*. Blackwell Science, Oxford.
- Csillag, F., and S. Kabos. 2002. Wavelets, boundaries, and the spatial analysis of landscape pattern. *Ecoscience* 9:177-190.

- Curran, L. M., I. Caniago, G. D. Paoli, D. Astianti, M. Kusneti, M. Leighton, C. E. Nirarita, and H. Haeruman. 1999. Impact of El Nino and logging on canopy tree recruitment in Borneo. *Science* 286:2184-2188.
- Curran, L. M., S. N. Trigg, A. K. McDonald, D. Astiani, Y. M. Hardiono, P. Siregar, I. Caniago, and E. Kasischke. 2004. Lowland forest loss in protected areas of Indonesian Borneo. *Science* 303:1000-1003.
- Davies-Colley, R. J., G. W. Payne, and M. van Elswijk. 2000. Microclimate gradients across a forest edge. *New Zealand Journal of Ecology* 24:111-121.
- DeBano L. F., D. G. Neary, and P. F. Ffolliott. 1998. *Fire's effect on ecosystems*. Wiley, New York.
- Demaynadier, P. G., and M. L. Hunter. 1998. Effects of silvicultural edges on the distribution and abundance of amphibians in Maine. *Conservation Biology* 12:340-352.
- Devineau, J. L. 1976. Cycles de la biomasse et des repousses après coupe en savane de Côte-d'Ivoire. *Oecologia Plantarum* 11:375-395.
- Didham, R. K., and J. H. Lawton. 1999. Edge structure determines the magnitude of changes in microclimate and vegetation structure in tropical forest fragments. *Biotropica* 31:17-30.
- Dierschke H. 1994. *Pflanzensoziologie: Grundlagen und Methoden*. Ulmer, Stuttgart.
- Diggle, P. J. 1975. Robust density estimation using distance methods. *Biometrika* 62:39-48.
- Direction des Mines et de la Géologie. 1995. Carte Géologique de la Côte d'Ivoire à 1/200.000, Feuille NASSIAN. Abidjan.
- Drake, D. R., C. P. H. Mulder, D. R. Towns, and C. H. Daugherty. 2002. The biology of insularity: an introduction. *Journal of biogeography* 29:563-569.
- Eldin, M. 1971. Le climat. Pages 73-108 *in* *Le Milieu Naturel de la Côte d'Ivoire*. Orstom, Paris.
- Engeman, R. M., R. T. Sugihara, L. F. Pank, and W. E. Dusenberry. 1994. A comparison of plotless density estimators using Monte Carlo simulation. *Ecology* 75:1769-1779.
- Ernest, S. K. M., and J. H. Brown. 2001. Delayed compensation for missing keystone species by colonization. *Science* 292:101-104.
- Fagan, W. F., M. J. Fortin, and C. Soykan. 2003. Integrating edge detection and dynamic modeling in quantitative analyses of ecological boundaries. *Bioscience* 53:730-738.
- Fahrig, L. 2003. Effects of habitat fragmentation on biodiversity. *Annual Review of Ecology Evolution and Systematics* 34:487-515.
- Fairhead J., and M. Leach. 1996. *Misreading the African landscape. Society and ecology in a forest-savanna mosaic*. Cambridge University Press, Cambridge.
- Fairhead J., and M. Leach. 1998. *Reframing deforestation: global analysis and local realities: studies in West Africa*. Routledge, London, New York.
- Farnsworth, K. D., and A. R. A. Anderson. 2001. How simple grazing rules can lead to persistent boundaries in vegetation communities. *Oikos* 95:15-24.

- Favier, C., J. Chave, A. Fabing, D. Schwartz, and M. A. Dubois. 2004. Modelling forest-savanna mosaic dynamics in man-influenced environments: effects of fire, climate and soil heterogeneity. *Ecological Modelling* 171:85-102.
- Fearnside, P. M., and W. F. Laurance. 2003. Comment on "Determination of deforestation rates of the world's humid tropical forests". *Science* 299:1015a.
- Fernandez, C., F. J. Acosta, G. Abella, F. Lopez, and M. Diaz. 2002. Complex edge effect fields as additive processes in patches of ecological systems. *Ecological Modelling* 149:273-283.
- FGU-Kronberg. 1979. Gegenwärtiger Status der Comoé- und Tai-Nationalparks sowie des Azagny-Reservats und Vorschläge zu deren Erhaltung und Entwicklung zur Förderung des Tourismus. II. Comoé-Nationalpark. 1. Bestandsaufnahme der ökologischen und biologischen Verhältnisse. GTZ GmbH, Eschborn.
- Finegan, B. 1984. Forest succession. *Nature* 312:109-114.
- Fischer, F., M. Gross, and K. E. Linsenmair. 2002. Updated list of the larger mammals of the Comoé National Park, Ivory Coast. *Mammalia* 66:83-92.
- Fischer, F., and K. E. Linsenmair. 2001. Decreases in ungulate population densities. Examples from the Comoé National Park, Ivory Coast. *Biological Conservation* 101:131-135.
- Fölster H. 1983. Bodenkunde Westafrika (Nigeria, Kamerun). Afrika-Kartenwerk, Beiheft zu Blatt 4, Gebrüder Borntraeger, Berlin.
- Fortin, M. J., R. J. Olson, S. Ferson, L. Iverson, C. Hunsaker, G. Edwards, D. Levine, K. Butera, and V. Klemas. 2000. Issues related to the detection of boundaries. *Landscape Ecology* 15:453-466.
- Fortin, M.-J. 1994. Edge detection algorithms for two-dimensional ecological data. *Ecology* 75:956-965.
- Fournier A. 1991. Phénologie, croissance et production végétales dans quelques savanes d'Afrique de l'Ouest. Variation selon un gradient climatique. ORSTOM, Paris.
- Fournier, A., O. Hoffmann, and J.-L. Devineau. 1982. Variations de la phytomasse herbacée le long d'une toposéquence en zone soudano-guinéenne, Ouango-Fitini (Côte d'Ivoire). *Bulletin de l'Institut Fondamental d'Afrique Noire, sér. A* 44:71-77.
- Fraver, S. 1994. Vegetation responses along edge-to-interior gradients in the mixed hardwood forests of the Roanoke river basin, North-Carolina. *Conservation Biology* 8:822-832.
- Fuls, E. R. 1992. Ecosystem modification created by patch-overgrazing in semiarid grassland. *Journal of Arid Environments* 23:59-69.
- Furley P. A., J. Proctor, and J. A. Ratter. 1992. Nature and dynamics of forest-savanna boundaries. Chapman & Hall, London.
- Gascon, C., G. B. Williamson, and G. A. B. Da Fonseca. 2000. Receding forest edges and vanishing reserves. *Science* 288:1356-1358.
- Giambelluca, T. W., A. D. Ziegler, M. A. Nullet, D. M. Truong, and L. T. Tran. 2003. Transpiration in a small tropical forest patch. *Agricultural and Forest Meteorology* 117:1-22.

- Gibson, D. J. 1996. Textbook misconceptions: the climax concept of succession. *American Biology Teacher* 58:135-140.
- Gignoux, J., J. Clobert, and J. C. Menaut. 1997. Alternative fire resistance strategies in savanna trees. *Oecologia* 110:576-583.
- Goldammer J. G. (ed.) 1990. Fire in the tropical biota: ecosystem processes and global changes. Springer-Verlag, Berlin.
- Gosz, J. R. 1991. Fundamental ecological characteristics of landscape boundaries. Pages 8-30 in M. M. Holland, P. G. Risser, and R. J. Naiman editors. *Ecotones: the role of landscape boundaries in the management and restoration of changing environments*. Chapman & Hall, New York.
- Griggs, R. F. 1938. Timberlines in northern Rocky Mountains. *Ecology* 19:548-564.
- Guillaumet, J. L., and E. Adjanohoun. 1971. La végétation de la Côte d'Ivoire. Pages 161-262 in *Le Milieu Naturel de la Côte d'Ivoire*. Orstom, Paris.
- Guinko, S. 1985. Contribution à l'étude de la végétation et de la flore du Burkina Faso. 1. Les reliques boisées ou bois sacrés. *Revue Bois et Forêts des Tropiques* 208:29-36.
- Hahn-Hadjali, K. 1998. Les groupements végétaux des savanes du sud-est du Burkina Faso (Afrique de l'ouest). *Études sur la flore et la végétation du Burkina Faso et des pays avoisinants* 3:3-79.
- Hall J. B., and M. D. Swaine. 1981. Distribution and ecology of vascular plants in a tropical rain forest: forest vegetation in Ghana. Junk, The Hague, Boston, London.
- Harper, K. A., and S. E. Macdonald. 2001. Structure and composition of riparian boreal forest: new methods for analyzing edge influence. *Ecology* 82:649-659.
- Harper, K. A., and S. E. Macdonald. 2002. Structure and composition of edges next to regenerating clear-cuts in mixed-wood boreal forest. *Journal of Vegetation Science* 13:535-546.
- Harris W. V. 1971. Termites - their recognition and control. 2nd edition. Longman, Green and Co., London.
- Hart, T. B., J. A. Hart, and P. G. Murphy. 1989. Monodominant and species-rich forests of the humid tropics: causes for their cooccurrence. *American Naturalist* 133:613-633.
- Hartge K. H., and R. Horn. 1992. *Die physikalische Untersuchung von Böden*. 3rd edition. Enke, Stuttgart.
- Hastie T., R. Tibshirani, and J. Friedman. 2003. *The elements of statistical learning: data mining, inference, and prediction*. Springer, New York.
- Hastie, T. J., and D. Pregibon. 1992. Generalized linear models. Page 196-247 in J. M. Chambers, and T. J. Hastie editors. *Statistical Models in S*. Wadsworth & Brooks/Cole, Wadsworth.
- Henle, K., S. Sarre, and K. Wiegand. 2004. The role of density regulation in extinction processes and population viability analysis. *Biodiversity and Conservation* 13:9-52.
- Hennenberg, K. J., D. Goetze, V. Minden, D. Traoré, and S. Porembski, *in press*. Size class distribution of *Anogeissus leiocarpus* (Combretaceae) along forest-savanna ecotones in northern Ivory Coast. *Journal of Tropical Ecology*.

- Heywood, V. H. (ed.) 1998. Flowering plants of the world. Batsford, London.
- Higgins, S. I., W. J. Bond, and W. S. W. Trollope. 2000. Fire, resprouting and variability: a recipe for grass-tree coexistence in savanna. *Journal of Ecology* 88:213-229.
- Hill, J. L., and P. J. Curran. 2001. Species composition in fragmented forests: conservation implications of changing forest area. *Applied Geography* 21:157-174.
- Hill, J. L., and P. J. Curran. 2003. Area, shape and isolation of tropical forest fragments: effects on tree species diversity and implications for conservation. *Journal of biogeography* 30:1391-1403.
- Hochberg, M. E., J. C. Menaut, and J. Gignoux. 1994. The influences of tree biology and fire in the spatial structure of the West African savannah. *Journal of Ecology* 82:217-226.
- Holmquist, J. G. 1998. Permeability of patch boundaries to benthic invertebrates: influences of boundary contrast, light level, and faunal density and mobility. *Oikos* 81:558-566.
- Honnay, O., K. Verheyen, and M. Hermy. 2002. Permeability of ancient forest edges for weedy plant species invasion. *Forest Ecology and Management* 161:109-122.
- Hopkins, B. 1992. Ecological processes at the forest-savanna boundaries. Pages 21-33 in P. A. Furley, J. Proctor, and J. A. Ratter editors. *Nature and dynamics of forest-savanna boundaries*. Chapman & Hall, London.
- Hovestadt T. 1997. Fruchtmerkmale, endozoochore Samenausbreitung und ihre Bedeutung für die Zusammensetzung der Pflanzengemeinschaft: Untersuchungen im Wald-Savannenmosaik des Comoé Nationalparks, Elfenbeinküste. *Wissenschaft & Technik*, Berlin.
- Hovestadt, T., H. J. Poethke, and K. E. Linsenmair, *in press*. Spatial patterns in species-area relationships and species distribution in a West Africa forest-savannah mosaic. *Journal of biogeography*.
- Hovestadt, T., H. J. Poethke, and S. Messner. 2000. Variability in dispersal distances generates typical successional patterns: a simple simulation model. *Oikos* 90:612-619.
- Hovestadt, T., P. Yao, and K. E. Linsenmair. 1999. Seed dispersal mechanisms and the vegetation of forest islands in a West African forest-savanna mosaic (Comoé National Park, Ivory Coast). *Plant Ecology* 144:1-25.
- Huntley B. J. and B. H. Walker (eds) 1982. *Ecology of tropical savannas*. Springer, Berlin.
- Huston, M., and T. Smith. 1987. Plant succession - life-history and competition. *American Naturalist* 130:168-198.
- Hutchinson J., J. M. Dalziel, R. W. J. Keay, and F. N. Hepper. 1954-1972. *Flora of west tropical Africa*. 2nd edition. Vol. I-II, The Whitefriars Press, London.
- Irvine F. R. 1961. *Woody plants of Ghana*. Oxford University Press, London.
- Jacquez, G. M., S. Maruca, and M.-J. Fortin. 2000. From fields to objects: a review of geographic boundary analysis. *Journal of Geographical Systems* 2:221-241.
- Jeltsch, F., G. E. Weber, and V. Grimm. 2000. Ecological buffering mechanisms in savannas: a unifying theory of long-term tree-grass coexistence. *Plant Ecology* 161:161-171.
- Jones, E. W. 1963. The forest outliers in the Guinea Zone of northern Nigeria. *Journal of Ecology* 51:415-434.

- Kapos, V. 1989. Effects of isolation on the water status of forest patches in the Brazilian Amazon. *Journal of Tropical Ecology* 5:173-185.
- Kapos, V., G. Ganade, E. Matsui, and R. L. Victoria. 1993. Partial-derivative-C-13 as an indicator of edge effects in tropical rainforest reserves. *Journal of Ecology* 81:425-432.
- Keay R.W.J. 1949. An example of Sudan zone vegetation in Nigeria. *Journal of Ecology* 37:335-364.
- Keay R. W. J. 1959a. An outline of Nigerian vegetation. Lagos Govt. Printer, Lagos.
- Keay R. W. J. 1959b. Derived savanna: derived from what? *Bulletin d'IFAN, Ser. A.*, 21:427-438
- Keesing, F. 1998. Impacts of ungulates on the demography and diversity of small mammals in central Kenya. *Oecologia* 116:381-389.
- Keesing, F. 2000. Cryptic consumers and the ecology of an African savanna. *Bioscience* 50:205-215.
- Kellman, M., and J. Meave. 1997. Fire in the tropical gallery forests of Belize. *Journal of biogeography* 24:23-34.
- Kellman, M., R. Tackaberry, and L. Rigg. 1998. Structure and function in two tropical gallery forest communities: implications for forest conservation in fragmented systems. *Journal of Applied Ecology* 35:195-206.
- Kemp, P. R., J. M. Cornelius, and J. F. Reynolds. 1994. Temporal discontinuities in precipitation in the central North-American prairie. *International Journal of Climatology* 14:539-557.
- Kent, M., W. J. Gill, R. E. Weaver, and R. P. Armitage. 1997. Landscape and plant community boundaries in biogeography. *Progress in Physical Geography* 21:315-353.
- Kersting P. 2003. Geoökologische Untersuchung im Comoé-Nationalpark mit Schwerpunkt Bodenkunde. University of Mainz, Diploma thesis, Mainz.
- Knapp R. 1973. Die Vegetation von Afrika. Gustav Fischer, Stuttgart.
- Krebs C. J. 1999. Ecological methodology. 2nd edition. Addison Wesley Longman, Menlo Park, California.
- Krieger, A., S. Porembski, and W. Barthlott. 2003. Temporal dynamics of an ephemeral plant community: species turnover in seasonal rock pools on Ivorian inselbergs. *Plant Ecology* 167:283-292.
- Küper, W., J. H. Sommer, J. C. Lovett, J. Mutke, H. P. Linder, H. J. Beentje, R. S. A. R. Van Rompaey, C. Chatelain, M. Sosef, and W. Barthlott, *in press*. African hotspots of biodiversity redefined. *Annals Missouri Botanical Garden*.
- Lauer W., and M. D. Rafiqpoor. 2002. Die Klima der Erde: eine Klassifikation auf der Grundlage der ökophysiologischen Merkmale der realen Vegetation. Steiner, Stuttgart.
- Lauginie F. 1995. Problèmes lies a la conservation de la grande faune en Afrique. L'exemple des grands mammiferes du parc national de la Comoé (Côte d'Ivoire). Unversity of Orleans, Disseration, Orleans.

- Laurance, W. F. 2000. Do edge effects occur over large spatial scales? *Trends in Ecology & Evolution* 15:134-135.
- Laurance, W. F. 2003. Slow burn: the insidious effects of surface fires on tropical forests. *Trends in Ecology & Evolution* 18:209-212.
- Laurance, W. F., A. K. M. Albernaz, and C. Da Costa. 2001. Is deforestation accelerating in the Brazilian Amazon? *Environmental Conservation* 28:305-311.
- Laurance W.F., P. Delamónica, H.L. Vasconcelos, and T.E. Lovejoy 2000. Rainforest fragmentation kills big trees. *Nature* 404:836.
- Laurance, W. F., L. V. Ferreira, J. M. Rankin-de Merona, and S. G. Laurance. 1998. Rain forest fragmentation and the dynamics of Amazonian tree communities. *Ecology* 79:2032-2040.
- Laurance, W. F., T. E. Lovejoy, H. L. Vasconcelos, E. M. Bruna, R. K. Didham, P. C. Stouffer, C. Gascon, R. O. Bierregaard, S. G. Laurance, and E. Sampaio. 2002. Ecosystem decay of Amazonian forest fragments: a 22-year investigation. *Conservation Biology* 16:605-618.
- Laurance, W. F., and E. Yensen. 1991. Predicting the impacts of edge effects in fragmented habitats. *Biological Conservation* 55:77-92.
- Lawesson, J. E. 1994. Some comments on the classification of African vegetation. *Journal of Vegetation Science* 5:441-444.
- Lawson, G. W., J. Jeník, and K. O. Armstrong-Mensah. 1968. A study of a vegetation catena in Guinea savanna at Mole game reserve (Ghana). *Journal of Ecology* 56:505-522.
- Le Houérou H. N. 1989. *The grazing land ecosystems of the African Sahel*. Springer Verlag, Berlin.
- Lebrun J. P., and A. L. Storck. 1991-1997. *Énumération des plantes à fleurs d'Afrique tropicale*. Conservatoire et Jardin Botaniques de Genève, Geneva, Vol. I-IV.
- Lehmann E. L. 1999. *Theory of point estimation*. 2nd edition. Springer, New York.
- Leopold A. 1933. *Game management*. Charles Scribner's Sons, New York.
- Letouzey, R. 1969. Observations phytogéographiques concernant le plateau africain de l'Adamaoua. *Adansonia ser.2* 14:321-337.
- Lindstrom, M. J., and D. M. Bates. 1988. Newton-Raphson and EM algorithms for linear mixed-effects models for repeated-measures data. *Journal of the American Statistical Association* 83:1014-1022.
- Lindstrom, M. J., and D. M. Bates. 1990. Nonlinear mixed-effects models for repeated-measures data. *Biometrics* 46:673-687.
- Lloyd, K. M., A. A. M. McQueen, B. J. Lee, R. C. B. Wilson, S. Walker, and J. B. Wilson. 2000. Evidence on ecotone concepts from switch, environmental and anthropogenic ecotones. *Journal of Vegetation Science* 11:903-910.
- Lomolino, M. V. 1994. An evaluation of alternative strategies for building networks of nature-reserves. *Biological Conservation* 69:243-249.
- Lomolino, M. V., and M. D. Weiser. 2001. Towards a more general species-area relationship: diversity on all islands, great and small. *Journal of biogeography* 28:431-445.

- Louppe, D., N. Ouattara, and A. Coulibaly. 1995. Effet des feux de brousse sur la végétation. *Bois et Forêts des Tropiques* 245:59-74.
- Ludwig, J. A., and J. M. Cornelius. 1987. Locating discontinuities along ecological gradients. *Ecology* 68:448-450.
- Mabberley D. J. 2000. *The plant book - a portable dictionary of the vascular plants*. 2 edition. Cambridge university press, Cambridge.
- MacArthur R. H., and E. O. Wilson. 1967. *The theory of island biogeography*. Princeton University Press, Princeton (NJ) .
- MacKay, J. H. 1936. Problems of ecology in Nigeria. *Empire forestry journal* 15:190-200.
- Maignien R. 1966. Review of research on laterites. UNESCO, Paris.
- Malcolm, J. R. 1994. Edge effects in central Amazonian forest fragments. *Ecology* 75:2438-2445.
- Malcolm, J. R. 1998. A model of conductive heat flow in forest edges and fragmented landscapes. *Climatic Change* 39:487-502.
- Matlack, G. R. 1993. Microenvironment variation within and among forest edge sites in the eastern United-States. *Biological Conservation* 66:185-194.
- Matlack, G. R. 1994. Vegetation dynamics of the forest edge - trends in space and successional time. *Journal of Ecology* 82:113-123.
- McCook, L. J. 1994. Understanding ecological community succession: causal-models and theories, a review. *Vegetatio* 110:115-147.
- McGregor G. R., and S. Nieuwolt. 1998. *Tropical climatology: an introduction to the climates of the low latitudes*. Wiley, Chichester.
- Menaut, J. C., and J. César. 1979. Structure and primary productivity of Lamto savannas, Ivory Coast. *Ecology* 60:1197-1210.
- Menaut, J. C., and J. César. 1982. The structure and dynamics of a West African savanna. Pages 80-100 *in* B. J. Huntley, and B. H. Walker editors. *Ecology of tropical savannas*. Springer, Berlin.
- Mordelet, P. 1993. Influence of tree shading on carbon assimilation of grass leaves in Lamto savanna, Côte d'Ivoire. *Acta Oecologica-International Journal of Ecology* 14:119-127.
- Mordelet, P., and J. C. Menaut. 1995. Influence of trees on above-ground production dynamics of grasses in a humid savanna. *Journal of Vegetation Science* 6:223-228.
- Morison, C. G. T., A. C. Hoyle, and J. F. Hope-Simpson. 1948. Tropical soil-vegetation catenas and mosaics. *Journal of Ecology* 36:1-84.
- Müller, J., and R. Wittig. 2002. L'état actuel du peuplement ligneux et la perception de sa dynamique par la population dans le Sahel burkinabé - présenté à l'exemple de Tintaboora et de Kollangal Alyaakum. *Etudes sur la flore et la végétation du Burkina Faso et des pays avoisinants* 6:19-30.
- Murcia, C. 1995. Edge effects in fragmented forests: implications for conservation. *Trends in Ecology and Evolution* 10:58-62.

- Myers, N., R. A. Mittermeier, C. G. Mittermeier, G. A. B. Da Fonseca, and J. Kent. 2000. Biodiversity hotspots for conservation priorities. *Nature* 403:853-858.
- Nansen, C., A. Tchabi, and W. G. Meikle. 2001. Successional sequence of forest types in a disturbed dry forest reserve in southern Benin, West Africa. *Journal of Tropical Ecology* 17:525-539.
- Neumann, K., and P. Müller-Haude. 1999. Forêts sèches au sud-ouest du Burkina Faso: végétation - sols - action de l'homme. *Phytocoenologia* 29:53-85.
- Newmark, W. D. 2001. Tanzanian forest edge microclimatic gradients: dynamic patterns. *Biotropica* 33:2-11.
- Nishimura, T. B., and T. Kohyama. 2002. Formation and maintenance of community boundaries in a sub-alpine forest landscape in northern Japan. *Journal of Vegetation Science* 13:555-564.
- Ojo O. 1977. The climates of West Africa. Heinemann, London.
- Oosting, H. J., and P. J. Kramer. 1946. Water and light in relation to pine reproduction. *Ecology* 27:47-53.
- Palik, B. J., and P. G. Murphy. 1990. Disturbance versus edge effects in sugar-maple/beech forest fragments. *Forest Ecology and Management* 32:187-202.
- Perry, G. L. W. 2002. Landscapes, space and equilibrium: shifting viewpoints. *Progress in Physical Geography* 26:339-359.
- Pickett, S. T. A., and M. L. Cadenasso. 1995. Landscape ecology: spatial heterogeneity in ecological systems. *Science* 269:331-334.
- Pinheiro J. C., and D. M. Bates. 2000. *Mixed-effects models in S and S-plus*. Springer, New York.
- Poilecot P. 1995. *Les Poaceae de Côte-d'Ivoire*. Conservatoire et Jardin Botaniques, Geneva.
- Poilecot P., K. Bonfou, H. Dosso, F. Lauginie, K. N'Dri, M. Nicole, and Y. Sangare. 1991. *Un écosystème de savane soudanienne: le Parc National de la Comoé (Côte d'Ivoire)*. UNESCO, Paris.
- Porembski, S. 1991. Beiträge zur Pflanzenwelt des Comoé-Nationalparks (Elfenbeinküste). *Natur und Museum* 121:61-83.
- Porembski, S. 2001. Phytodiversity and structure of the Comoé river gallery forest (NE Ivory Coast). Pages 1-10 *in* G. Gottsberger, and S. Liede editors. *Life forms and dynamics in tropical forests*. Cramer, Berlin, Stuttgart.
- Putz, F. E., G. M. Blate, K. H. Redford, R. Fimbel, and J. Robinson. 2001. Tropical forest management and conservation of biodiversity: an overview. *Conservation Biology* 15:7-20.
- R 1.8.0. 2003. The R Project for Statistical Computing. <http://www.r-project.org/>
- Ramsey, J. M., and R. Rose Innes. 1963. Some quantitative observations on the effects of fire on the Guinea savanna vegetation of northern Ghana over a period of eleven years. *African Soils* 8:41-86.

- Ranta, P., T. Blom, J. Niemela, E. Joensuu, and M. Siitonen. 1998. The fragmented Atlantic rain forest of Brazil: size, shape and distribution of forest fragments. *Biodiversity and Conservation* 7:385-403.
- Redding, T. E., G. D. Hope, M. J. Fortin, M. G. Schmidt, and W. G. Bailey. 2003. Spatial patterns of soil temperature and moisture across subalpine forest-clearcut edges in the southern interior of British Columbia. *Canadian Journal of Soil Science* 83:121-130.
- Rheault, H., P. Drapeau, Y. Bergeron, and P. A. Esseen. 2003. Edge effects on epiphytic lichens in managed black spruce forests of eastern North America. *Canadian Journal of Forest Research-Revue Canadienne de Recherche Forestiere* 33:23-32.
- Risser, P. G. 1995. The status of the science examining ecotones - a dynamic aspect of landscape is the area of steep gradients between more homogeneous vegetation associations. *Bioscience* 45:318-325.
- Russell, W. H., and C. Jones. 2001. The effects of timber harvesting on the structure and composition of adjacent old-growth coast redwood forest, California, USA. *Landscape Ecology* 16:731-741.
- Salzmann U. 1999. Zur holozänen Vegetations- und Klimaentwicklung der westafrikanischen Savannen: paläoökologische Untersuchungen in der Sahel- und Sudanzone NO-Nigerias. Johann Wolfgang Goethe-Universität Frankfurt am Main, Frankfurt am Main.
- Salzmann, U. 2000. Are modern savannas degraded forests? - A Holocene pollen record from the Sudanian vegetation zone of NE Nigeria. *Vegetation History and Archaeobotany* 9:1-15.
- Salzmann, U., P. Hoelzmann, and I. Morczinek. 2002. Late Quaternary climate and vegetation of the Sudanian zone of northeast Nigeria. *Quaternary Research* 58:73-83.
- San Jose, J. J., and R. A. Montes. 1997. Fire effect on the coexistence of trees and grasses in savannas and the resulting outcome on organic matter budget. *Interciencia* 22:289-298.
- Saunders, D. A., R. J. Hobbs, and C. R. Margules. 1991. Biological consequences of ecosystem fragmentation: a review. *Conservation Biology* 5:18-32.
- Saunders, S. C., J. Q. Chen, T. R. Crow, and K. D. Brososfske. 1998. Hierarchical relationships between landscape structure and temperature in a managed forest landscape. *Landscape Ecology* 13:381-395.
- Saunders, S. C., J. Q. Chen, T. D. Drummer, and T. R. Crow. 1999. Modeling temperature gradients across edges over time in a managed landscape. *Forest Ecology and Management* 117:17-31.
- Scholes, R. J., and S. R. Archer. 1997. Tree-grass interactions in savannas. *Annual Review of Ecology and Systematics* 28:517-544.
- Schultz, C. B., and E. E. Crone. 2001. Edge-mediated dispersal behavior in a prairie butterfly. *Ecology* 82:1879-1892.
- Schwartz, D., H. De Foresta, A. Mariotti, J. Balesdent, J. P. Massimba, and C. Girardin. 1996. Present dynamics of the savanna-forest boundary in the Congolese Mayombe: a pedological, botanical and isotopic (^{13}C and ^{14}C) study. *Oecologia* 106:516-524.

- Sheil, D., S. Jennings, and P. Savill. 2000. Long-term permanent plot observations of vegetation dynamics in Budongo, a Ugandan rain forest. *Journal of Tropical Ecology* 16:765-800.
- Simberloff, D. 1988. The contribution of population and community biology to conservation science. *Annual Review of Ecology and Systematics* 19:473-511.
- Sobey, D. G. 1978. *Anogeissus* groves on abandoned village sites in the Mole National Park, Ghana. *Biotropica* 10:87-99.
- Spichiger, R., and C. Pamard. 1973. Recherches sur le contact forêt-savane en Côte-d'Ivoire: étude du recrû forestier sur des parcelles cultivées en lisière d'un îlot forestier dans le sud du pays Baoulé. *Candollea* 28:21-37.
- Stocks, B. J., B. W. vanWilgen, W. S. W. Trollope, D. J. Mccrae, J. A. Mason, F. Weirich, and A. L. F. Potgieter. 1996. Fuels and fire behavior dynamics on large-scale savanna fires in Kruger National Park, South Africa. *Journal of Geophysical Research-Atmospheres* 101:23541-23550.
- Stott, P. 2000. Combustion in tropical biomass fires: a critical review. *Progress in Physical Geography* 24:355-377.
- Sträßer M. 1998. Klimadiagramme zur Köppenschen Klimaklassifikation: 201 Klimadiagramme. Justus Perthes Verlag Gotha, Gotha.
- Sturm, H.-J. 1993. Auswirkungen von Feuer- und Beweidungsausschluß auf die Produktion der Krautschicht einer Strauchsavanne. *Verhandlungen der Gesellschaft für Ökologie* 22:323-328.
- Swaine, M. D., W. D. Hawthorne, and T. K. Orgle. 1992. The effects of fire exclusion on savanna vegetation at Kpong, Ghana. *Biotropica* 24:166-172.
- Swaine, M. D., and T. C. Whitmore. 1988. On the definition of ecological species groups in tropical rain forests. *Vegetatio* 75:81-86.
- Takhtajan A. L. 1986. *Floristical regions of the world*. University of California Press, Berkeley.
- Talling, J. F. 1957. The phytoplankton population as a compound photosynthetic system. *New phytologist* 56:133-149.
- ter Braak C. J. F., and P. Smilauer. 2002. *CANOCO reference manual and CanoDraw for Windows user's guide: software for canonical community ordination (version 4.5)*. Biometrics, Wageningen.
- Thomas, D. C., A. Cameron, R. E. Green, M. Bakkenes, L. B. Beaumont, Y. C. Collingham, B. F. N. Erasmus, M. Ferreira de Siqueira, A. Grainger, L. Hannah, H. Hughes, B. Huntley, A. S. van Jaarsveld, G. F. Midgley, L. Miles, M. A. Ortega-Huerta, A. T. Peterson, O. L. Phillips, and S. E. Williams. 2004. Extinction risk from climate change. *Nature* 427:145-148.
- Toms, J. D., and M. L. Lesperance. 2003. Piecewise regression: a tool for identifying ecological thresholds. *Ecology* 84:2034-2041.
- Torti, S. D., P. D. Coley, and T. A. Kursar. 2001. Causes and consequences of monodominance in tropical lowland forests. *American Naturalist* 157:141-153.
- Turner, I. M. 1996. Species loss in fragments of tropical rain forest: a review of the evidence. *Journal of Applied Ecology* 33:200-209.

- Turner, I. M., and R. T. Cortlett. 1996. The conservation value of small, isolated fragments of lowland tropical rain forest. *Trends in Ecology and Evolution* 11:330-331.
- UN. 1992. Convention on biological diversity NA.92-7807.
<http://www.biodiv.org/convention/articles.asp>
- UN. 1994 Convention to combat desertification GE.94-64371.
<http://www.unccd.int/convention/menu.php>
- van de Vijver, C. A. D. M. 1999. Fire and life in Tarangire. Effects of burning and herbivory on an East African savanna system. Wageningen University.
- van der Maarel, E. 1990. Ecotones and ecoclines are different. *Journal of Vegetation Science* 1:135-138.
- van Langevelde, F., C. A. D. M. van de Vijver, L. Kumar, J. van de Koppel, N. de Ridder, J. van Andel, A. K. Skidmore, J. W. Hearne, L. Stroosnijder, W. J. Bond, H. H. T. Prins, and M. Rietkerk. 2003. Effects of fire and herbivory on the stability of savanna ecosystems. *Ecology* 84:337-350.
- Vazquez, J. A., and T. J. Givnish. 1998. Altitudinal gradients in tropical forest composition, structure, and diversity in the Sierra de Manantlan. *Journal of Ecology* 86:999-1020.
- Villecourt, P., W. Schmidt, and J. César. 1979. Recherche sur la composition chimique (N, P, K) de la strate herbacée de la savane de Lamto (Côte d'Ivoire). *Revue d'Ecologie et de Biologie du Sol* 16:9-15.
- Villecourt, P., W. Schmidt, and J. César. 1980. Pertes d'un écosystème à l'occasion du feu de brousse (Savane tropicale de Lamto, Côte d'Ivoire). *Revue d'Ecologie et de Biologie du Sol* 17:7-12.
- Walker S., W. Steffen, J. Canadell, and J. Ingram. 1999. The terrestrial biosphere and global change. Cambridge University Press, Cambridge.
- Walker, S., J. B. Wilson, J. B. Steel, G. L. Rapson, B. Smith, W. M. King, and Y. H. Cottam. 2003. Properties of ecotones: evidence from five ecotones objectively determined from a coastal vegetation gradient. *Journal of Vegetation Science* 14:579-590.
- Walter H. 1979. *Vegetation und Klimazonen*. Ulmer, Stuttgart.
- WBGU. 2000. *Welt im Wandel: Erhalt und nachhaltige Nutzung der Biosphäre*. Springer Verlag, Berlin.
- White F. 1983. *The vegetation of Africa*. United Nations, Paris.
- Whittaker, R. H. 1953. A consideration of climax theory - the climax as a population and pattern. *Ecological Monographs* 23:41-78.
- Whittaker, R. H. 1967. Gradient analysis of vegetation. *Biological Reviews of the Cambridge Philosophical Society* 42:207-264.
- Wickens G. E. 1976. *The flora of Jebel Marra (Sudan Republic) and its geographical affinities*. Her Majesty's Stationery Office, London.
- Wiens, J. A., C. S. Crawford, and J. R. Gosz. 1985. Boundary dynamics: a conceptual framework for studying landscape ecosystems. *Oikos* 45:421-427.
- Williams-Linera, G., V. Dominguez-Gastelu, and M. E. Garcia-Zurita. 1998. Micro-environment and floristics of different edges in a fragmented tropical rainforest. *Conservation Biology* 12:1091-1102.

- Wolters, V., W. L. Silver, D. E. Bignell, D. C. Coleman, P. Lavelle, W. H. van der Putten, P. De Ruiter, J. Rusek, D. H. Wall, D. A. Wardle, L. Brussaard, J. M. Dangerfield, V. K. Brown, K. E. Giller, D. U. Hooper, O. Sala, J. Tiedje, and J. A. van Veen. 2000. Effects of global changes on above- and belowground biodiversity in terrestrial ecosystems: implications for ecosystem functioning. *Bioscience* 50:1089-1098.
- Young, A., and N. Mitchell. 1994. Microclimate and vegetation edge effects in a fragmented podocarp-broadleaf forest in New-Zealand. *Biological Conservation* 67:63-72.
- Zalatnai, M., and L. Körmöczi. 2004. Fine-scale pattern of the boundary zones in alkaline grassland communities. *Community Ecology* 5:235-246.
- Zheng, D. L., and J. Q. Chen. 2000. Edge effects in fragmented landscapes: a generic model for delineating area of edge influences (D-AEI). *Ecological Modelling* 132:175-190.

Acknowledgements

Many people contributed to this work in different ways. My sincere thanks go to all of them, also those not mentioned explicitly. Warm thanks to

... Prof. Dr. Stefan Porembski who gave me the opportunity to work at the Department of Botany. Thank you very much for valuable suggestions, both during field work and in seminars and discussions.

... our Ivorian counterparts at the Universities of Cocody and Abobo-Adjamé, namely Prof. Dr. Dossahoua Traoré, Prof. Dr. Laurent Aké Assi, Dr. Eduard N'Guessan, and Dr. Martine Tahoux Touao. The Ivorian Ministry of Eaux et Forêts kindly gave the permission to conduct research in the CNP.

... Prof. Dr. K. Eduard Linsenmair, Dr. Frauke Fischer, and employees of the 'Projet Biodiversité' who enabled me to carry out the studies in the CNP at the research station of the University of Würzburg as well as to Minnattallah Boutros for the coordination of BIOTA project in West Africa.

... Prof. Dr. Brice Sinsin, Dr. Adjima Thiombiano, Henri Guesio Téré, Koffi Kouadio, Pierre Agbani, Jean Assi, and Justin Kevin Kassi for their valuable support on plant determination.

... my field assistant Lucien Kouamé. Thank you very much for your dedicated work and the nice time in the field!

... Dr. Dethardt Goetze for coordinating the sub-project W04 and for indefatigably correcting my manuscript more often than tow ;-) times!

... Prof. Dr. Florian Jeltsch, Dr. Anja Eggert, Sven Adler, Bettina Orthmann, and Björn Reineking for constructive methodical discussions and especially to Ingo Steinke for his help on the derivations of confidence intervals.

... Dr. Thomas Hovestadt for constructive discussions at the beginning of this study and for providing tree data of the study area.

... all members of the Department of Botany, especially Petra Kiehl and Gabriele Schöley, for their contribution in the background of this study.

... Ute Becker, Dr. Else Bünemann, Dr. Njikoa Ebigbo, Dr. Alexandra Erfmeier, Dr. Ulmar Grafe, Daniela Gurlin, Dr. Dieter Mahsberg, Dr. Karen Hahn-Hadjali, Dr. Ursula Karlowski, Christian Kost, Annick Koulibaly, Dr. Karsten Modi, Dr. Norbert Reintjes, and Dr. Jörg

Szarzynski for their constructive discussion during field work and for their valuable comments on the manuscript of this thesis.

This study was embedded in the program BIOTA (Biodiversity Monitoring Transect Analysis in Africa), funded by the German Federal Ministry of Education and Research (BMBF, project ID: 01 LC 0017/01 LC 0017A409

Appendix

Appendix A. Estimation of total area (TA) in dependence on an aspired relative core area (rCA) (compare Chapter 2.6.5)

Let rCA and TA denote the relative core area and the total area of forest islands, respectively. For the given data values rCA_i and TA_i we assume the non-linear regression model

$$rCA_i = a \cdot TA_i / (TA_i + b) + e_i \quad (\text{A } 1)$$

with zero-mean error terms e_i and unknown coefficients a and b . By non-linear least squares, the estimates \hat{a} and \hat{b} for a and b are determined. The corresponding estimates for their standard deviation and its covariance are denoted by $S\hat{D}_a$, $S\hat{D}_b$, and $S\hat{D}_{a,b}$. The deterministic functional relationship between TA and rCA from A 1 gives $TA = TA(rCA) = (rCA \cdot b) / (a - rCA) = f(a, b)$. Therefore, for a given rCA we can estimate $TA(rCA)$ by

$$T\hat{A} = f(\hat{a}, \hat{b}) = (rCA \cdot \hat{b}) / (\hat{a} - rCA).$$

Applying the Delta-Method (see Lehmann 1999) to $f(\hat{a}, \hat{b})$ we get an estimate for the standard deviation of $T\hat{A}$ by

$$S\hat{D}_{TA}^2 = rCA^2 \cdot \left[\frac{\hat{b}^2 \cdot S\hat{D}_a^2}{(\hat{a} - rCA)^4} + \frac{S\hat{D}_b^2}{(\hat{a} - rCA)^2} - \frac{2 \cdot \hat{b} \cdot S\hat{D}_{a,b}}{(\hat{a} - rCA)^3} \right]$$

Assuming a ‘normal distribution’ for the distribution of \hat{a} and \hat{b} , which can be justified for sufficiently large sample sizes, a confidence interval CI for $TA(rCA)$ can be constructed by

$$\left[T\hat{A} - z_{1-\alpha/2} S\hat{D}_{TA}, T\hat{A} + z_{1-\alpha/2} S\hat{D}_{TA} \right],$$

where $z_{1-\alpha/2}$ is the $(1-\alpha/2)$ -quantile of the standard normal distribution.

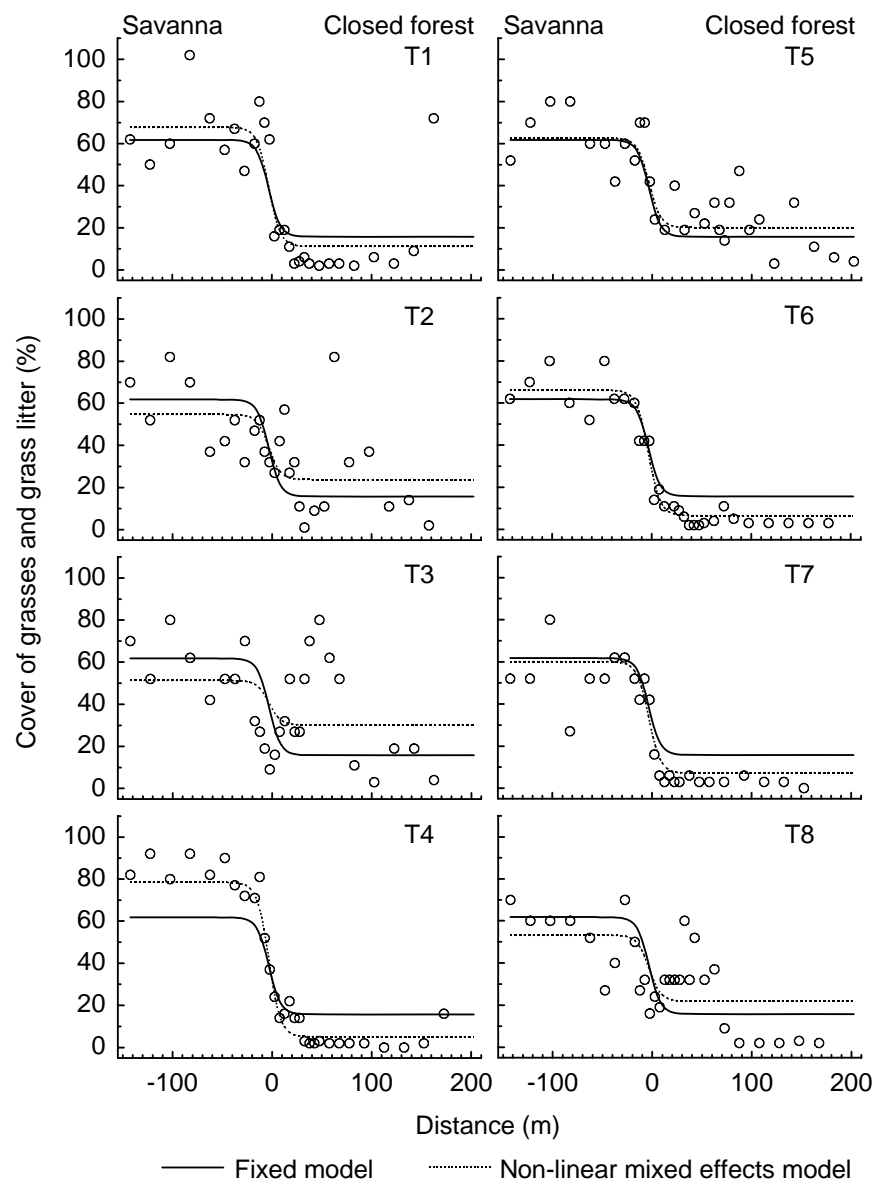


Fig. A. 1. Graphic comparison of the non-linear mixed effects model (significant random effect for the coefficient a and c representing the left and right asymptotes (see Chapter 2.5); dashed lines) and the fixed model (no transect effect; lines) for the structural parameter cover of grasses and grass litter. Random transect effects for the coefficients b and d were not significant. Dots = sample points, T1-T8 = transects (compare Fig. 2.1)

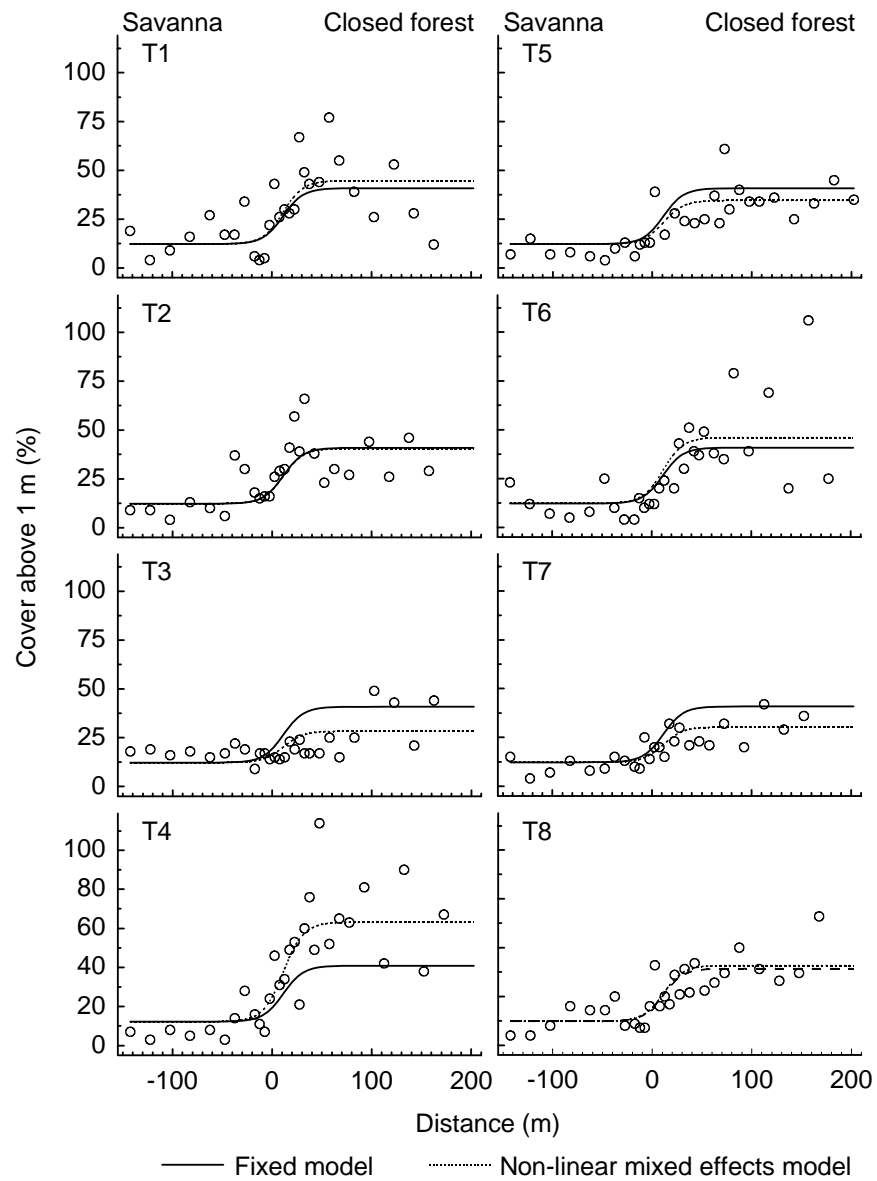


Fig. A. 2. Graphic comparison of the non-linear mixed effects model (significant random effect for the coefficient a representing the right asymptote (see Chapter 2.5); dashed lines) and the fixed model (no transect effect; lines) for the structural parameter cover above 1 m. Random transect effects for the coefficients b , c , and d were not significant. Dots = sample points, T1-T8 = transects (compare Fig. 2.1)

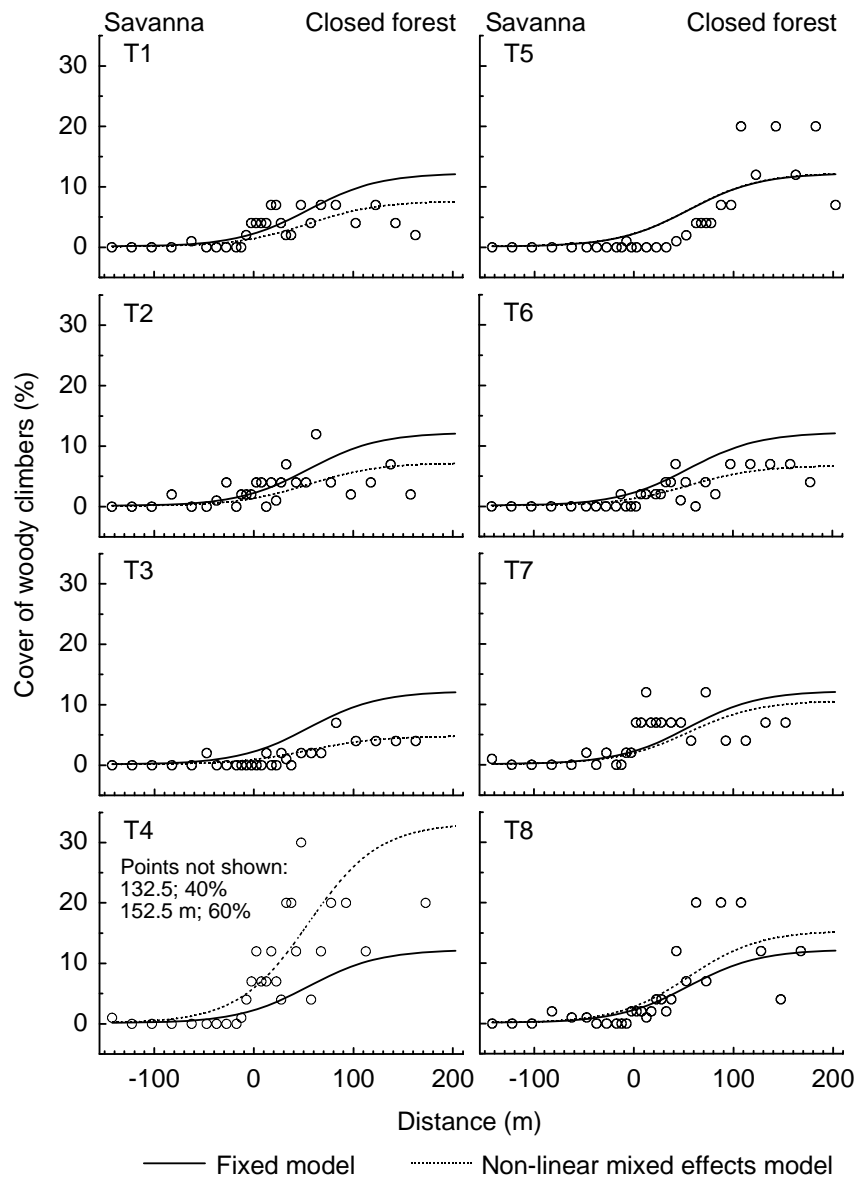


Fig. A. 3. Graphic comparison of the non-linear mixed effects model (significant random effect for the coefficient a representing the right asymptote (see Chapter 2.5); dashed lines) and the fixed model (no transect effect; lines) for the structural parameter cover of woody climbers. Random transect effects for the coefficients b , c , and d were not significant. Dots = sample points, T1-T8 = transects (compare Fig. 2.1).

Table. A. 1. Summary of detected depth-of-edge influence (DEI) regarding different parameters studied along forest-savanna transects in the CNP. Errors represent the 95%-confidence intervals. n = number of transect replicates, min = minimum, med = median, max = maximum, MP = measurement period. See Chapter 3.1 – 3.4 for details.

	n	DEI (m)
Vegetation composition (Chapter 3.4):		
Cover of all species	1	75
Cover of grass species	1	10
Cover of herb species	1	65
Cover of woody climbers	1	45
Cover of tree and shrub species	1	120
Trees and shrubs 1-10 cm dbh	1	75
Trees and shrubs 10-20 cm dbh	1	120
Trees > 20 cm dbh (min, med, max)	8	(35) 55 (100)
Structural parameters (Chapter 3.1):		
Cover of grass and grass litter (fixed model)	8	11.4 ±9.8
Cover above 1 m (fixed model)	8	32.0 ±15.5
Cover of woody climbers (fixed model)	8	119.4 ±74.8
Mass of dry grasses (Chapter 3.2):		
single models (min, med, max)	8	(0) 6.8 (147.6)
fixed model	8	27.2 ±22.0
Limit of burned surface (min, med, max) (Chapter 3.2)	8	(0) 0 (27.5)
Microclimate (Chapter 3.3):		
MP	Parameter	transect effect (n=8) DEI
1	stdT _{mean}	yes 137.3 ±138.3
	stdH _{5%-quantil}	yes -
	stdVPD _{amp.}	no 57.5 ±60.8
2	stdT _{mean}	yes 42.4 ±37.8
	stdH _{5%-quantil}	yes 21.5 ±41.0
	stdVPD _{amp.}	no 36.1 ±45.4
3	stdT _{mean}	yes 60.3 ±43.1
	stdH _{5%-quantil}	yes 108.4 ±135.4
	stdVPD _{amp.}	no 32.5 ±41.3
4	stdT _{mean}	yes 44.9 ±26.7
	stdH _{5%-quantil}	yes 32.4 ±15.7
	stdVPD _{amp.}	no 37.3 ±19.5
5	stdT _{mean}	yes 39.1 ±36.3
	stdH _{5%-quantil}	yes 27.4 ±15.5
	stdVPD _{amp.}	no 30.3 ±21.0

Curriculum vitae of Klaus Josef Hennenberg:

Dec. 18, 1970	Born in Münster (Westf.), Germany
08/77-06/81	Primary school, Albersloh
08/81-05/90	Gymnasium Wolbeck, Münster (Westf.) (Abitur)
10/90-09/92	Studies in biology at the University of Münster (Westf.) (Vordiplom)
10/92-09/93	Practical training
10/93-09/98	Studies in biology at the University of Göttingen (Diploma), subjects: botany, soil science, nature conservation Diploma thesis: Ecological and population biological investigations on the northern distribution range of <i>Hippocrepis comosa</i>
11/98-10/99	Graduate assistant at the Department of Nature Conservation, University of Göttingen: Forest conservation in Slovakia
10/99-12/00	Advanced studies on 'Energy and Environment – efficient use of energy' at the University of Kassel.
11/99-03/00	Scientific employee at the Department of Botany, University of Kaiserslautern: Feasibility study for the experimental station of silviculture in Trippstadt
07-10/00	Research assistant in the EU-project TRANSPLANT, Department of Plant Ecology, University of Marburg
01/01-12/04	Scientific employee in the BMBF-project BIOTA (Biodiversity Transect Monitoring Analysis), Department of Botany, University of Rostock

Rostock, December 2004

Hiermit erkläre ich, dass ich die eingereichte Dissertation selbständig und ohne fremde Hilfe verfasst, andere als die von mir angegebenen Quellen und Hilfsmittel nicht benutzt und die den benutzten Werken wörtlich oder inhaltlich entnommenen Stellen als solche kenntlich gemacht habe.

Rostock, Dezember 2004

Klaus Josef Hennenberg